

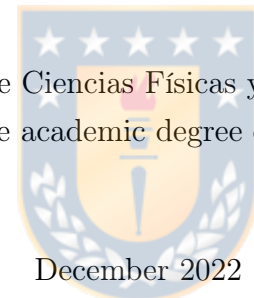


UNIVERSIDAD DE CONCEPCIÓN  
FACULTAD DE CIENCIAS FÍSICAS Y MATEMÁTICAS

# Theoretical Models of Black Holes and some implications for Q-balls

**By: Sumeet Mohan Chougule**

Thesis presented to the Facultad de Ciencias Físicas y Matemáticas of the Universidad de  
Concepción to qualify for the academic degree of Doctor in Physical Sciences



December 2022  
Concepción, Chile

**Thesis Advisor: Dr. Fernando Izaurieta**



© 2022, Sumeet Chougule

The total or partial reproduction is authorized, for academic purposes, by any means or procedure, including the bibliographic citation of the document.



Thesis Advisor : Dr. Fernando Izaurieta

*Departamento de Física,  
Universidad de Concepción (UdeC),  
Concepción, Chile.*

Assessment Committee : Dr. Jorge Zanelli

*Laboratorio de Física Teórica,  
Centro de Estudios Científicos (CECs),  
Valdivia, Chile.*

: Dr. Fabrizio Canfora

*Laboratorio de Física Teórica,  
Centro de Estudios Científicos (CECs),  
Valdivia, Chile.*



*To the memory of my father,  
Mohan Annasaheb Chougule  
We miss you!*



## ACKNOWLEDGEMENTS

I am grateful beyond words to my dad, mom, and brother for supporting me in doing the things I want to do. Nothing would have been possible without their unparalleled love!

I want to express my sincere gratitude to my advisor Dr. Jorge Zanelli. I am deeply grateful for your guidance, support, and encouragement throughout my Ph.D. journey. Your expertise and insight have been invaluable to me, and I am grateful for the time and energy you have dedicated to my research. Your guidance and mentorship have been instrumental in helping me to develop as a researcher and a scholar, and I am forever grateful for the opportunity to work with you. I feel fortunate to have had the opportunity to learn from you and to benefit from your expertise and wisdom. Thank you for your patience, support, and unwavering belief in me.

I want to express my sincere gratitude to Dr. Fabrizio Canfora. Your contributions have been invaluable, and I am deeply grateful for your time, energy, and expertise. Your insights and ideas have helped to shape this work in countless ways, and I am grateful for the opportunity to have worked with you. Your support and encouragement have meant a great deal to me, and I am grateful for your positive impact on my research. Thank you for your collaboration and for being such a vital part of this thesis.

With pleasure, I would like to thank Centro de Estudios Científicos (CECs), Valdivia, where I spent most of my Ph.D. time. With special thanks to the secretary Patricia Fernandoy at CECs, without whom I would have kept spiraling down the bureaucratic hole.

I would also like to thank Departamento de Física, UdeC, for providing the resources and facilities that have made this research possible. I want to especially acknowledge Dr. Jaime Araneda, Dr. Fernando Izaurieta, and secretary Soledad Daroch. In particular, I would like to thank Agencia Nacional de Investigación y Desarrollo (ANID) for their financial support, which has enabled me to focus on my research and complete this work.

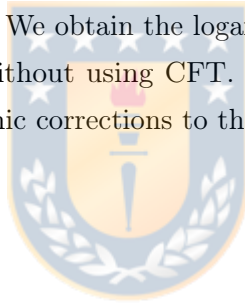
Special thanks to my collaborators Dr. Andres Gomberoff, Dr. Debaprasad Maity, Dr. Sayan Chakrabarti, Dr. Behnam Pourhassan, Dr. Sanjib Dey, and Dr. Mir Faizal. I also appreciate enormous discussions on physics with Dr. Krishnamohan Parattu, Dr. Fábio Novaes, and Dr. Alfredo Pérez.

Finally, I would like to thank my friends, Satyajeet Lokhande, Akash Gulankar, Jaime Peñailillo, José Ilić, and Dr. Marco Rivera, for their support and encouragement throughout this process.



## Abstract

The study of black holes is a fascinating and active area of research in theoretical physics. In recent years, the development of effective field theory (EFT) has provided a robust framework for studying the properties and behavior of black holes. In this thesis, we apply the principles of EFT to study black holes and Q-balls. Using the EFT for the black holes in 3+1 D, we will look at the hairy black hole background to study its fluctuations in a model-independent way and analyze the quasinormal modes of the hairy black holes. This allowed us to show the possible gravitational wave signatures of hairy black holes. Skyrme model is an EFT of QCD which describes mesons, and we will focus on the pions with vanishing topological/Baryonic charge. This opens the door for studying non-topological solitonic configurations, which are Q-balls. We also research the mini-superspace of the 2+1 D pure gravity, which lets us explore the Lorentzian path integral and the Euclidean geometries' partition function. We obtain the logarithmic correction to the BTZ black hole entropy naked singularities without using CFT. Using the Euclidean partition function, we also calculate the logarithmic corrections to the entropy of the finite temperature BIon solution.



**Keywords** – Hairy black hole, Effective Field Theory, Quasinormal modes, Thermodynamics, Thermal fluctuations, Q-balls, Skyrme model, 3D pure gravity



# Contents

<b>ACKNOWLEDGEMENTS</b>	<b>i</b>
<b>Abstract</b>	<b>iii</b>
<b>1 Introduction</b>	<b>1</b>
1.1 But, what is Effective Field Theory?	3
1.1.1 EFT of Goldstone bosons	6
1.2 Metric notations	7
1.3 But, what is the outline of the thesis?	8
<b>2 Effective Field Theory of Hairy Black Holes and Their flat/dS limit</b>	<b>11</b>
2.1 Introduction	12
2.2 Effective field theory setup	14
2.2.1 Stückelberg mechanism: Goldstone boson mode	17
2.2.2 dS, AdS and flat Schwarzschild limit	20
2.3 Underlying theory	28
2.3.1 Quasinormal mode analysis in asymptotically dS/flat hairy black holes	31
2.3.2 Quasinormal frequencies for asymptotically flat Schwarzschild black hole	34
2.3.3 Quasinormal frequencies for Schwarzschild de Sitter black holes	37
2.4 Conclusion	39
<b>3 Gauged Q-Balls in the gauged Skyrme model</b>	<b>41</b>
3.1 Introduction	42
3.2 The gauged Skyrme model	44
3.2.1 Field equations	44
3.2.2 Energy-momentum tensor and topological charge	45
3.3 Review of Q-balls	46
3.3.1 Q-balls of complex scalar field	46
3.3.2 Gaged Q-balls of complex scalar field	47
3.4 The ansatz and the corresponding field equations	48
3.5 Q-Balls in Skyrme model	50
3.6 Gauged Q-balls in Skyrme model	54
3.6.1 Energy per unit charge	56

3.7	Stability analysis . . . . .	57
3.8	Phenomenological implications . . . . .	59
3.9	Conclusion . . . . .	59
<b>4</b>	<b>But, what about Quantum Gravity?</b>	<b>61</b>
4.1	Roadblocks in quantizing gravity . . . . .	61
4.2	Wait, but why should we quantize gravity? . . . . .	62
4.3	But, what about the path integral of gravity? . . . . .	63
4.3.1	Euclidean quantum gravity . . . . .	63
4.3.1.1	Wait, but how is it related to a path integral? . . . . .	64
4.4	But, what would it imply if nature doesn't follow QG? . . . . .	64
<b>5</b>	<b>Quantum Corrections to a Finite Temperature BIon</b>	<b>66</b>
5.1	Introduction . . . . .	66
5.2	Gravitational Partition Function . . . . .	68
5.3	Corrected Thermodynamics for the BIon . . . . .	72
5.4	Conclusion . . . . .	78
<b>6</b>	<b>Lorentzian path integral of 3D pure gravity</b>	<b>80</b>
6.1	Introduction . . . . .	80
6.2	Proposal for the gravitational path integral measure . . . . .	81
6.3	Gravitational Hamiltonian and the Boundary term . . . . .	83
<b>7</b>	<b>Partition function of 3D pure gravity</b>	<b>88</b>
7.1	Introduction . . . . .	88
7.2	BTZ mini-superspace of 2+1 AdS gravity . . . . .	89
7.3	Temperature of Naked Singularities (NS) . . . . .	90
7.4	Partition function . . . . .	91
<b>8</b>	<b>Conclusion</b>	<b>93</b>
	<b>Appendix</b>	<b>96</b>
<b>A</b>		<b>96</b>
A1	Supplements for the EFT of Black holes . . . . .	96
A2	Q-balls . . . . .	96
A2.1	Energy of Q-balls . . . . .	96
A2.2	Asymptotic energy of ungauged Q-balls . . . . .	97
A3	Determinant of the Wheeler-DeWitt metric . . . . .	97
	<b>Referencias</b>	<b>100</b>

# List of Tables

2.3.1 Quasinormal frequencies of Schwarzschild black hole for overtone numbers $n = 1$ to 10 for $m_0^2 = 10^{-6}$ . Different multipole numbers ( $l = 1$ to 3) corresponding to the different overtones are shown in the table. . . . .	35
2.3.2 Quasinormal frequencies of Schwarzschild black hole for a different value of $m_0^2 = 10^{-1}$ . . . . .	36
2.3.3 Quasinormal frequencies of Schwarzschild-dS black hole for $m_0^2 = 10^{-6}$ and $\tilde{l}^2 = 10^8$ . . . . .	38
2.3.4 Quasinormal frequencies of Schwarzschild-dS black hole for $m_0^2 = 0.1$ and $\tilde{l}^2 = 10^8$ . . . . .	39



# List of Figures

2.2.1 Left one is a plot of the potential vs. radial distance for different $l$ values with $n = 0$ . $l$ increases from 0 to 4 in steps of 1 from bottom to top. Asymptotically flat Schwarzschild geometry is chosen as the metric function in the potential (2.2.29). The right one is a plot of Re. vs. Im. $\omega$ for different values of $l$ . The red curve has $n = 0$ , blue has $n = 1$ and black has $n = 2$ , showing a clear difference with the standard behavior of QN frequencies with multipole number and overtone. . . . .	26
2.2.2 Plot of the real and imaginary parts of $\omega$ vs multipole number $l = 2, 3, 4$ and 5 for different $n$ values. The blue dashed plot corresponds to $n = 0$ , the red dotted curve corresponds to $n = 1$ , and the black one corresponds to $n = 2$ . . . . .	27
2.3.1 Plot of the real and imaginary parts of $W_0$ for the Schwarzschild black hole for the first 10 overtones . . . . .	36
3.5.1 Minima of $U(\alpha)$ at $\alpha_0 \neq 0$ . . . . .	50
3.5.2 Minima of $U(H)$ at $H_0 \neq 0$ . . . . .	52
3.5.3 $U(H)$ and $V_{eff}$ plots . . . . .	53
5.3.1 Behavior of the corrected entropy as a function of $t \equiv \bar{T}$ for $\mathcal{K} = 1$ and $T_{D3} = 1$ . . . . .	73
5.3.2 Behavior of the corrected entropy as a function of $\sigma_0$ for $\mathcal{K} = 1$ , $T_{D3} = 1$ (a) $\bar{T} = 0.5$ (b) $\bar{T} = 1$ . . . . .	73
5.3.3 Behavior of the corrected entropy in terms of $\gamma$ to see cases of $\gamma = 0$ and $\gamma = 1$ . We set $\mathcal{K} = 1$ , $\bar{T} = 1$ and $T_{D3} = 1$ . . . . .	75
5.3.4 Behavior of internal energy in terms of $\gamma$ , with $\mathcal{K} = 1$ and $T_{D3} = 1$ (a) $\bar{T} = 0.9$ (b) $\bar{T} = 1$ . . . . .	75
5.3.5 Behavior of the specific heat with respect $\sigma_0$ for $\mathcal{K} = 1$ and $T_{D3} = 1$ (a) $\bar{T} = 0.9$ (b) $\bar{T} = 0.7$ . . . . .	76
5.3.6 Behavior of the specific heat with respect to $\gamma$ for $\mathcal{K} = 1$ , $\bar{T} = 0.9$ and $T_{D3} = 1$ . . . . .	76
5.3.7 Behavior of the specific heat with respect to $\bar{T}$ for $\mathcal{K} = 1$ , $\sigma_0 = 0.02$ and $T_{D3} = 1$ . . . . .	77

# Chapter 1

## Introduction

Quantum gravity (QG) is undoubtedly one of the biggest open problems in physics and is often considered one of the field's most fundamental and challenging problems. The problem of quantum gravity is searching for a theory that can reconcile the principles of quantum mechanics and general relativity, two of the most successful and well-established theories in physics.

In almost the last hundred years, there has not been any significant improvement in our understanding apart from realizing the difficulties involved in considering a quantum version of the gravitational field. Generations of physicists and mathematicians have attacked the problem with their ingenuity which mainly led to mathematical and theoretical models of how the Universe at the Planck scale should behave. Some primary models include string theory, loop quantum gravity, and causal dynamical triangulation. So far, the Universe doesn't seem to care about those models keeping our glass everlastingly filled with curiosity.

We cannot comprehend gravity at the quantum scale for various fundamental reasons/limitations. Quantum mechanics (QM) requires a well-defined Hilbert space on a spacetime background, but in the case of QG, the spacetime itself should be part of the Hilbert space. This is a limitation put forth by our well-established theory of QM. There is also a lack of understanding of what exactly the two degrees of freedom of the gravitational field represent at the quantum level. There are many other fundamental and technical reasons for our failures, which will be discussed later.

In this thesis, we will explore physics with fundamental tools that have shown the experimental and observational prevalence in the past. Of course, we should be open

---

to novel mathematical and physical ideas like string theory, AdS/CFT, etc. But, so far, it has neither improved our fundamental understanding of nature's internal mechanism nor shown any experimental/observational hope! It also makes fundamental principles of physics obscure. It is better to return to our roots and rethink our approach toward QG. We may even discover that nature does not have gravity quantized, and gravity might be an emergent phenomenon of some other fundamental field<sup>1</sup>.

Here, we will explore toy models using fundamental tools, giving us a better insight into the path toward QG. Studying these toy models doesn't give us a full sight of QG problems. Still, it helps us understand different aspects of it through the fundamental principles, which might eventually have experimental/observational consequences. The toys we will be playing with are the black holes and Q-balls.

Black holes have been a testing ground for QG for many decades. There is a fascinating and active area of research in theoretical physics. Black holes are among the most extreme and mysterious objects in the universe, and they have long captured the imagination of scientists and the public alike. Despite their exotic nature, black holes are a well-established prediction of Einstein's theory of general relativity. According to this theory, black holes are formed when a massive star collapses under its own gravity, creating a region of space-time with a strong gravitational pull that nothing, not even light, can escape.

Since their discovery, black holes have been the subject of intense study by physicists, who have developed a range of theoretical models and computational techniques to understand their properties and behavior. In recent years, the detection of gravitational waves from black hole mergers (3) by the LIGO has opened up new avenues of research, providing unprecedented insights into the dynamics of these fascinating objects.

On the other hand, venturing into Q-balls exposes us to the intricacies of a gauge theory which will eventually improve our understanding of general relativity (GR), which can be understood as a gauge theory. Q-ball is a class of non-topological solitonic objects that can arise in specific theories of scalar fields. They have been proposed as a possible candidate for dark matter (44; 47; 48; 49; 50; 51; 52) and could be related to the asymmetry observed between matter and antimatter (53; 54). They could also have observable gravitational wave signatures (55; 56). Both black holes and Q-balls can be studied using theoretical models based on the fundamental principles of physics. In particular, the development of

---

<sup>1</sup>In that case, one possibility of the emergence of graviton could be as a Goldstone boson from the underlying fundamental theory, (9).

effective field theory (EFT) has provided a robust framework for studying the properties and behavior of these objects.

GR can be understood as a gauge theory, a theoretical framework used to describe the behavior of physical systems in terms of local symmetries. In general, a gauge theory is characterized by the presence of a gauge field, which is a field that describes the local symmetries of the system, and a set of gauge transformations, which are transformations that leave the physical laws of the system invariant.

In the case of general relativity, the gauge field is the metric tensor, which describes the curvature of spacetime, and the gauge transformations are diffeomorphisms, which are smooth, continuous transformations of spacetime coordinates. The gauge transformations in general relativity are associated with the principle of general covariance, which states that the physical laws of the theory should be invariant under arbitrary coordinate transformations.

One of the key benefits of understanding general relativity as a gauge theory is that it allows for a systematic and controlled expansion in powers of energy/derivatives, making it easier to study the behavior of the theory at different energy scales. It also provides a framework for understanding the behavior of the theory in the presence of perturbations and for understanding the role of symmetries in the behavior of the theory. Even though the gauge symmetries of GR and Q-balls are different, the study of Q-balls lets us explore the gauge theory aspect.

In this thesis, we will use the methods of EFT to study theoretical models of black holes and Q-balls. By constructing effective Lagrangians for the relevant degrees of freedom of these objects and using the techniques of EFT, we will investigate the behavior of black holes and Q-balls in various regimes and explore their implications for our understanding of the fundamental laws of physics. We will also explore the mini-superspace of 2+1 dimensional AdS pure gravity with techniques of the path integral and the partition function.

## 1.1 But, what is Effective Field Theory?

Effective field theory (EFT) is a theoretical framework to construct approximate descriptions of physical systems at low energies or long distances. It is a powerful tool for studying systems that exhibit a separation of scales. The relevant degrees of freedom and interactions at a given energy or length scale can be described by an effective theory valid only within a limited range of energies or distances.

In EFT, one identifies a physical system's relevant degrees of freedom and the symmetries that constrain their interactions. The effective Lagrangian, which encodes the dynamics of these degrees of freedom, is then constructed as an expansion in powers of the relevant energy or distance scale, with the lowest-order term in the expansion corresponding to the most relevant interactions. Higher-order terms in the expansion encode the effects of less relevant interactions and can be systematically included to improve the theory's accuracy.

EFT has found a wide range of applications in various areas of physics, including particle physics, condensed matter physics, and cosmology. In particle physics, EFTs describe the interactions of elementary particles at energies much lower than the scale at which the underlying fundamental theory is expected to break down. In condensed matter physics, EFTs are used to describe the behavior of systems with many interacting degrees of freedom, such as superconductors and superfluids. In cosmology, EFTs describe the universe's evolution and the properties of dark matter and dark energy.

Overall, EFT is an essential tool in the arsenal of theoretical physicists and has played a central role in many significant developments in our understanding of the physical world. EFT allows us to write down the action principle for the energy scale of interest. For example, let's consider the case of a scalar field theory with a single real scalar field denoted by  $\phi(x)$ . The action for this theory is given by

$$S_\phi = \int d^4x \sqrt{-g} \left[ \frac{1}{2} (\partial_\mu \phi)^2 - \frac{1}{2} m^2 \phi^2 - \frac{\lambda}{4!} \phi^4 \right] \quad (1.1.1)$$

where  $m$  is the mass of the scalar field and  $\lambda$  is the coupling constant. This action is written in terms of the most relevant degrees of freedom at the low-energy scale, which are the value of the field  $\phi(x)$  and its derivative  $\partial_\mu \phi(x)$ .

The expansion in powers of energy is then performed by introducing a momentum scale  $\Lambda$  and expanding the action in powers of  $p_\phi/\Lambda$ , where  $p$  is the momentum of the field. The leading-order term in the expansion is the so-called tree-level action, given by the first two terms in the action above. The higher-order terms in the expansion, called loop corrections, represent the effects of virtual particles with momenta higher than  $\Lambda$  on the low-energy dynamics of the system. These higher-order terms can be computed systematically using perturbation theory.

In practice, constructing an EFT involves several technical steps, including identifying the relevant degrees of freedom, the symmetry properties of the system, and the power counting



rules that determine the importance of different terms in the action. We can formulate GR as an EFT which allows us to consider an expansion in the powers of metric derivatives. For an excellent review of GR as an EFT, please check (6; 7).

At low energies, the gravitational action consists of the Einstein-Hilbert term, the Ricci scalar,  $R$ . Varying it leads to Einstein's equation of motion, and we can do great physics with it at low energies. To probe at higher energies, we should consider the most general Lagrangian with higher derivative terms that remain invariant under the gauge symmetries of GR, the diffeomorphisms. This way, the gravitational action will capture the physics at high energies without knowing the underlying theory of QG. The energy scale is set by the reduced Planck mass  $M_p^2 = (8\pi G)^{-1}$  and the first few terms of the most general action ordered in the energy/derivative expansion are

$$\mathcal{S} = \frac{M_p^2}{2} \int d^4x \sqrt{-g} \left[ 2\Lambda + R + \frac{1}{M_p^2} (c_1 R^2 + c_2 R_{\mu\nu} R^{\mu\nu}) + \dots \right] \quad (1.1.2)$$

with  $\Lambda$  of order  $\partial^0$ ,  $R$  of order  $\partial^2$ ,  $R^2$  and  $R_{\mu\nu} R^{\mu\nu}$  of order  $\partial^4$  and the ellipses are for the higher order terms. The coefficients like  $c_1$  and  $c_2$  are used to renormalize any divergences coming from the higher derivative terms. Renormalized  $c_1$  and  $c_2$  take care of the one-loop divergences, which were calculated by 't Hooft and Veltman (8).

The small-scale/high-energy physics will correspond to a quantum field which will be a fluctuation in the background metric

$$g_{\mu\nu} = \bar{g}_{\mu\nu} + \delta g_{\mu\nu} \quad (1.1.3)$$

The effective action 1.1.2 tends to capture the physics of these quantum fluctuations. Now that we have identified the relevant degree of freedom, we expand all the terms in the action up to one's desire of the order in fluctuations and derivatives<sup>2</sup>. The simplest case of fluctuations in Minkowski background with  $\Lambda \ll M_p$

$$g_{\mu\nu} = \eta_{\mu\nu} + h_{\mu\nu}/M_p \quad (1.1.4)$$

---

<sup>2</sup>Caveat: As we have no idea of the underlying theory, we just hope that the higher order terms manifest some physics from the QG which could lead to some phenomenology.

will lead to an expansion

$$\mathcal{S} = \int d^4x \left[ (\partial h)^2 + \frac{h(\partial h)^2}{M_p} + \frac{h^2(\partial h)^2}{M_p^2} + \dots \right] \quad (1.1.5)$$

where we have suppressed indices of  $h_{\mu\nu}$  for simplicity. We will receive corrections from higher-order terms as we go to higher energies ( $\geq M_p$ ).

### 1.1.1 EFT of Goldstone bosons

This thesis explores the solutions in  $3 + 1$  dimensions of the theories with spontaneously broken symmetries. Goldstone's theorem shows that when a continuous symmetry is spontaneously broken in a physical system, a massless particle must be associated with each broken symmetry generator. These particles are called Goldstone bosons, a consequence of the symmetry-breaking process. Hence, we will explore an effective action for Goldstone bosons as they are the relevant degrees of freedom.

Here we will be studying hairy black hole solutions as a solution to an EFT that has an effective action for the Goldstone boson associated with the breaking of  $r$  diffeomorphism symmetry. We will construct an effective action for the Goldstone boson of broken  $r$ -diffeomorphism and study features of its solution, hairy black holes. Its construction follows similar to the effective actions in Eqs. 1.1.2 and 1.1.5, written down for the fluctuations around a hairy black hole background. It is a well-curated action that considers the dynamics of scalar fluctuations at the quadratic order in a hairy black hole background. The scalar hair breaks the  $r$ -diffeomorphism symmetry, so the generic action in the unitary gauge consists of all the invariant terms on a constant  $r$ -hypersurface

$$\mathcal{S} = \int d^4x \sqrt{-g} \mathcal{L}(g_{\mu\nu}, R_{\mu\nu\alpha\beta}, g^{rr}, K_{\mu\nu}, \nabla_\mu, r) \quad (1.1.6)$$

The terms are invariant under the residual symmetries on the hypersurface, which are temporal and angular variance. A detailed description of the action can be found in the 2nd chapter.

We will study Q-balls in the Skyrme model, an EFT of quantum chromodynamics (QCD). In the low energy limit, the relevant degrees of freedom are mesons because the quark and gluon degrees of freedom are confined. The lightest quarks' masses are negligible in this low energy limit, and they are the up and down quarks. The approximate description of the flavor symmetry corresponds to  $SU_L(N) \times SU_R(N)$ , with  $N$  being the number of flavors.

QCD famously exhibits spontaneous breaking of approximated chiral symmetry, which gives rise to a Goldstone boson with a small mass term<sup>3</sup>. For  $N = 2$ , the effective action of QCD with two flavors is given by  $SU(2)$  Skyrme action. The relevant degrees of freedom in this action consists of the PNGB. This associated PNGBs are the pions with masses ( $\pi^\pm \approx 140 \text{ MeV}$ ,  $\pi^0 \approx 135 \text{ MeV}$ ). The solutions of the Skyrme equation are topological solitons (Skyrmions) with a baryonic charge. We will study solutions of the Skyrme equation of motion with zero baryonic charges, which is possible with a suitable hedgehog ansatz, which leads to the pionic Q-balls.

## 1.2 Metric notations

The generic metric in terms of the lapse and shift functions  $N(x^\mu)$  and  $N^i(x^\mu)$ , respectively, is

$$ds^2 = -N^2(x^\mu)dt^2 + g_{ij}(x^\mu) (dx^i + N^i(x^\mu)dt) (dx^j + N^j(x^\mu)dt) \quad (1.2.1)$$

where  $\mu$  goes over all the spacetime coordinates while  $i$  runs over spatial coordinates. For a 3+1 D spacetime,  $x^i \equiv (r, \theta, \phi)$  and for a 2+1 D spacetime  $x^i \equiv (r, \phi)$ . This thesis will explore solutions in 2+1 D and 3+1 D.

We will study less generic cases of the 1.2.1, which motivates us to utilize EFT techniques. In 3+1 D, we will look at hairy black hole solutions and Q-balls. For a generic static black hole considered in chapter 2 there is no shift, so we have

$$N^2(r) = f(r) \text{ and } g_{ij}(r) \equiv (f^{-1}(r), r^2, r^2 \sin^2 \theta) \quad (1.2.2)$$

while chapter 6.2.2 on Q-balls consists of a flat metric

$$N^2(r) = 1 \text{ and } g_{ij}(r) \equiv (1, r^2, r^2 \sin^2 \theta) \quad (1.2.3)$$

In 2+1 D, we will look at the BTZ black hole and naked singularities whose collective set is called BTZ mini-superspace characterized by

$$N^2(r) = \left( \frac{r^2}{l^2} - 8GM + \frac{16G^2 J^2}{r^2} \right), \quad N^\phi(r) = -\frac{4GJ}{r^2} \quad (1.2.4)$$

<sup>3</sup>When the broken symmetry is not exact, the Goldstone boson is not massless, and it is also known as a pseudo-Nambu-Goldstone boson (PNGB).

$$g_{ij}(r) \equiv (N^{-2}(r), r^2) \text{ now with } i \equiv (r, \phi) \quad (1.2.5)$$

### 1.3 But, what is the outline of the thesis?

In chapter 2, which is based on (1), we applied the EFT approach toward understanding black holes in a model-independent manner. With the focus on the following question: *does the effective theory of black holes provide any information about the possible existence of hair?* To probe any physical system, the behavior of fluctuation in a specific background under consideration is most important. In this chapter, we consider black hole space-time with hair as a particular type of background whose properties can only be understood by looking at the nature of fluctuation around it. The conventional EFT approach deals with writing down the theory of background itself in terms of fundamental fields. In the present context, the approach was to consider the prior existence of a background of interest and then write down the most general theory for the fluctuations in the given background based on symmetry. This approach has been successfully applied in inflationary cosmology, which is popularly known as an effective theory of inflation (19). In this chapter, we use the same technique in the background of spherically symmetric black holes with hair which also enjoys the exact symmetry.

We have first written down the most general model-independent effective Lagrangian for the fluctuation in a given hairy black hole background. We have considered an asymptotically flat and de-Sitter black hole background for our detailed analysis. The background cosmological constant is assumed to be generated from the hair. Generally, the behavior of fluctuation encodes essential information about background hair. Therefore, to understand the behavior of the fluctuation, we have chosen a particular set of effective theory parameters. Using the sixth-order WKB approximation associated with those fluctuations, we have computed the quasinormal modes, which appeared to carry different features compared to usual black hole quasinormal modes. In general, for the four-dimensional Schwarzschild black hole in the asymptotically flat/dS background, the real oscillation frequency of the quasinormal modes decreases, and the imaginary part of the frequency increases with the increase of the overtone number ( $n$ ) while the multipole number ( $l$ ) is kept fixed. Interestingly what came out from our quasinormal mode analysis for the effective field theory fluctuation is that both the real and imaginary frequencies increase with increasing overtone number. Motivated by our EFT analysis, we also constructed a class of higher derivative scalar field theory. For this theory also, we confirmed the aforementioned exciting behavior of the quasinormal

modes.

In the next chapter, chapter 3, we will study a non-trivial configuration of scalar fields that form a condensate called Q-balls without gravity. In other words, Q-balls are localized, non-topological lumps of the scalar field with a continuous charge distribution. It was first proposed by Coleman in the complex scalar field theory (66). Our focus in this chapter is on the question: *can Pionic Q-balls exist in the Skyrme model?*

This chapter will demonstrate how under suitable hedgehog ansatz, we can bring the Skyrme equation of motion in a form analogous to the equations in the complex scalar theories. The Skyrme model is an EFT of the QCD (78; 79; 81; 82; 80). The Skyrme model possesses a conserved topological charge interpreted as a Baryonic charge. Thus, configurations with vanishing Baryonic charges are interpreted as Pionic configurations, while configurations with non-vanishing topological charges contain Baryons. Hence, we will only consider configurations with disappearing topological charges in the present work. As we will see, one of the advantages of the Skyrme model is that the geometry of the action uniquely determines the effective potential appearing in the "Q-ball equations" (so that any arbitrariness in the choice of the potential disappears).

Chapter 3 is an ongoing project. Still, we have successfully demonstrated how, under the suitable ansatz, the effective potential satisfies all the critical requirements for a theory to sustain a Q-ball solution. So, a Q-ball in the Skyrme model will correspond to a Pion condensate held together by the non-linearity of the theory. This is a more pragmatic scenario than previous Q-ball solutions in the literature. This project is not yet finished due to the sensitivity associated with the numerical analysis.

Chapter 4 is an overview of the quantum mechanics of the gravitational field. It also has a short review of the partition function and Euclidean quantum gravity, which will set the stage for the subsequent chapters.

In chapter 5, which is based on (2), we applied the techniques of Euclidean quantum gravity to a finite temperature BIon solution to analyze the quantum fluctuations. A finite temperature BIon solution is a brane-anti-brane wormhole configuration. In this chapter, it will be shown that these quantum fluctuations produce logarithmic corrections to the entropy of this finite temperature BIon solution. These corrections to the entropy also correct the internal energy and the specific heat for this finite temperature BIon.

Chapter 6 is more of a pedagogical introduction to the Hamiltonian formalism in 2+1 D

gravity and surface terms. It highlights the difficulties involved in the path toward QG. We propose a possible measure for the gravitational path integral, but not much can be done in this formalism! In short, approaching QG seems intractable. Maybe, Universe doesn't have a quantized graviton, and gravity might be an emergent phenomenon of some other fundamental field.

Chapter 7 is still an ongoing project which uses EFT to construct a mini-superspace of 2+1 D AdS pure gravity and Euclidean partition function to calculate the logarithmic corrections to the BTZ black hole entropy. This mini-superspace contains all the stationary geometries which are locally  $AdS_3$  with  $J/l \leq |M|$ . They consist of BTZ black holes, conical defects and excesses (CD/CE), and over-spinning (OS) singularities, (4; 5).

Chapter 8 summarizes the results found in this thesis.



## Chapter 2

# Effective Field Theory of Hairy Black Holes and Their flat/dS limit



### Abstract

Effective theory of fluctuations based on underlying symmetry plays a vital role in understanding the low energy phenomena. Using this powerful technique, we study the fluctuation dynamics keeping in mind the following central question: does the effective theory of black holes provide any information about the possible existence of hair? Assuming the symmetry of the hair is that of the underlying black hole space-time, we start by writing down the most general action for the background and the fluctuation in the effective field theory framework. Considering the Schwarzschild and Schwarzschild de Sitter black hole background with a spherically symmetric hair we derived the most general equation of motion for the fluctuation. For a particular choice of theory parameters, quasinormal modes corresponding to those fluctuations appeared to have distinct features compared to the usual black hole quasinormal modes. On the other hand, the background equations from the effective theory of Lagrangian seemed to suggest that the underlying theory of the hair under consideration should be a higher derivative in nature. Therefore as a concrete example, we construct a class of higher derivative scalar field theory that gives rise to spherically symmetric hair through background cosmological constant. We also calculated the quasinormal modes whose behavior was similar to the one discussed in the effective theory.

## 2.1 Introduction

The general theory of relativity has been proven to successfully explain a large variety of gravitational phenomena in a wide range of length scales. The theory also provides us with a class of vacuum solutions called black holes. Black holes are the most fascinating objects in general relativity, which has not been clearly understood from different aspects despite having a long history of various path-breaking research. On the other hand, it is believed to be the simplest object in our universe, which is characterized by only three parameters: mass, charge, and angular momentum. Over the years, it has also been understood that those are the only three charges that a black hole can carry. In black hole physics, this is known as the black hole no-hair theorem (10; 11). A lot of work has been done in the literature on the possible existence of hairy black holes for various theories. Let us particularly mention a class of modified gravity theories (12), which has gained significant attention in the recent past because of their applicability in various physical contexts. The existence of black hole hairs has been extensively discussed in those theories in (13; 14; 15). We will also discuss a particular class of these theories in the present chapter. Having talked about an extensive research area in the domain of black hole physics, it has to be admitted that all those endeavors towards understanding black holes are mostly confined within the theoretical regime, without much to do with the observation. Thanks to the recent breakthrough on the observational front in gravitational waves (16; 17) originating from the merger of binary black holes, has finally opened up the exciting possibility of verifying as well as understanding those large volumes of theoretical works and most importantly in understanding the more profound underlying principles of the nature of space-time. All the studies on black holes so far were model-dependent, where one considers a specific theory of gravity and its black hole solutions.

On the other hand, when it comes to observations, all the observable quantities are based upon the properties of fluctuations around the black hole background without much to do with a specific theory of gravity. This motivates us to understand black holes in an effective field theory framework. As the name suggests, it will be a model-independent description of fluctuations around a black hole in space-time. In this chapter, our analysis will be focused on the following question: *does the effective theory of black holes provide any information about the possible existence of hair?* Our study of possible hairy black hole solutions will be valid for a class of asymptotically flat and dS black holes. As has been pointed out before, black holes with hair have been the subject of intense research for many years. For



a fascinating short review, the reader is referred to (18) and *references therein*.

The effective field theory approach has been proven to be a universal tool for understanding low-energy phenomena in many areas of physics. One exciting application of this approach, which has gained significant attention in the recent past, is the effective theory of inflation (19). The idea behind this theory was to understand the model-independent dynamics of fluctuation in a time-dependent inflaton background. The inflaton's spontaneous breaking of time translation symmetry is the most crucial ingredient. Motivated by this, we initiated the present work. Our basic underlying assumption in this work would be to consider the existence of a hairy black hole that breaks spatial translation symmetry. For a generic theory, a non-trivial background solution always breaks a certain amount of symmetry of the underlying theory. For a theory of gravity, a diffeomorphism is the fundamental underlying symmetry. The existence of non-trivial black hole hair will break the symmetry mentioned above. Therefore, the main idea in our approach will be to write down all possible terms in the effective Lagrangian, which obey the residual diffeomorphism symmetry in the above-mentioned hairy black hole background.

Our present study will consider the most straightforward situation where the background is a spherically symmetric black hole with the hair having the exact symmetry. The origin of the hair in the effective field theory framework is not essential for our study. More general situations will be discussed in our future publications. Before we embark on our analysis, let us mention some independent studies on fluctuations in the black hole background. In reference (20), the authors have studied the fluctuation dynamics in static black hole background considering the less symmetric situation with angular diffeomorphism invariance. This, in principle, will lead to more than one degree of freedom as opposed to the case considered in our current chapter for a hairy black hole. In another work, (21), more elaborate formalism has been developed irrespective of specific hairy background, and it is valid even for non-hairy black holes. However, to achieve the full diffeomorphism invariant action, the formalism requires starting with a large number of independent parameters. Then systematic analysis needs to be performed to reduce the number of parameters. While we were studying properties of fluctuations in a hairy black hole background based on the formalism used in the effective theory of inflation, the paper (22) came up where the same formalism has been considered. They studied the properties in greater detail.

This chapter is organized as follows: in section 2, we write down the most general Lagrangian for the background and the associated fluctuations assuming  $r$ -diffeomorphism symmetry

to be broken by some unknown field. We aim to understand the hairy black holes in the effective field theory framework. Therefore we will assume a spherically symmetric black hole background with hair which also inherits the symmetry of the background. By using the well-known Stückelberg mechanism, we identify the scalar Goldstone mode associated with the broken  $r$ -diffeomorphism symmetry and derive its equation of motion. While deriving the equation, the background naturally plays a vital role. Therefore, the fluctuation equation encodes the information about the nature of hair in the background. Considering the most straightforward asymptotically flat/dS/AdS black hole backgrounds, our effective field theory approach shows that they can support hair, generating background cosmological constant dynamically. However, it turns out that the theory of hair, in general, should be a higher derivative in nature. This fact may be intimately tied with the conventional no-hair theorem, which will be discussed in the future. Considering this observation, we will construct a specific higher derivative scalar field theory in the subsequent section. This section is ended by discussing the qualitative behavior of the quasinormal modes for the Goldstone modes, which behave distinctly as opposed to the conventional black hole quasinormal modes. Interestingly enough, this distinct behavior also can be seen from our underlying theory, discussed in detail in section 3. This section will discuss a class of higher derivative theory of the scalar field. The vacuum expectation value of the scalar breaks  $r$ -diffeomorphism symmetry with a background cosmological constant. With this background, we study the behavior of quasinormal modes. Finally, we finish the chapter with the conclusion.

## 2.2 Effective field theory setup

In this section, we will formulate the theory. As already mentioned, we assume there exists a hairy black hole with spherical symmetry. It naturally breaks the  $r$ -diffeomorphism symmetry. Therefore, without requiring any specific gravity model, we can write down the most generic Lagrangian, which will be invariant under the residual diffeomorphism symmetry. Under the residual symmetry transformation  $x'^i = x^i + \xi^i$  ( $i \equiv t, \theta, \phi$ ), the list of covariant quantities contains  $g^{rr}$  and all the geometrical objects defined on an arbitrary  $r = \text{constant}$  hypersurface, namely the extrinsic curvature  $K_{\mu\nu}$ , three-dimensional Ricci scalar  $\mathcal{R}^{(3)}$ . However, one important point we missed is the degree of symmetry of the  $r$ -constant hypersurface, which is not maximally symmetric. The spatially flat cosmological background is one example where the  $t$ -constant hypersurface is maximally symmetric. Therefore, for any spherically symmetric background, the extrinsic curvature  $K_{\mu\nu}$  of  $r$ -

constant hyper-surface does not become proportional to the induced metric. As a result, one needs to consider the rotational symmetry and general time reparametrization invariance separately, as pointed out and discussed in detail in the reference (22). Therefore, in the framework of effective field theory, we need many independent parameters compared to the extremal case to understand the dynamics of fluctuation in the hairy black hole background. With these important points and ingredients, the most generic Lagrangian for the background and the fluctuation can be expressed as

$$\begin{aligned}
\mathcal{S} = \int d^4x \sqrt{-g} \left\{ \frac{M_{Pl}^2}{2} \mathcal{R} - \Lambda(r) - c(r)g^{rr} - \alpha(r)\bar{K}_{\mu\nu}K^{\mu\nu} + \frac{1}{2!}M_2(r)^4(\delta g^{rr})^2 \right. \\
+ \frac{1}{3!}M_3(r)^4(\delta g^{rr})^3 - \frac{\bar{M}_1(r)^3}{2}(\delta g^{rr})(\delta K^\mu{}_\mu) + \bar{M}_4^2(r)\bar{K}_{\mu\nu}\delta g^{rr}\delta K^{\mu\nu} \\
+ M_5^2(r)(\partial_r\delta g^{rr})^2 + M_6^2(r)(\partial_r\delta g^{rr})\delta K^\beta{}_\beta + M_7^2(r)\bar{K}_{\alpha\beta}(\partial_r\delta g^{rr})\delta K^{\alpha\beta} \\
+ \frac{\hat{m}_2^2(r)}{8}g^{\mu\nu}\partial_\mu(\delta g^{rr})\partial_\nu(\delta g^{rr}) - \frac{\bar{M}_2(r)^2}{2}(\delta K^\mu{}_\mu)^2 - \frac{\bar{M}_3(r)^2}{2}\delta K^\mu{}_\nu\delta K^\nu{}_\mu \\
+ M_{11}(r)\bar{K}_{\mu\nu}\delta K^\beta{}_\beta\delta K^{\mu\nu} + M_{12}(r)\bar{K}_{\mu\nu}\delta K^{\mu\rho}\delta K^\nu{}_\rho + \lambda_1(r)\bar{K}_{\mu\rho}\bar{K}^\rho{}_\nu\delta K^\beta{}_\beta\delta K^{\mu\nu} \\
\left. - \frac{\hat{m}_1^2(r)}{2}\delta g^{rr}\delta\mathcal{R}^{(3)} + M_{14}(r)\bar{K}_{\mu\nu}\delta g^{rr}\delta R^{\mu\nu(3)} \right\}. \tag{2.2.1}
\end{aligned}$$

All the parameters take care of the dimensions of the corresponding term, and all are functions of  $r$ . The background extrinsic curvature is given by  $\bar{K}_{\mu\nu} = \frac{1}{2}\frac{g_{\mu\nu}}{\sqrt{g(r)}}$ . The above action contains all the possible terms at the quadratic level. The interested reader can find an excellent description of why these are the only terms possible in the appendix of (22). In the following discussion, we will keep up to the fourth derivative order of the fluctuation. For the above general Lagrangian, we consider the following form of the spherically symmetric hairy black hole background:

$$ds^2 = -f(r)dt^2 + g(r)dr^2 + R(r)d\Omega^2 \quad ; \quad \phi \equiv \phi_0(r). \tag{2.2.2}$$

At this point, let us mention that  $\phi$  represents the hair, whose explicit nature is unimportant to us. Because of  $r$ -diffeomorphism symmetry of the underlying theory, one can always choose unitary gauge,  $\delta\phi = 0$  such that the extra scalar degree of freedom is eaten in the metric and manifest itself as a gravitational degree of freedom which we parametrized by the fluctuation of the metric  $\delta g^{rr} = g^{rr} - 1/g(r)$ . Consequently, we can express all the covariant geometric quantities defined on  $r$ -constant hypersurface in terms of those metric fluctuations. Based on these general arguments, the first four terms in the above action

encode the information about the hairy black hole background given in Eq. (2.2.2). Since the coefficient of arbitrary linear fluctuation is proportional to the equation of motion, the rest of the terms in the Lagrangian will start from quadratic order in fluctuation. Hence unperturbed background will be parametrised by three unknown functions  $\Lambda(r)$ ,  $c(r)$  and  $\alpha(r)$ , and associated stress-energy tensor can be expressed as

$$T_{\mu\nu} = -\frac{2}{\sqrt{-g}} \frac{\delta\mathcal{S}}{\delta g^{\mu\nu}} = -g_{\mu\nu} \left[ c(r)g^{rr} + \Lambda(r) + \alpha(r)K_{\alpha\beta}K^{\alpha\beta} \right] + 2c(r)\delta_{\mu}^r\delta_{\nu}^r - \alpha(r)K_{\alpha\beta}K^{\alpha\beta}n_{\mu}n_{\nu} - \nabla_{\beta}(\alpha(r)K^{\beta}_{\mu}n_{\nu}) - \nabla_{\beta}(\alpha(r)K^{\beta}_{\nu}n_{\mu}) + \nabla_{\beta}(\alpha(r)K_{\mu\nu}n^{\beta}). \quad (2.2.3)$$

By using the Einstein's equation  $R_{\mu\nu} - \frac{1}{2}Rg_{\mu\nu} = (1/M_{Pl}^2)T_{\mu\nu}$ , the expressions for the two unknown parameters ( $\Lambda(r)$ ,  $c(r)$ ) are given in the appendix A1. Equation for  $\alpha(r)$  satisfies the following constraint equation,

$$\left( \frac{f'(r)}{f(r)} - \frac{R'(r)}{R(r)} \right) \alpha'(r) + \left( \frac{f''(r)}{f(r)} - \frac{f'^2(r)}{2f^2(r)} - \frac{R''(r)}{R(r)} - \frac{f'(r)g'(r)}{2g^{3/2}(r)\sqrt{f(r)}} + \frac{f'(r)R'(r)}{2f(r)R(r)} + \frac{g'(r)R'(r)}{2g(r)R(r)} + 2\frac{g(r)}{R(r)} \right) (M_{Pl}^2 + \alpha(r)) + \left( \frac{R'^2(r)}{R^2(r)} - \frac{f'^2(r)}{f^2(r)} - 2\frac{g(r)}{R(r)} \right) \alpha(r) = 0. \quad (2.2.4)$$

For a given black hole background,  $\alpha(r)$  can take different solutions, which essentially encode the information about the hair and the underlying gravity theory. For simplicity, we will take the trivial solution of the Eq. 2.2.4 i.e.,  $\alpha(r) = 0$ , provided we satisfy the following constraint:

$$\left( \frac{f''(r)}{f(r)} - \frac{f'^2(r)}{2f^2(r)} - \frac{R''(r)}{R(r)} - \frac{f'(r)g'(r)}{2g^{3/2}(r)\sqrt{f(r)}} + \frac{f'(r)R'(r)}{2f(r)R(r)} + \frac{g'(r)R'(r)}{2g(r)R(r)} + 2\frac{g(r)}{R(r)} \right) = 0. \quad (2.2.5)$$

In this chapter, we will be considering mainly Schwarzschild, Schwarzschild-AdS, and Schwarzschild-dS background solutions. One can check that for those backgrounds, Eq. 2.2.5 is automatically satisfied. We will consider the more general cases involving  $\alpha$  elsewhere. Considering the above background effective theory parameters, we are now in a position to consider the experimentally observable fluctuation dynamics. Using the diffeomorphism symmetry, in the next section, we will identify the Goldstone boson mode and its dynamical equation in the hairy black hole background mentioned above.

### 2.2.1 Stückelberg mechanism: Goldstone boson mode

We have already discussed the extra scalar degree of freedom is contained in the  $r$ -diffeomorphism broken Lagrangian given by Eq. 2.2.2. As emphasized before, in the last section, we have expressed the  $r$ -symmetry broken Lagrangian (Eq. 2.2.1) in unitary gauge. Therefore, the associated Goldstone mode is absorbed inside the gravitational degree of freedom. The well-known Stückelberg mechanism extracts the Goldstone mode described above by unfolding the unitary gauge. By this, one also can restore the  $r$ -symmetry, which the mode will non-linearly realize. To restore the symmetry, one reparametrises the broken symmetry again as:

$$r \rightarrow \tilde{r} = r + \pi(x^\mu), \quad (2.2.6)$$

$$t \rightarrow \tilde{t} = t, \quad x^i \rightarrow \tilde{x}^i = x^i, \quad (2.2.7)$$

which will transform the background scalar field  $\phi_0(r)$  as

$$\phi_0(\tilde{r}) = \phi_0(r) + \phi_0'(r)\pi. \quad (2.2.8)$$

Therefore, by using this trick, we can restore the  $r$ -diffeomorphism symmetry by considering the following combined transformations:

$$r \rightarrow r + \xi^r \quad ; \quad \pi(x) \rightarrow \pi(x) - \xi^r, \quad (2.2.9)$$

and simultaneously extract the dynamical degrees of freedom as  $\pi(x)$  field, identified as the Goldstone boson mode. Using these new coordinates, we separate the Goldstone boson mode considering all transformed quantities:

$$\tilde{g}^{\alpha\beta} = g^{\alpha\beta} + \delta_r^\beta g^{\alpha\nu} \partial_\nu \pi + \delta_r^\alpha g^{\mu\beta} \partial_\mu \pi + \delta_r^\alpha \delta_r^\beta g^{\mu\nu} \partial_\mu \pi \partial_\nu \pi, \quad (2.2.10)$$

$$\tilde{g}_{\mu\nu} = g_{\mu\nu} - g_{r\nu} \partial_\mu \pi - g_{\mu r} \partial_\nu \pi + g_{rr} \partial_\mu \pi \partial_\nu \pi, \quad (2.2.11)$$

$$\tilde{\partial}_r = (-\partial_r \pi + (\partial_r \pi)^2) \partial_r + \partial_r, \quad (2.2.12)$$

$$\tilde{\partial}_i = (-\partial_i \pi + \partial_i(\pi \partial_r \pi)) \partial_r + \partial_i, \quad (2.2.13)$$

$$\delta \tilde{K}_{\tilde{i}\tilde{j}} = -\tilde{K}'_{\tilde{i}\tilde{j}} \pi + \frac{1}{\sqrt{g^{rr}}} \nabla_{\tilde{i}} \partial_{\tilde{j}} \pi. \quad (2.2.14)$$

While calculating the action, in the present chapter, we will consider terms up to quadratic order in the  $\pi$  field. At this level, the tensor mode will not be coupled with the scalar

mode. Therefore, the tensor mode analysis will be done separately. However, the reader can see the reference (22) for details on this issue. Higher-order interaction terms will be considered separately. Specifically, it would be interesting to understand the correction to the quasinormal modes considering the loop effect. Finally, the covariant quadratic Lagrangian for the Goldstone boson turns out to be,

$$\begin{aligned}
\mathcal{L}_{\pi\pi} = & \frac{1}{4}c(r)g^{\mu\nu}\partial_\mu\pi\partial_\nu\pi - \frac{1}{2}\left(\Lambda''(r) - \frac{c''(r)}{4g(r)} + \frac{\alpha'(r)}{4g(r)}g^{\bar{i}\bar{l}}g^{\bar{k}\bar{j}}\partial_r g_{\bar{l}\bar{k}}\partial_r g_{\bar{i}\bar{j}}\right)\pi^2 + \frac{c'(r)}{2g(r)}\pi\partial_r\pi \\
& + \frac{2M_2(r)^4}{g^2(r)}(\partial_r\pi)^2 - \frac{\alpha(r)}{4}g^{\bar{i}\bar{m}}g^{\bar{n}\bar{j}}\partial_r g_{\bar{m}\bar{n}}\left[-\frac{1}{g(r)}\partial_r(g(r)\partial_{\bar{i}}\pi\partial_{\bar{j}}\pi) + \frac{g^{\alpha\beta}}{2}\partial_r g_{\bar{i}\bar{j}}\partial_\alpha\pi\partial_\beta\pi\right. \\
& + g^{\bar{l}\bar{k}}\partial_{\bar{k}}\pi(\partial_{\bar{i}}\pi\partial_r g_{\bar{l}\bar{j}} + \partial_{\bar{j}}\pi\partial_r g_{\bar{i}\bar{l}} - \partial_{\bar{l}}\pi\partial_r g_{\bar{i}\bar{j}})\left. - \frac{\alpha'(r)}{2}g^{\bar{i}\bar{l}}g^{\bar{k}\bar{j}}\partial_r g_{\bar{l}\bar{k}}\pi\nabla_{\bar{i}}\partial_{\bar{j}}\pi\right. \\
& - \frac{1}{2}\bar{M}_2(r)^2g(r)(\bar{\square}\pi)^2 - \frac{1}{2}\bar{M}_3(r)^2g(r)g^{\bar{i}\bar{k}}g^{\bar{l}\bar{j}}[\nabla_{\bar{i}}\partial_{\bar{l}}\pi][\nabla_{\bar{k}}\partial_{\bar{j}}\pi] - \frac{\bar{M}_1(r)^3}{\sqrt{g(r)}}\partial_r\pi(\bar{\square}\pi) \\
& - \frac{1}{2}\left(\bar{M}_2(r)^2\bar{K}^{\bar{n}\bar{i}}\bar{K}^{\bar{l}\bar{j}} + \bar{M}_3(r)^2\bar{K}^{\bar{n}\bar{j}}\bar{K}^{\bar{l}\bar{i}}\right)\pi^2 + \bar{M}_2(r)^2\bar{K}^{\bar{n}\bar{i}}\sqrt{g(r)}\pi\bar{\square}\pi \\
& + \bar{M}_3(r)^2\bar{K}^{\bar{n}\bar{j}}\sqrt{g(r)}\pi\nabla^{\bar{j}}\partial_{\bar{i}}\pi + \bar{M}_1(r)^3\frac{\bar{K}^{\bar{n}\bar{i}}}{g(r)}\pi\pi' - \bar{M}_4(r)^2\frac{\bar{K}^{\bar{i}\bar{j}}\bar{K}^{\bar{n}\bar{j}}}{g(r)}\pi\pi' - 2M_6^2(r)\bar{K}^{\bar{n}\bar{i}}\partial_r\left(\frac{\partial_r\pi}{g(r)}\right)\pi \\
& + \frac{M_{11}(r)}{2}\partial_r g_{\bar{l}\bar{k}}\left(\bar{K}^{\bar{n}\bar{i}}\bar{K}^{\bar{l}\bar{k}}\pi^2 - \bar{K}^{\bar{n}\bar{i}}\sqrt{g(r)}\pi\nabla^{\bar{l}}\partial_{\bar{k}}\pi - \bar{K}^{\bar{l}\bar{k}}\sqrt{g(r)}\pi\bar{\square}\pi\right) \\
& + \frac{M_{12}(r)}{2}\partial_r g_{\bar{i}\bar{l}}\left(\bar{K}^{\bar{n}\bar{l}\bar{k}}\bar{K}^{\bar{n}\bar{i}}\pi^2 - 2\bar{K}^{\bar{n}\bar{l}\bar{k}}\sqrt{g(r)}\pi\nabla^{\bar{i}}\partial_{\bar{k}}\pi\right) \\
& + \frac{\lambda_1(r)}{4}\partial_r g_{\bar{i}\bar{l}}\partial_r g_{\bar{m}\bar{j}}g^{\bar{l}\bar{m}}\left(\bar{K}^{\bar{n}\bar{k}}\bar{K}^{\bar{l}\bar{j}}\pi^2 - \bar{K}^{\bar{n}\bar{k}}\sqrt{g(r)}\pi\nabla^{\bar{i}}\partial_{\bar{j}}\pi - \bar{K}^{\bar{l}\bar{j}}\sqrt{g(r)}\pi\bar{\square}\pi\right) \\
& + \frac{\hat{m}_2^2(r)}{2g^5(r)}g'(r)^2(\partial_r\pi)^2 + \frac{\hat{m}_2^2(r)}{2g^3(r)}(\partial_r^2\pi)^2 - \frac{\hat{m}_2^2(r)}{g^4(r)}g'(r)\partial_r\pi\partial_r^2\pi + \frac{\hat{m}_2^2(r)}{2g^2(r)}g^{\bar{i}\bar{j}}(\partial_r\partial_{\bar{i}}\pi)(\partial_r\partial_{\bar{j}}\pi) \\
& - \bar{M}_4^2(r)g^{\bar{i}\bar{l}}g^{\bar{k}\bar{j}}\partial_r g_{\bar{l}\bar{k}}\partial_r\pi\nabla_{\bar{i}}\partial_{\bar{j}}\pi + \frac{\lambda_1(r)}{4}\partial_r g_{\bar{i}\bar{j}}\partial_r g_{\bar{n}\bar{l}}g^{\bar{j}\bar{n}}g^{\bar{i}\bar{o}}g^{\bar{l}\bar{s}}\bar{\square}\pi\nabla_{\bar{o}}\partial_{\bar{s}}\pi \\
& + 4M_5^2(r)\left[\partial_r\left(\frac{\partial_r\pi}{g(r)}\right)\right]^2 + 2M_6^2(r)\sqrt{g(r)}\partial_r\left(\frac{\partial_r\pi}{g(r)}\right)\bar{\square}\pi - M_7(r)g^{\bar{i}\bar{l}}g^{\bar{k}\bar{j}}\partial_r g_{\bar{l}\bar{k}}\partial_r\left(\frac{\partial_r\pi}{g(r)}\right)\nabla_{\bar{i}}\partial_{\bar{j}}\pi \\
& + \frac{M_{11}(r)}{2}\sqrt{g(r)}\partial_r g_{\bar{i}\bar{j}}g^{\bar{i}\bar{m}}g^{\bar{j}\bar{n}}\bar{\square}\pi\nabla_{\bar{m}}\partial_{\bar{n}}\pi + \frac{M_{12}(r)}{2}\sqrt{g(r)}\partial_r g_{\bar{i}\bar{j}}g^{\bar{i}\bar{n}}g^{\bar{j}\bar{m}}\nabla_{\bar{n}}\partial_{\bar{k}}\pi\nabla_{\bar{m}}\partial_{\bar{l}}\pi \\
& - \left(\frac{\hat{m}_1^2(r)}{g(r)}g^{\bar{i}\bar{j}} + M_{14}(r)(g^{rr})^{3/2}g^{\bar{a}\bar{i}}g^{\bar{b}\bar{j}}\partial_r g_{\bar{a}\bar{b}}\right)\partial_r\pi\left[-\partial_{\bar{l}}\pi\partial_r\Gamma_{\bar{i}\bar{j}}^{\bar{l}} + \partial_{\bar{j}}\pi\partial_r\Gamma_{\bar{i}\bar{l}}^{\bar{l}} - \partial_{\bar{l}}(g^{\bar{l}\bar{k}}\partial_{\bar{i}}\pi\partial_r g_{\bar{k}\bar{j}})\right. \\
& + \partial_{\bar{j}}\left(\frac{g^{\bar{l}\bar{k}}}{2}(\partial_{\bar{i}}\pi\partial_r g_{\bar{k}\bar{l}} + \partial_{\bar{l}}\pi\partial_r g_{\bar{i}\bar{k}})\right) - g^{\bar{m}\bar{k}}(\partial_{\bar{i}}\pi\partial_r g_{\bar{k}\bar{j}})\Gamma_{\bar{l}\bar{m}}^{\bar{l}} - \frac{g^{\bar{l}\bar{k}}}{2}(\partial_{\bar{l}}\pi\partial_r g_{\bar{k}\bar{m}} + \partial_{\bar{m}}\pi\partial_r g_{\bar{l}\bar{k}})\Gamma_{\bar{i}\bar{j}}^{\bar{m}} \\
& \left. + \frac{g^{\bar{m}\bar{k}}}{2}(\partial_{\bar{i}}\pi\partial_r g_{\bar{k}\bar{l}} + \partial_{\bar{l}}\pi\partial_r g_{\bar{i}\bar{k}})\Gamma_{\bar{j}\bar{m}}^{\bar{l}} + \frac{g^{\bar{l}\bar{k}}}{2}(\partial_{\bar{j}}\pi\partial_r g_{\bar{k}\bar{m}} + \partial_{\bar{m}}\pi\partial_r g_{\bar{j}\bar{k}})\Gamma_{\bar{i}\bar{l}}^{\bar{m}}\right] \tag{2.2.15}
\end{aligned}$$

where  $\bar{\square} = g^{\bar{i}\bar{j}} \nabla_{\bar{i}} \partial_{\bar{j}}$  and  $\bar{i}, \bar{j} = 0, 2, 3$ . In the above Lagrangian, there exist higher time derivative terms such as  $(\ddot{\pi}^2, \ddot{\pi}^{\prime 2}, \dot{\pi} \ddot{\pi})$ . In general, those terms may contribute to unwanted ghosts, leading to instability, unless we fine-tune the model parameters in such a way that at the equation of motion level, it cancels all the higher derivative terms. For simplicity of our calculation, in order to remove the ghost, we impose the following straightforward constraints on our effective theory parameters:  $\bar{M}_2(r)^2 = -\bar{M}_3(r)^2$  and  $M_{11}(r) = -M_{12}(r)$ .

In the present work, as mentioned, we will consider simple cases where the background space-time is asymptotically flat and de Sitter with scalar hair from the effective theory perspective. From the action, we can clearly see that the leading order kinetic term for the scalar field fluctuation comes from the background  $c(r)$  function. However, an important observation that will be discussed in detail in the subsequent section is that the  $c(r)$  function becomes zero in the asymptotic region for asymptotically flat/dS/AdS black holes. Therefore, fluctuating Goldstone boson mode seems to become strongly coupled as one goes towards the asymptotic region of the black holes under consideration. This fact may have some interesting connection with the no-hair theorem, which we plan to study in the future. For the case of asymptotically AdS black holes, a hairy solution with the minimally coupled scalar field was first found for a 2+1 dimensional black hole in (23), and in 2004 hairy solution for a 3+1 dimensional black hole was found in (24). In both cases, the well-known Breitenlohner-Freedman (BF) bound (26) is satisfied, guaranteeing that global AdS spacetime is stable under perturbations. While in the case of (25), one needs to introduce local instability, specifically near the horizon, either by introducing electromagnetic coupling or considering the mass of the real scalar field violating the Breitenlohner-Freedman (BF) bound. For our present purpose, we will not be considering those situations. However, we can realize an interesting particular case when the function  $c(r)$  is zero throughout the region of the black hole space-time. Our Lagrangian seems to suggest that we still can have Goldstone boson fluctuations, whose dynamics will be controlled by the set of effective theory parameters  $(M_i, \bar{M}_i, \hat{m}_i)$ . Therefore, pure flat/dS/AdS metric can support the hair having the same symmetry as the black holes with well-behaved fluctuation. However, the cosmological constant will be generated dynamically from the shift symmetry-breaking scalar hair solution for these cases. In the subsequent sections, we will study in detail two exceptional cases.

### 2.2.2 dS, AdS and flat Schwarzschild limit

Our goal for this subsection would be to understand the details of the special cases we mentioned at the end of the previous section. Given the second-order action for the Goldstone mode, it won't be easy to understand the fundamental properties of Goldstone mode. Therefore, we restrict our discussion to particular black hole backgrounds widely studied in the literature. Our major discussion will mainly be focused on asymptotically dS/flat Schwarzschild black holes. However, the AdS case will be briefly discussed for completeness. We consider the following background metric components,

$$f(r) = 1 - \frac{2M}{r} + \epsilon \frac{r^2}{l_c^2}, \quad (2.2.16)$$

$$g(r) = \left(1 - \frac{2M}{r} + \epsilon \frac{r^2}{l_c^2}\right)^{-1}, \quad (2.2.17)$$

$$R(r) = r^2 ; \quad \phi = \phi_0^\epsilon(r), \quad (2.2.18)$$

where  $\epsilon = (-1, 1, 0)$  corresponds to asymptotically AdS, dS, and flat Schwarzschild black holes, respectively. For these metric functions, the background parameters of our effective field theory Eq.A1.1 and Eq.A1.2 turn out to be  $\Lambda(r) = -\epsilon \frac{3}{l_c^2}$ ,  $c(r) = 0$  and  $\alpha(r) = 0$ . Important to notice that the background cosmological constant is induced dynamically from the background scalar field. Therefore, any bare value of the cosmological constant can be absorbed in the scalar field vacuum expectation value, and the effective cosmological constant would be  $\Lambda(r)$ , which is constant.

In this limit, the quadratic action for the scalar fluctuation boils down to the following expression:

$$\begin{aligned} \mathcal{L}_{\pi\pi} = & \frac{2M_2(r)^4}{g^2(r)} (\partial_r \pi)^2 + \frac{1}{2} \bar{M}_3(r)^2 g(r) (\bar{\square} \pi)^2 - \frac{1}{2} \bar{M}_3(r)^2 g(r) g^{\bar{i}\bar{k}} g^{\bar{l}\bar{j}} [\nabla_{\bar{i}} \partial_{\bar{l}} \pi] [\nabla_{\bar{k}} \partial_{\bar{j}} \pi] \\ & - \frac{\bar{M}_1(r)^3}{\sqrt{g(r)}} \partial_r \pi (\bar{\square} \pi) + \frac{\hat{m}_2^2(r)}{2g^5(r)} g'(r)^2 (\partial_r \pi)^2 + \frac{\hat{m}_2^2(r)}{2g^3(r)} (\partial_r^2 \pi)^2 - \frac{\hat{m}_2^2(r)}{g^4(r)} g'(r) \partial_r \pi \partial_r^2 \pi \\ & + \frac{\hat{m}_2^2(r)}{2g^2(r)} g^{\bar{i}\bar{j}} (\partial_r \partial_{\bar{i}} \pi) (\partial_r \partial_{\bar{j}} \pi) - \bar{M}_4^2(r) g^{\bar{i}\bar{l}} g^{\bar{k}\bar{j}} \partial_r g_{\bar{l}\bar{k}} \partial_r \pi \nabla_{\bar{i}} \partial_{\bar{j}} \pi + 4M_5^2(r) \left[ \partial_r \left( \frac{\partial_r \pi}{g(r)} \right) \right]^2 \\ & + 2M_6^2(r) \sqrt{g(r)} \partial_r \left( \frac{\partial_r \pi}{g(r)} \right) \bar{\square} \pi - M_7(r) g^{\bar{i}\bar{l}} g^{\bar{k}\bar{j}} \partial_r g_{\bar{l}\bar{k}} \partial_r \left( \frac{\partial_r \pi}{g(r)} \right) \nabla_{\bar{i}} \partial_{\bar{j}} \pi \\ & - \frac{M_{12}(r)}{2} \sqrt{g(r)} \partial_r g_{\bar{i}\bar{j}} g^{\bar{i}\bar{m}} g^{\bar{j}\bar{n}} \bar{\square} \pi \nabla_{\bar{m}} \partial_{\bar{n}} \pi + \frac{M_{12}(r)}{2} \sqrt{g(r)} \partial_r g_{\bar{i}\bar{j}} g^{\bar{i}\bar{n}} g^{\bar{l}\bar{k}} g^{\bar{j}\bar{m}} \nabla_{\bar{n}} \partial_{\bar{k}} \pi \nabla_{\bar{m}} \partial_{\bar{l}} \pi \\ & - \left( \frac{\hat{m}_1^2(r)}{g(r)} g^{\bar{i}\bar{j}} + \frac{M_{14}(r)}{g^{3/2}(r)} g^{\bar{a}\bar{i}} g^{\bar{b}\bar{j}} \partial_r g_{\bar{a}\bar{b}} \right) \partial_r \pi \left[ -\partial_{\bar{l}} \pi \partial_r \Gamma_{\bar{i}\bar{j}}^{\bar{l}} + \partial_{\bar{j}} \pi \partial_r \Gamma_{\bar{i}\bar{l}}^{\bar{l}} - \partial_{\bar{l}} (g^{\bar{l}\bar{k}} \partial_{\bar{i}} \pi \partial_r g_{\bar{k}\bar{j}}) \right] \end{aligned}$$



$$\begin{aligned}
& +\partial_{\bar{j}}\left(\frac{g^{\bar{l}\bar{k}}}{2}(\partial_{\bar{i}}\pi\partial_r g_{\bar{k}\bar{l}}+\partial_{\bar{l}}\pi\partial_r g_{\bar{i}\bar{k}})\right)-g^{\bar{m}\bar{k}}(\partial_{\bar{i}}\pi\partial_r g_{\bar{k}\bar{j}})\Gamma_{\bar{l}\bar{m}}^{\bar{l}}-\frac{g^{\bar{l}\bar{k}}}{2}(\partial_{\bar{l}}\pi\partial_r g_{\bar{k}\bar{m}}+\partial_{\bar{m}}\pi\partial_r g_{\bar{l}\bar{k}})\Gamma_{\bar{i}\bar{j}}^{\bar{m}} \\
& +\frac{g^{\bar{m}\bar{k}}}{2}(\partial_{\bar{i}}\pi\partial_r g_{\bar{k}\bar{l}}+\partial_{\bar{l}}\pi\partial_r g_{\bar{i}\bar{k}})\Gamma_{\bar{j}\bar{m}}^{\bar{l}}+\frac{g^{\bar{l}\bar{k}}}{2}(\partial_{\bar{j}}\pi\partial_r g_{\bar{k}\bar{m}}+\partial_{\bar{m}}\pi\partial_r g_{\bar{j}\bar{k}})\Gamma_{\bar{i}\bar{l}}^{\bar{m}} \\
& +\frac{\lambda_1(r)}{4}\partial_r g_{\bar{i}\bar{j}}\partial_r g_{\bar{n}\bar{l}}g^{\bar{j}\bar{n}}g^{\bar{i}\bar{o}}g^{\bar{l}\bar{s}}\square\pi\nabla_{\bar{o}}\partial_{\bar{s}}\pi-\frac{\lambda_1(r)}{4}\partial_r g_{\bar{i}\bar{l}}\partial_r g_{\bar{m}\bar{j}}g^{\bar{l}\bar{m}}\left(\bar{K}^{\bar{l}\bar{k}}_{\bar{k}}\sqrt{g(r)}\nabla^{\bar{i}}\partial^{\bar{j}}\pi+\bar{K}^{\bar{n}\bar{j}}_{\bar{j}}\sqrt{g(r)}\square\pi\right)\pi \\
& +\left[\frac{\bar{M}_3(r)^2}{2}\left(\bar{K}^{\bar{n}\bar{i}}_{\bar{i}}\bar{K}^{\bar{l}\bar{j}}_{\bar{j}}-\bar{K}^{\bar{n}\bar{i}}_{\bar{j}}\bar{K}^{\bar{l}\bar{j}}_{\bar{i}}\right)+\frac{M_{12}(r)}{2}\left(\partial_r g_{\bar{i}\bar{l}}\bar{K}^{\bar{l}\bar{k}}_{\bar{k}}\bar{K}^{\bar{n}\bar{i}}_{\bar{i}}-\partial_r g_{\bar{l}\bar{k}}\bar{K}^{\bar{n}\bar{i}}_{\bar{i}}\bar{K}^{\bar{l}\bar{k}}_{\bar{k}}\right)\right. \\
& \left.+\frac{\lambda_1(r)}{4}\partial_r g_{\bar{i}\bar{l}}\partial_r g_{\bar{m}\bar{j}}g^{\bar{l}\bar{m}}\bar{K}^{\bar{l}\bar{k}}_{\bar{k}}\bar{K}^{\bar{n}\bar{j}}_{\bar{j}}\right]\pi^2+\bar{M}_1(r)^3\frac{\bar{K}^{\bar{l}\bar{i}}_{\bar{i}}}{g(r)}\pi\pi'-\bar{M}_3(r)^2\bar{K}^{\bar{n}\bar{i}}_{\bar{i}}\sqrt{g(r)}\pi\square\pi \\
& +\bar{M}_3(r)^2\bar{K}^{\bar{n}\bar{i}}_{\bar{j}}\sqrt{g(r)}\pi\nabla^{\bar{j}}\partial_{\bar{i}}\pi-\bar{M}_4(r)^2\frac{\bar{K}^{\bar{i}\bar{j}}_{\bar{i}\bar{j}}\bar{K}^{\bar{n}\bar{j}}_{\bar{j}}}{g(r)}\pi\pi'-2M_6^2(r)\bar{K}^{\bar{n}\bar{i}}_{\bar{i}}\partial_r\left(\frac{\partial_r\pi}{g(r)}\right)\pi \\
& +\frac{M_{12}(r)}{2}\partial_r g_{\bar{l}\bar{k}}\left(\bar{K}^{\bar{n}\bar{i}}_{\bar{i}}\sqrt{g(r)}\nabla^{\bar{l}}\partial^{\bar{k}}\pi+\bar{K}^{\bar{l}\bar{k}}_{\bar{k}}\sqrt{g(r)}\square\pi\right)\pi-M_{12}(r)\partial_r g_{\bar{i}\bar{l}}\bar{K}^{\bar{l}\bar{k}}_{\bar{k}}\sqrt{g(r)}\pi\nabla^{\bar{i}}\partial_{\bar{k}}\pi.
\end{aligned} \tag{2.2.19}$$

Our plan is to understand the properties of hairs from the effective field theory perspective. So far, the usual approach to figuring out the hairy black hole solutions was from the background effective field theory. In the present approach, we consider the effective theory of fluctuations. Most importantly, our starting point is the existence of background scalar hair which enjoys the same symmetry as that of the black holes. Importantly, this was one of the main criteria of the black hole no-hair theorem. Our study is based on the idea of the effective theory of inflation. In the inflation model, the approximate shift symmetry plays a very important role in constraining the theory parameters, which can be assumed to be time-independent and study the properties of fluctuation. However, for the present case, we do not have special symmetry which can help us to understand the nature of the effective theory parameters  $(M_2(r)^4, \bar{M}_3(r)^2, \bar{M}_1^3(r), \hat{m}_2^2(r), \bar{M}_4^2(r), M_5^2(r), M_6^2(r), M_7(r), M_{12}(r), M_{14}(r), \lambda_1(r), \hat{m}_1^2(r))$ . From our action's structure, we can construct the theory for a background, which we will do in the next section. Our action shows that for three different asymptotic limits, we may have hair with its detectable fluctuating degrees of freedom identified as  $\pi(x)$  field. In order to understand further, let us consider the following decomposition of  $\pi = e^{-i\omega t}S(r)Y_{lm}(\theta, \phi)$ , and the equation of motion for  $S(r)$  turns out to be

$$\begin{aligned}
& 4\frac{d}{dr}\left(M_2(r)^4 f^2(r)r^2\frac{dS(r)}{dr}\right)+\hat{m}_1^2(r)\left[\frac{f'(r)}{f(r)}r^2\omega^2-\left(\frac{f'(r)}{2}+\frac{f(r)}{r}\right)l(l+1)\right]S'(r) \\
& -\frac{d}{dr}\left(\hat{m}_2^2(r)r^2 f(r)\frac{dS(r)}{dr}\right)\omega^2+\frac{d}{dr}\left(\hat{m}_2^2(r)f^2(r)\frac{dS(r)}{dr}\right)l(l+1)
\end{aligned}$$

$$\begin{aligned}
& -\frac{d^2}{dr^2} \left[ r^2 \hat{m}_2^2(r) f^3(r) \frac{d^2 S(r)}{dr^2} + r^2 \hat{m}_2^2(r) f'(r) f^2(r) \frac{dS(r)}{dr} \right] + V_l(r) S(r) \\
& + \frac{d}{dr} \left[ r^2 \hat{m}_2^2(r) f(r) f'(r)^2 \frac{dS(r)}{dr} + r^2 \hat{m}_2^2(r) f'(r) f^2(r) \frac{d^2 S(r)}{dr^2} \right] \\
& + 8 \frac{d}{dr} \left[ r^2 M_5^2(r) f'(r) \frac{d}{dr} (S'(r) f(r)) \right] - 8 \frac{d^2}{dr^2} \left[ r^2 M_5^2(r) f(r) \frac{d}{dr} (S'(r) f(r)) \right] \\
& - 4 M_6^2(r) \frac{f'(r)}{f^{1/2}(r)} l(l+1) S'(r) - 4 \frac{d}{dr} \left[ r^2 \frac{M_6^2(r) \omega^2}{f^{1/2}(r)} \right] S'(r) - 4 \frac{M_6^2(r) r^2 \omega^2}{f^{1/2}(r)} S''(r) \\
& + 4 \frac{d}{dr} \left[ M_6^2(r) f^{1/2}(r) \right] l(l+1) S'(r) + 2 \frac{d}{dr} \left[ M_7(r) \frac{f'(r)}{f(r)} r^2 \omega^2 \right] S'(r) + 2 M_7(r) \frac{f'(r)}{f(r)} r^2 \omega^2 S''(r) \\
& - 4 \frac{d}{dr} \left( M_7(r) \frac{f(r)}{r} \right) l(l+1) S'(r) - \frac{4}{r} M_7(r) f(r) l(l+1) S''(r) - 2 M_6^2(r) \bar{K}^{\bar{n}}_{\bar{i}} r^2 \partial_r \left( S'(r) f(r) \right) \\
& + M_{14}(r) f^{3/2}(r) \left[ \frac{2f'(r)}{f^2(r)} r \omega^2 - \left( \frac{f'(r)}{r f(r)} + \frac{2}{r^2} \right) l(l+1) \right] S'(r) \\
& + \left[ \bar{M}_3(r)^2 \left( \bar{K}^{\bar{n}}_{\bar{i}} \bar{K}^{\bar{i}j}_{\bar{j}} - \bar{K}^{\bar{n}}_{\bar{j}} \bar{K}^{\bar{i}j}_{\bar{i}} \right) + M_{12}(r) \left( \partial_r g_{\bar{i}\bar{l}} \bar{K}^{\bar{l}k} \bar{K}^{\bar{n}}_{\bar{k}} - \partial_r g_{\bar{l}\bar{k}} \bar{K}^{\bar{n}}_{\bar{i}} \bar{K}^{\bar{l}k} \right) \right. \\
& \left. + \frac{\lambda_1(r)}{2} \partial_r g_{\bar{i}\bar{l}} \partial_r g_{\bar{m}\bar{j}} g^{\bar{l}\bar{m}} \bar{K}^{\bar{i}k}_{\bar{k}} \bar{K}^{\bar{n}j}_{\bar{j}} \right] r^2 S(r) - \frac{d}{dr} \left( \bar{M}_1(r)^3 r^2 \bar{K}^{\bar{n}}_{\bar{i}} f(r) + \bar{M}_4(r)^2 r^2 \bar{K}^{\bar{i}j}_{\bar{j}} \bar{K}^{\bar{n}j}_{\bar{j}} f(r) \right) S(r) \\
& = \left[ \bar{M}_3(r)^2 r^2 \frac{\bar{K}^{\bar{n}}_{\bar{i}}}{f^{3/2}(r)} + \frac{\lambda_1(r)}{4} \partial_r g_{\bar{i}\bar{l}} \partial_r g_{\bar{k}\bar{j}} g^{\bar{l}\bar{k}} r^2 \frac{\bar{K}^{\bar{n}j}_{\bar{j}}}{f^{3/2}(r)} + \frac{d}{dr} \left( \frac{\bar{M}_1^3(r) r^2}{\sqrt{f(r)}} \right) + \frac{d}{dr} \left( \hat{m}_1^2(r) r^2 \frac{f'(r)}{f(r)} \right) \right. \\
& \left. + \frac{d}{dr} \left( r^2 M_4^2(r) \frac{f'(r)}{f^2(r)} \right) - 2 \frac{d}{dr} \left( r^2 M_6^2(r) \frac{f'(r)}{f^{3/2}(r)} \right) - \frac{d}{dr} \left( r^2 M_7(r) \frac{f'^2(r)}{f^2(r)} \right) - \frac{d^2}{dr^2} \left( r^2 M_7(r) \frac{f'(r)}{f(r)} \right) \right. \\
& \left. + 2 \frac{d}{dr} \left( r M_{14}(r) \frac{f'(r)}{f^{1/2}(r)} \right) \right] \omega^2 S(r), \tag{2.2.20}
\end{aligned}$$

where  $\omega$  is identified as the frequency of the mode and  $l$  is the multipole number corresponding to the mode.  $V_l(r)$  is called the "effective potential" which takes the following form,

$$\begin{aligned}
V_l(r) = & \left[ \bar{M}_3(r)^2 \frac{\bar{K}^{\bar{n}}_{\bar{i}}}{f^{1/2}(r)} + \frac{\lambda_1(r)}{4} \partial_r g_{\bar{i}\bar{l}} \partial_r g_{\bar{k}\bar{j}} g^{\bar{l}\bar{k}} \frac{\bar{K}^{\bar{n}j}_{\bar{j}}}{f^{1/2}(r)} - \frac{\bar{M}_3(r)^2}{r^2 f(r)} \right. \\
& - \frac{d}{dr} \left( \bar{M}_1^3(r) \sqrt{f(r)} \right) + \frac{d}{dr} \left( \hat{m}_1^2(r) \left( \frac{f'(r)}{2} + \frac{f(r)}{r} \right) \right) + \frac{\lambda_1(r)}{r^4} + \frac{d}{dr} \left( \frac{M_4^2(r)}{r} \right) \\
& - 2 \frac{d}{dr} \left( M_6^2(r) \frac{f'(r)}{f^{1/2}(r)} \right) + 2 \frac{d^2}{dr^2} \left( M_6^2(r) f^{1/2}(r) \right) + 2 \frac{d}{dr} \left( M_7(r) \frac{f'(r)}{r} \right) \\
& \left. - 2 \frac{d^2}{dr^2} \left( M_7(r) \frac{f(r)}{r} \right) + 2 \frac{M_{12}(r)}{r^3 \sqrt{f(r)}} + 2 \frac{d}{dr} \left( M_{14}(r) \frac{f^{3/2}(r)}{r} \left( \frac{f'(r)}{2f(r)} + \frac{1}{r} \right) \right) \right] l(l+1). \tag{2.2.21}
\end{aligned}$$

One can clearly identify an important difference between the above fluctuation equation and

the usual black hole linear perturbation equation for the scalar mode. The above structure of the effective equation seems to suggest that the underlying theory for the black hole scalar hair should be a higher derivative in nature and therefore, in general, may not be stable under small fluctuations. Hence, it would be important to understand the underlying theory for scalar hair from the effective theory perspective. This is what we are going to study in the next section. To this end let us emphasize the fact that for a given set of theory parameters we can in principle solve the above fluctuation equation and compute the quasinormal frequencies. Therefore, as emphasized, we will restrict our study based on some assumptions which transform our complicated equation into a simplified form. These assumptions and restrictions may be able to capture the qualitative nature of the quasi-normal frequencies, which we will discuss subsequently. Considering all parameters to be zero except  $M_2(r)$ ,  $\bar{M}_1(r)$  and  $\bar{M}_3(r)$ , we get a simplified equation as

$$4\frac{d}{dr}\left(M_2(r)^4 f^2(r)r^2\frac{dS(r)}{dr}\right) + V_0(r)S(r) = \left[\bar{M}_3(r)^2\left(r^2\frac{f''(r)}{2f^2(r)} - r^2\frac{f'^2(r)}{4f^3(r)} + r\frac{f'(r)}{f^2(r)} - \frac{2}{f(r)}\right) + \frac{d}{dr}\left(\frac{\bar{M}_1^3(r)r^2}{\sqrt{f(r)}}\right)\right]\omega^2 S(r). \quad (2.2.22)$$

The potential  $V_0(r)$  is

$$V_0(r) = \bar{M}_3(r)^2\left(r\frac{f''(r)f'(r)}{f(r)} - \frac{2f''(r)}{f^{1/2}(r)} - r\frac{f'^3(r)}{2f^2(r)} + \frac{3f'^2(r)}{2f(r)} + \frac{2f(r)}{r^2} - \frac{2f'(r)}{r}\right) - \frac{d}{dr}\left[\bar{M}_1(r)^3\left(r^2\frac{f''(r)f^{1/2}(r)}{2} - r^2\frac{f'^2(r)}{4f^{1/2}(r)} + rf'(r)f^{1/2}(r) - 2f^{3/2}(r)\right)\right] + \left[\bar{M}_3(r)^2\left(\frac{f''(r)}{2f(r)} - \frac{f'^2(r)}{4f^2(r)} + \frac{f'(r)}{rf(r)} - \frac{2}{r^2} - \frac{1}{r^2f(r)}\right) - \frac{d}{dr}\left(\bar{M}_1^3(r)\sqrt{f(r)}\right)\right]l(l+1) \quad (2.2.23)$$

If one introduces the following coordinate transformation,  $dr^* = dr/(2M_2(r)^4 f^2(r)r^2)$ , then above equation transforms into

$$\frac{d^2 S}{dr^{*2}} + (\omega_{eff}^2 - V_{eff})S = 0, \quad (2.2.24)$$

where the effective frequency and the effective potential spectrum are expressed as

$$\omega_{eff}^2 = -r^2 M_2(r)^4 f^2(r) \left[ \bar{M}_3(r)^2 \left( r^2 \frac{f''(r)}{2f^2(r)} - r^2 \frac{f'^2(r)}{4f^3(r)} + r \frac{f'(r)}{f^2(r)} - \frac{2}{f(r)} \right) \right]$$

$$+ \frac{d}{dr} \left( \frac{\bar{M}_1^3(r)r^2}{\sqrt{f(r)}} \right) \Big] \omega^2, \quad (2.2.25)$$

$$V_{eff} = -r^2 M_2(r)^4 f^2(r) V_0(r). \quad (2.2.26)$$

Note the important difference between Eq. 2.2.24 and the usual Regge-Wheeler type black hole perturbation equation. The frequency is effectively position-dependent, and the potential has complicated parameter dependences. Therefore, an important constraint has been arrived at from the above equations, which is  $\bar{M}_1 \neq 0$ . We only need to specify two parameters to understand the dynamics of fluctuations. Considering the usual definition, the effective frequency function should be finite in all the regions of the radial coordinate. By choosing  $\bar{M}_3 = 0$  and selecting the other two parameters appropriately as

$$M_2(r)^4 \sim -\frac{1}{f(r)^2 r^2}, \quad \bar{M}_1(r)^3 \sim \frac{\sqrt{f(r)}}{r}, \quad (2.2.27)$$

which enables us to write  $\omega_{eff}$  and  $V_{eff}$  as

$$\omega_{eff}^2 \sim \omega^2, \quad \text{and} \quad (2.2.28)$$

$$V_{eff} \sim -\frac{d}{dr} \left[ r \frac{f''(r)f(r)}{2} - r \frac{f'^2(r)}{4} + \frac{(f^2(r))'}{2} - 2 \frac{f^2(r)}{r} + \frac{f(r)}{r} l(l+1) \right] \quad (2.2.29)$$

All equations are written up to their dimensional constant. For this parametrization, we also have  $r = r^*$ . One specifically should notice the important difference that the centrifugal term appears as a multiplicative factor in the expression for the effective potential as opposed to the potential for scalar perturbation in the usual black hole background. Some comments are in order for the complicated structure of the effective potential and the choices of parameters. First of all, it is to be noted that the  $\omega_{eff}$  in its most general form is dependent on position. This itself is a problem for solving the equations of perturbations. The particular choice of the parameters helps one write the frequency independent of position, thereby enabling one to use standard methods of finding the quasinormal frequencies. On the other hand, it is also challenging to work with the general form of the equation. Hence, the simplified equation above with the potential (2.2.29) can give us a hint into the behavior of the black hole towards small perturbations. We will, therefore, look at the particular potential given in Eq. 2.2.29, via the WKB approach (27) to gather information about the nature of the quasinormal frequencies.

There are a few reasons for using the WKB approach to find out quasinormal modes. It

is well known that these modes being the late-time responses of the black holes to any linear order perturbations, have already been observed in the gravitational wave signal from the black hole-black hole or black hole-neutron star mergers in recent gravitational wave detections. Therefore, the accuracy of calculation of the quasinormal modes is one of the most important issues among many others, because these modes will give information on black hole parameters as well as they will help in constraining possible gravitational theories via observations. It is to be mentioned here different numerical techniques already are present in the literature to find quasinormal modes up to the desired accuracy. However, as pointed out clearly in (28), although these techniques are mainly based on convergent procedures, the analysis is extremely non-trivial and is different for different spacetimes. One, therefore, needs different separate numerical procedures to study different black hole space-time depending on the nature of the master differential equation. WKB method, on the contrary, provides a unique procedure, which on one hand remains unchanged for various different master equations, and on the other hand, it provides sufficient numerical accuracy too. Because our goal is to look at different toy models in various black hole backgrounds, we found the WKB method to be a universal tool to comment on the stability of space-time. It has been already shown (28; 29) that when one increases the order in the WKB series from three to six, the relative error diminishes drastically by a few times or even by orders. However, in many scenarios, this formula does not allow one to compute quasinormal modes which have  $n \geq l$  with much accuracy. But, in this work, we have particularly omitted the modes with  $n \geq l$  to get some idea about the behavior of the perturbations with sixth order WKB method and keeping our main target as the understanding of hairy black holes in the effective field theory framework.

The sixth-order WKB method developed by Konoplya (29) gives values accurately as one gets by performing numerical integration of the master differential equation. The sixth-order WKB formula for a general black hole potential  $V(r)$  is given by

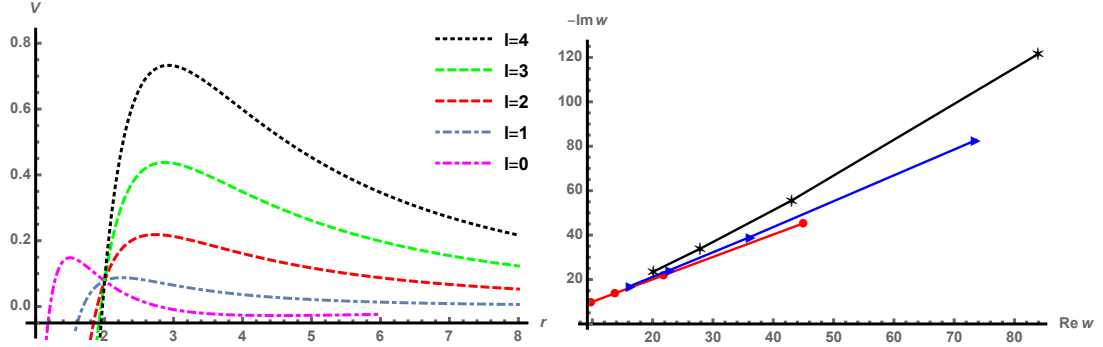


**Figure 2.2.1:** Left one is a plot of the potential vs. radial distance for different  $l$  values with  $n = 0$ .  $l$  increases from 0 to 4 in steps of 1 from bottom to top. Asymptotically flat Schwarzschild geometry is chosen as the metric function in the potential (2.2.29). The right one is a plot of  $\text{Re.}$  vs.  $\text{Im.}$   $\omega$  for different values of  $l$ . The red curve has  $n = 0$ , blue has  $n = 1$  and black has  $n = 2$ , showing a clear difference with the standard behavior of QN frequencies with multipole number and overtone.

$$\frac{i(\omega^2 - V(r_0))}{\sqrt{-2V''(r_0)}} - \Lambda_2 - \Lambda_3 - \Lambda_4 - \Lambda_5 - \Lambda_6 = n + \frac{1}{2}. \quad (2.2.30)$$

Here,  $V(r_0)$  is the peak value of  $V(r)$ ,  $V''(r_0) = \frac{d^2V}{dr_*^2}|_{r=r_0}$ ,  $r_0$  is the value of the radial coordinate corresponding to the maximum of the potential  $V(r)$  and  $n$  is the overtone number.  $\Lambda_i$ 's are the higher order WKB correction terms, whose expressions can be found in (29). Thus, using the potential  $V_{eff}$  given by Eq. 2.2.29 in Eq.2.2.30, we plot (see Fig. 2.2.1 and 2.2.2) the nature of the potential (for arbitrary choices of the parameters), variation of the real and imaginary parts of the quasinormal frequencies with multipole numbers  $l$  and overtone  $n$ . In finding out the quasinormal frequencies, we have used the asymptotically flat Schwarzschild metric as the metric function in the effective potential.

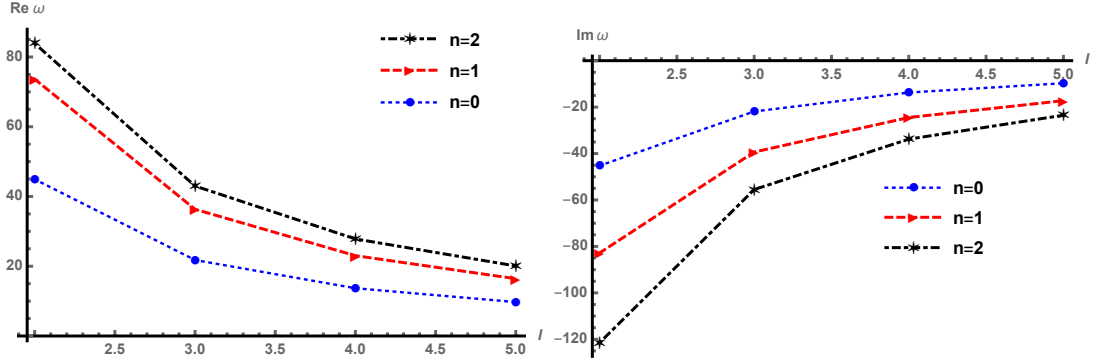


**Figure 2.2.2:** Plot of the real and imaginary parts of  $\omega$  vs multipole number  $l = 2, 3, 4$  and 5 for different  $n$  values. The blue dashed plot corresponds to  $n = 0$ , the red dotted curve corresponds to  $n = 1$ , and the black one corresponds to  $n = 2$ .

Note the fundamental difference in the behavior of the quasinormal frequencies with changing the overtone ( $n$ ) and multipole number ( $l$ ). In general, for the four-dimensional Schwarzschild black hole in an asymptotically flat background, the real oscillation frequency decreases, and the imaginary part of the frequency increases with the increase of the overtone number while the multipole number is kept fixed. However, in our case, both the real oscillation frequency as well as the imaginary part of the frequency increases with the increase of the overtone. We will see in the next sections that this behavior remains for a specific theory that contains all the information discussed above.

From the stability point of view, it is well known that the evolution of the perturbations in a black hole spacetime has three distinct parts: firstly, there is a response to perturbations at very early times, where the form of the signal depends crucially on the initial conditions, secondly, at an intermediate stage, the signal is dominated by quasinormal frequencies, i.e., the exponential decay, also called the ring down phase. The quasinormal modes determine the frequency and damping times. The signal depends only on the black hole parameters in this particular phase. Finally, due to the backscattering of the curvature of space-time, at late times, the propagating wave shows a falloff of the field at the tail phase. This tail phase is completely independent of the initial data, and it persists even if there is no horizon. In this work, we neglect the back reaction and solely focus on the second part of the perturbative response, i.e., the ringing phase.

For the general case, as we will see in the next section, it is tough to identify the effective potential for a particular underlying model.

## 2.3 Underlying theory

Based on our previous analysis, in this section, we will consider a possible underlying model which has a hairy solution with the flat/dS black holes. Our approach here will be the same as the model of ghost condensation (30). However, an important difference lies in the existence of spherically symmetric scalar hair. Therefore, the order parameter for spontaneous breaking of  $r$ -translation symmetry is given by vacuum expectation value of  $\langle \partial_\mu \phi \rangle$ . From this, it is supposed that the system has shift symmetry, implying the absence of non-derivative coupling. We are considering the spherically symmetric black holes with scalar hair, which enjoys the same symmetry as the black hole metric. Hence, we have  $\phi \equiv \phi(r)$ , and therefore,  $\langle \partial_r \phi \rangle \neq 0$ . Given the effective action we derived in the previous section, we consider the following two functions of the basic composite field variable  $X = -1/2(\partial\phi)^2$  as  $P(X) = -\alpha X^2 + \beta X^4$ , and  $F(X) = \tilde{M}_3 g^{\mu\nu} \partial_\mu X \partial_\nu X$ . For our purpose, we call  $P(X)$  as the kinetic potential term and  $F(X)$  as the kinetic gradient term. All the parameters,  $\alpha, \beta$ , are positive dimensionful constant with  $\alpha = \tilde{M}_1^{-4}, \beta = \tilde{M}_2^{-12}$  and  $\tilde{M}_3 \equiv \tilde{M}_3^{-6}$ . All  $\tilde{M}$ 's are of dimension one. The Lagrangian for the above scalar hair will be expressed as

$$\begin{aligned} \mathcal{L}_\phi &= \sqrt{-g} [P(X) + F(X)], \\ &= \sqrt{-g} \left[ -\tilde{M}_1^{-4} X^2 + \tilde{M}_2^{-12} X^4 + \tilde{M}_3^{-6} g^{\mu\nu} \partial_\mu X \partial_\nu X \right]. \end{aligned} \quad (2.3.1)$$

The expression for the action will be

$$\mathcal{S} = \int d^4x \left[ \sqrt{-g} \frac{M_{Pl}^2}{2} \mathcal{R} - \mathcal{L}_\phi + \mathcal{J} \right], \quad (2.3.2)$$

where  $\mathcal{J}$  is the parameter, we will tune to get different values of the cosmological constant. Here, we will not discuss this fine-tuning issue. Our goal for this chapter would be to understand the quasinormal modes of those hairy black holes, where the condensed spherically symmetric scalar hair contributes to the effective cosmological constant, which can add up with the bare cosmological constant parameterized by  $\mathcal{J}$ . The expression for the stress-energy tensor appears to be

$$\begin{aligned} T_{\mu\nu} &= -P(X)g_{\mu\nu} + \mathcal{J}g_{\mu\nu} - 2P'(X)\partial_\mu\phi\partial_\nu\phi - F(X)g_{\mu\nu} \\ &\quad + 2\tilde{M}_3^{-6}\partial_\mu X\partial_\nu X - 4\tilde{M}_3^{-6}g^{\alpha\beta}\partial_\alpha(\partial_\mu\phi\partial_\nu\phi)\partial_\beta X. \end{aligned} \quad (2.3.3)$$



At the minimum of the kinetic potential,  $P(X) = -\tilde{M}_1^{-4}X^2 + \tilde{M}_2^{-12}X^4$ ,

$$X_0 = \pm \sqrt{\frac{\tilde{M}_2^{12}}{2\tilde{M}_1^4}} = \pm \frac{\tilde{M}_2^6}{\sqrt{2}\tilde{M}_1} \equiv \pm c, \quad (2.3.4)$$

the energy-momentum tensor takes the following form,

$$T_{\mu\nu} = -P(X_0)g_{\mu\nu} + \mathcal{J}g_{\mu\nu}. \quad (2.3.5)$$

Therefore, by appropriate choice of the value of  $\mathcal{J}$ , we can have spherically symmetric hairy black holes which are asymptotically dS/AdS/flat. The solution for the scalar field is therefore parametrized by

$$P'(X_0) = 0, \quad F(X_0) = 0, \quad \partial_\mu X_0 = 0, \\ \Rightarrow \phi_0(r) = c^{1/2} \int \frac{dr}{(f(r))^{1/2}}. \quad (2.3.6)$$

At this point, it is worth pointing out that for  $X_0 > 0$  the solution must be of the cosmological type which is precisely the ghost condensation model (30). However, in order to have scalar hair with the same symmetry as that of the black hole, we need to consider  $X_0 < 0$ . Considering the value of  $X_0$ , one arrives at  $P(X_0 = -c) = -\frac{\tilde{M}_2^{12}}{4\tilde{M}_1^8} < 0$  which contributes negative cosmological constant (AdS) in the background. Therefore, by tuning the value of  $\mathcal{J}$ , we can also obtain dS and Schwarzschild solutions. Once we have spherically symmetric hair, the Lagrangian for the Goldstone fluctuation  $\phi = \phi_0(r) + \varphi(x)$  turns out to be

$$\begin{aligned} \mathcal{L}_{\varphi\varphi} = & 4 \left[ 4\tilde{M}_2^{-12}(g^{rr})^4(\partial_r\phi_0)^6 + \tilde{M}_3^{-6}g^{rr}[\partial_r(g^{rr}\partial_r\phi_0)]^2 \right] (\partial_r\varphi)^2 + 4\tilde{M}_3^{-6}g^{rr}(g^{rr}\partial_r\phi_0)^2(\partial_r^2\varphi)^2 \\ & + 8\tilde{M}_3^{-6}(g^{rr})^2\partial_r\phi_0\partial_r(g^{rr}\partial_r\phi_0)\partial_r\varphi\partial_r^2\varphi - 4\tilde{M}_3^{-6}g^{rr}(\partial_r\phi_0)^2(\partial_r\dot{\varphi})^2 \\ & + 4\tilde{M}_3^{-6}g^{ij}(g^{rr}\partial_r\phi_0)^2(\partial_r\partial_i\varphi)(\partial_r\partial_j\varphi) + 16\tilde{M}_2^{-12}X_0^2g^{rr}\partial_r\phi_0(g^{\mu\nu}\partial_\mu\varphi\partial_\nu\varphi)\partial_r\varphi \\ & + 4\tilde{M}_3^{-6}g^{\mu\nu}\partial_\mu(g^{rr}\partial_r\phi_0\partial_r\varphi)\partial_\nu(g^{\alpha\beta}\partial_\alpha\varphi\partial_\beta\varphi) + 32\tilde{M}_2^{-12}X_0^2(g^{rr})^2\partial_r\phi_0(\partial_r\varphi)^3 \end{aligned} \quad (2.3.7)$$

Now, let us mention the connection between the scalar field fluctuation  $\delta\phi = \varphi(x)$  with the previously discussed Goldstone boson mode in the gravity sector. Considering the general coordinate transformation  $r \rightarrow r + \pi$ , the scalar field transforms as  $\phi'(x') = \phi_0(r + \pi) + \varphi(r + \pi) = \phi_0(r) + \varphi(x) + \pi(x)\phi'_0(r) + \mathcal{O}(\pi^2)$ . Hence, to the linear order the scalar field fluctuation  $\varphi$  is identified with the Goldstone mode  $\pi(x)$  as  $\delta\phi(r) \equiv \varphi = -\pi\phi'_0(r)$ .

More importantly, in the spherically symmetric hairy background, the kinetic potential term  $P(X)$  does not contribute to the time variation of the fluctuation. This is the reason we have introduced the kinetic gradient term  $F(X)$ . Therefore,  $X$  can be thought of as an effective composite degree of freedom which is behaving like a Higgs field, and the formation of spherically symmetric hair is essential and is similar to the well-known Higgs mechanism in terms of the composite field  $X$  of dimension four operators. By combining the bare cosmological constant  $\mathcal{J}$  and the vacuum of the scalar field hair, the net effective cosmological constant is expressed as

$$\Lambda = \frac{3}{l_c^2} = \frac{1}{M_p^2} \left( \frac{\tilde{M}_2^{12}}{4\tilde{M}_1^8} + \mathcal{J} \right) = \frac{1}{M_p^2} \left( \frac{X_0^2}{2\tilde{M}_1^4} + \mathcal{J} \right). \quad (2.3.8)$$

The dependence of the cosmological constant on scalar hair is seen in the above equation. The governing equation for the radial component of the scalar field fluctuation  $\varphi(x) = e^{-i\omega t} S(r) Y_{lm}(\theta, \phi)$  will take the form of the following fourth-order differential equation,

$$\begin{aligned} S''''(r) + 4 \left( \frac{f'(r)}{f(r)} + \frac{1}{r} \right) S'''(r) & - \left[ \frac{2\tilde{M}_3^6}{\tilde{M}_1^4 f(r)} - \frac{9f'^2(r)}{4f^2(r)} - \frac{5f''(r)}{2f(r)} - \frac{9f'(r)}{f(r)r} - \frac{2}{r^2} - \frac{\omega^2}{f^2(r)} + \frac{l(l+1)}{f(r)r^2} \right] S''(r) \\ & - \left[ 2 \frac{\tilde{M}_3^6}{\tilde{M}_1^4} \left( \frac{f'(r)}{f^2(r)} + \frac{2}{f(r)r} \right) - \frac{f'(r)f''(r)}{f^2(r)} - \frac{3f'^2(r)}{2f^2(r)r} - \frac{f'''(r)}{2f(r)} \right. \\ & \left. - 2 \frac{f''(r)}{f(r)r} - \frac{f'(r)}{f(r)r^2} - \frac{2\omega^2}{f^2(r)r} + \frac{l(l+1)f'(r)}{f^2(r)r^2} \right] S'(r) = 0. \end{aligned} \quad (2.3.9)$$

In order to get the numerical solution for the quasinormal modes, it is convenient to express the above equation in terms of the dimensionless coordinate  $\tilde{r} = \frac{r}{r_0}$ , theory parameter  $m_0^2 = \frac{\tilde{M}_3^6 r_0^2}{M_1^4}$  and  $W_0^2 = (r_0 \omega)^2$ . So the above equation in the new coordinate is

$$\begin{aligned} \frac{d^4 S(\tilde{r})}{d\tilde{r}^4} + 4 \left( \frac{f'(\tilde{r})}{f(\tilde{r})} + \frac{1}{\tilde{r}} \right) \frac{d^3 S(\tilde{r})}{d\tilde{r}^3} & - \left[ \frac{2m_0^2}{f(\tilde{r})} - \frac{9f'^2(\tilde{r})}{4f^2(\tilde{r})} - \frac{5f''(\tilde{r})}{2f(\tilde{r})} - \frac{9f'(\tilde{r})}{f(\tilde{r})\tilde{r}} - \frac{2}{\tilde{r}^2} - \frac{W_0^2}{f^2(\tilde{r})} + \frac{l(l+1)}{f(\tilde{r})\tilde{r}^2} \right] \frac{d^2 S(\tilde{r})}{d\tilde{r}^2} \\ & - \left[ 2m_0^2 \left( \frac{f'(\tilde{r})}{f^2(\tilde{r})} + \frac{2}{f(\tilde{r})\tilde{r}} \right) - \frac{f'(\tilde{r})f''(\tilde{r})}{f^2(\tilde{r})} - \frac{3f'^2(\tilde{r})}{2f^2(\tilde{r})\tilde{r}} - \frac{f'''(\tilde{r})}{2f(\tilde{r})} \right. \\ & \left. - 2 \frac{f''(\tilde{r})}{f(\tilde{r})\tilde{r}} - \frac{f'(\tilde{r})}{f(\tilde{r})\tilde{r}^2} - \frac{2W_0^2}{f^2(\tilde{r})\tilde{r}} + \frac{l(l+1)f'(\tilde{r})}{f^2(\tilde{r})\tilde{r}^2} \right] \frac{dS(\tilde{r})}{d\tilde{r}} = 0 \end{aligned} \quad (2.3.10)$$

This is the final master equation that we will be analyzing for two different black hole backgrounds. Extra care must be taken as our master equation is the fourth order in the derivative. We have two theory parameters  $(m_0, X_0)$  which are functions of  $(\tilde{M}_1, \tilde{M}_2, \tilde{M}_3)$ .  $X_0$  sets the background value of the cosmological constant and also provides a scalar field profile. Now, in the following two sub-sections, our goal would be to compute the quasinormal modes considering asymptotically flat Schwarzschild and Schwarzschild de Sitter backgrounds. The present value of the cosmological constant of our universe will determine the value of  $X_0$ . For our analysis we consider two sample values of  $m_0^2 = 10^{-1}$  and  $10^{-6}$ .

### 2.3.1 Quasinormal mode analysis in asymptotically dS/flat hairy black holes

In anti-de Sitter space, we already know the existence of spherically symmetric scalar hair (24; 25) for minimally coupled and two derivative scalar fields. However, for an asymptotically dS/flat black hole background, it has been proven to be very difficult to find a hairy solution where hair also enjoys the same symmetry as the black holes. However, if one relaxes these assumptions, the time-dependent scalar hair in the spherically symmetric black holes has already been found (18). However, for a general shift symmetric scalar field theory known as Horndeski theory with an additional non-minimal coupling with Gauss-Bonnet gravity can give rise to spherically symmetric scalar hair as has recently been shown in (31). To the best of our knowledge, we are, for the first time pointing out the existence of scalar hair with the same symmetry as that of the black holes for a minimally coupled but higher derivative scalar field theory introduced earlier.

For simplicity, we also consider the shift symmetric theory, which we found easy to construct, observing the effective theory Lagrangian derived in previous sections. Our goal in this subsection would be to understand the behavior of quasinormal mode frequencies in the aforementioned hairy black hole background for asymptotically flat and dS black holes. AdS black holes will be discussed in a separate publication with their implications to AdS/CFT in detail.

Before going into the discussion of the quasinormal frequencies for black holes in the above-mentioned background, a little bit of discussion on black hole perturbations and corresponding quasinormal modes are in order. A perturbed black hole is generally described by the metric  $g_{\alpha\beta} = g_{\alpha\beta}^0 + \delta g_{\alpha\beta}$ , where  $g_{\alpha\beta}^0$  is the background space-time, i.e., the space-time

of the non-perturbed black hole and  $\delta g_{\alpha\beta}$  denotes the perturbation over the background. In the linear approximation, the perturbations  $\delta g_{\alpha\beta}$  are much smaller than the background, i.e.  $\delta g_{\alpha\beta} \ll g_{\alpha\beta}^0$ . Once we perturb a black hole by some fields or by perturbing the metric itself, the background responds to the perturbations by the emission of gravitational waves, which evolves in time in the following three stages: first, there is a relatively short period of initial outburst of radiation; second, a long period of damped oscillations dominated by the quasinormal modes and lastly, at very late times the quasinormal modes are suppressed by a power law or exponential tails in certain specific space-time geometries (see (37; 38; 39; 40) for a review). For all practical purposes, the second stage, i.e., the quasinormal ringing, is the most important one in the context of gravitational waves because these modes carry unique information about the black hole parameters.

In general, in a spherically symmetric black hole background, the study of perturbations due to linearised fields (with spin 0, 1, or 2) can be reduced to the study of an Schrödinger like second order differential equation. To determine the oscillation modes of a black hole, which corresponds to the solutions of the mentioned differential equation, one has to impose physically motivated boundary conditions at the two boundaries of the problem, viz. at the horizon and spatial infinity. For the spacetimes of our interest, the potential in the Schrödinger-like equation goes to zero at the horizon and at the asymptotic infinity/cosmological horizon. In this limit, solutions to the wave equations are purely ingoing at the horizon and purely outgoing at infinity. This means that at the classical level, nothing should leave the horizon, and nothing should come out from infinity to disturb the system.

Quasinormal modes differ from other problems involving small oscillations in the sense that the black hole system is dissipative. Waves can move either to infinity or into the black hole horizon. Therefore, a normal mode analysis of the system is not possible. However, there exists a discrete infinity of quasinormal modes, which are defined as eigenfunctions of the operators describing the governing equation of the perturbation, which satisfies the above-mentioned boundary conditions. The corresponding eigenfrequencies consist of a real and an imaginary part; the latter is related to the damping time of the mode. Quasinormal frequencies are sorted out generally by their imaginary part and are labeled by an integer  $n$ , which, in the literature, is called the overtone number. The fundamental quasinormal mode corresponding to the overtone number  $n = 0$  is the least damped mode. It usually dominates the ringdown waveform because it has the smallest imaginary part and is the longest-lived mode.

We have already introduced the dimensionless coordinates, and with the help of that, the metric in new coordinate with  $M_0 = \frac{M}{r_0} = \frac{\tilde{l}^2 - \epsilon}{2\tilde{l}^2}$  and  $\tilde{l}^2 = \frac{l_c^2}{r_0^2}$  takes the following form,

$$f(\tilde{r}) = 1 - \frac{2M_0}{\tilde{r}} + \epsilon \frac{\tilde{r}^2}{\tilde{l}^2}. \quad (2.3.11)$$

We will employ the usual numerical methodology to solve the system's quasinormal modes. In the usual quasinormal mode analysis, in most cases, the governing equation is Schrödinger-like wave equation. Therefore, by looking at the effective potential various analytical approximate methods have been developed over the years. However, our equation is in the fourth order for the present case. Therefore, we will solve the problem numerically. In the transformed coordinate, the near horizon limit, namely, in  $\tilde{r} \rightarrow 1$ , the master equation will take the following form,

$$S''''(\tilde{r}) + 4 \frac{S'''(\tilde{r})}{(\tilde{r} - 1)} + \left( \frac{9}{4} + \frac{W_0^2}{f'^2(1)} \right) \frac{S''(\tilde{r})}{(\tilde{r} - 1)^2} - \left( \frac{2m_0^2}{f'(1)} - \frac{f''(1)}{f'(1)} - \frac{3}{2} \pm \frac{l(l+1)}{f'(1)} - \frac{2W_0^2}{f'^2(1)} \right) \frac{S'(\tilde{r})}{(\tilde{r} - 1)^2} = 0. \quad (2.3.12)$$

Assuming the near horizon solution to be  $S(\tilde{r}) = (\tilde{r} - 1)^\nu$  we get,

$$\nu(\nu - 1) \left\{ \nu^2 - \nu - 2 + \left( \frac{9}{4} + \frac{W_0^2}{f'^2(1)} \right) \right\} = 0. \quad (2.3.13)$$

We have four roots which are  $\nu = 0, 1$ , and

$$\nu^\pm = \frac{1}{2} \pm \frac{iW_0}{f'(1)}. \quad (2.3.14)$$

For the asymptotically flat Schwarzschild and Schwarzschild de Sitter black holes, the above two imaginary roots will take the following forms respectively,

$$\nu_{Sch}^\pm = \frac{1}{2} \pm iW_0, \quad (2.3.15)$$

$$\nu_{dS}^\pm = \frac{1}{2} \pm \frac{iW_0 \tilde{l}^2}{\tilde{l}^2 - 1}, \quad (2.3.16)$$

where “+” corresponds to outgoing and “-” corresponds to ingoing mode near the horizon of the black hole. For very large values of  $\tilde{l}^2$  we will have  $\nu_{Sch}^\pm \sim \nu_{dS}^\pm$ . From Eq. 2.3.10, we have only one free parameter in theory, which is  $m_0^2$ . In the following two sub-sections, our goal would be to find out the behavior of the Goldstone mode in the asymptotic region and

the associated quasinormal frequencies.

### 2.3.2 Quasinormal frequencies for asymptotically flat Schwarzschild black hole

This section will deal with numerically finding out the quasinormal frequencies for the asymptotically flat Schwarzschild black holes with scalar hair, as discussed in the previous sections. We employed the method developed by Chandrasekhar and Detweiler (32) for finding the quasinormal frequencies. The procedure is to integrate the equation numerically by using "shooting" from both ends of the radial coordinate. Two asymptotic solutions, one near the horizon with the ingoing mode  $(\tilde{r}-1)^{\nu^-}$  and another one near the asymptotic infinity with the outgoing mode  $(\tilde{r}-1)^{\nu^+}$  are matched at some intermediate point  $\tilde{r}_{int}$ . While doing this matching, we need to ensure that at the matching point, the two aforesaid solutions assume the same numerical value and their derivative, or in other words, the Wronskian of the two solutions must vanish. Given the fixed boundary conditions near the horizon and at the infinity, the above matching condition will follow only for specific discrete but complex frequency values  $W_0$ . This gives us the required quasinormal frequencies. However, while doing this numerical analysis, we need to choose the value of the intermediate point judiciously and the numerical infinity  $\tilde{r}_{inf}$  so that the frequency obtained remains stable. Within the range of  $\tilde{r}_{inf} = (50, 100)$  with a given value of the intermediate point  $\tilde{r}_{int} \sim 7$ , we found stable quasinormal frequencies. One of the main difficulties probably lies in the fact that our equation is a higher derivative in nature, and we can not extract a well-defined potential that generically exists in the usual quasinormal mode analysis. The importance of the effective potential is that its nature along the radial coordinate provides valuable information while doing numerical quasi-normal mode analysis. Hence in addition to the non-applicability of the standard analytic WKB method, which we have used already in the previous section, numerical analysis for the present higher derivative equation also becomes non-trivial. In fact, at both boundaries, the general solution of our differential equation is a mixture of exponentially growing and exponentially decaying modes. One must choose the pure exponentially growing modes to calculate the quasinormal frequencies. Numerically, too large values of the radial coordinate attract contributions from unwanted exponentially suppressed modes, which may become significant after the integration. This gives rise to different frequency values for different infinity choices in the same mode. This problem is generally avoided by choosing small values of numerical infinities but keeping large enough order in the series expansion.

	$l = 1$	$l = 2$	$l = 3$
$n$	$W_{0R} - iW_{0I}$	$W_{0R} - iW_{0I}$	$W_{0R} - iW_{0I}$
1	$0.728 - 0.218i$	$0.965 - 0.242i$	$1.153 - 0.206i$
2	$0.871 - 0.313i$	$1.444 - 0.424i$	$1.721 - 0.337i$
3	$1.302 - 0.416i$	$1.628 - 0.429i$	$2.132 - 0.450i$
4	$1.594 - 0.447i$	$2.038 - 0.451i$	$2.436 - 0.456i$
5	$1.979 - 0.456i$	$2.377 - 0.465i$	$2.800 - 0.470i$
6	$2.336 - 0.469i$	$2.742 - 0.474i$	$3.151 - 0.479i$
7	$2.704 - 0.477i$	$3.102 - 0.483i$	$3.510 - 0.487i$
8	$3.069 - 0.486i$	$3.466 - 0.490i$	$3.871 - 0.494i$
9	$3.437 - 0.492i$	$3.831 - 0.497i$	$4.233 - 0.500i$
10	$3.804 - 0.498i$	$4.196 - 0.503i$	$4.596 - 0.506i$

**Table 2.3.1:** Quasinormal frequencies of Schwarzschild black hole for overtone numbers  $n = 1$  to 10 for  $m_0^2 = 10^{-6}$ . Different multipole numbers ( $l = 1$  to 3) corresponding to the different overtones are shown in the table.

Keeping all these things in mind, in order to proceed, we first figure out the asymptotic behavior of the solution for the Goldstone mode fluctuation  $\pi$  in the  $r \rightarrow \infty$  limit. For asymptotically flat black holes, the master Eq.2.3.10 takes the following asymptotic form as

$$S''''(\tilde{r}) + \frac{4}{\tilde{r}}S'''(\tilde{r}) + (W_0^2 - 2m_0^2)S''(\tilde{r}) + \frac{2}{\tilde{r}}(W_0^2 - 2m_0^2)S'(\tilde{r}) = 0. \quad (2.3.17)$$

The corresponding general solution turns out to be

$$S(\tilde{r}) \sim -\frac{B_1}{\tilde{r}} - B_2 \frac{e^{-i\tilde{r}\sqrt{W_0^2 - 2m_0^2}}}{\tilde{r}(W_0^2 - 2m_0^2)} + B_3 \frac{ie^{i\tilde{r}\sqrt{W_0^2 - 2m_0^2}}}{2\tilde{r}(W_0^2 - 2m_0^2)^{3/2}} + B_4, \quad (2.3.18)$$

where  $B$ 's are the integration constants fixed by the appropriate boundary conditions. The outgoing boundary condition is fixed by the mode corresponding to the coefficient of  $B_3$ , and the condition on the theory parameters should be  $2m_0^2 = \frac{4\tilde{M}_3^6 r_0^2}{c^2} < W_0^2$ . Another important point we want to make at this point is that as the spacetime is asymptotically flat, the bare cosmological constant  $\mathcal{J}$  satisfies

$$\Lambda = \frac{3}{l_c^2} = \frac{1}{M_p^2} \left( \frac{\tilde{M}_2^{12}}{4\tilde{M}_1^8} + \mathcal{J} \right) = 0, \quad (2.3.19)$$

which immediately sets the bare value of the cosmological constant in terms of our theoretical parameters. With this ingredient, we further proceed to solve for the quasinormal modes for a class of asymptotically flat Schwarzschild black holes. In the numerical integration

	$l = 1$	$l = 2$	$l = 3$
$n$	$W_{0R} - iW_{0I}$	$W_{0R} - iW_{0I}$	$W_{0R} - iW_{0I}$
1	$0.770 - 0.208i$	$1.026 - 0.219i$	$1.211 - 0.194i$
2	$0.905 - 0.304i$	$1.466 - 0.442i$	$1.756 - 0.332i$
3	$1.331 - 0.418i$	$1.651 - 0.410i$	$2.147 - 0.451i$
4	$1.613 - 0.437i$	$2.055 - 0.449i$	$2.451 - 0.451i$
5	$1.996 - 0.453i$	$2.391 - 0.461i$	$2.812 - 0.468i$
6	$2.350 - 0.466i$	$2.754 - 0.472i$	$3.162 - 0.477i$
7	$2.716 - 0.475i$	$3.113 - 0.481i$	$3.520 - 0.486i$
8	$3.081 - 0.484i$	$3.476 - 0.489i$	$3.879 - 0.493i$
9	$3.447 - 0.491i$	$3.840 - 0.496i$	$4.241 - 0.499i$
10	$3.813 - 0.497i$	$4.205 - 0.502i$	$4.604 - 0.505i$

**Table 2.3.2:** Quasinormal frequencies of Schwarzschild black hole for a different value of  $m_0^2 = 10^{-1}$ .

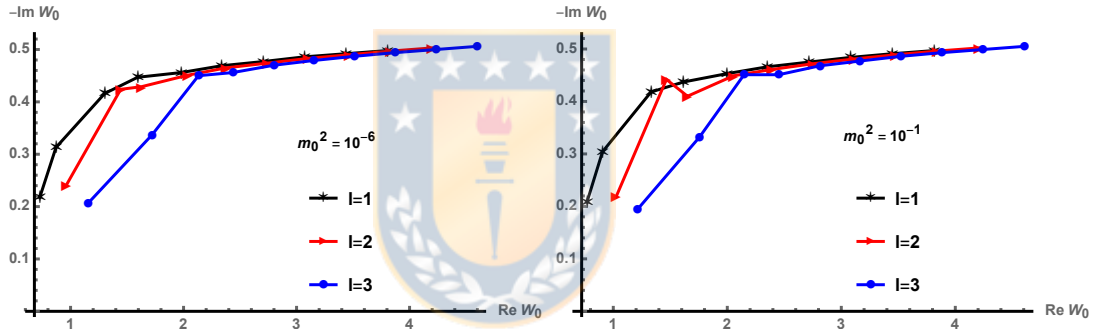


**Figure 2.3.1:** Plot of the real and imaginary parts of  $W_0$  for the Schwarzschild black hole for the first 10 overtones

method described above, we express the solution for  $S(\tilde{r})$  for finite but large  $\tilde{r}$  as an infinite series as

$$S(\tilde{r}) = \frac{e^{i\tilde{r}\sqrt{W_0^2 - 2m_0^2}}}{\tilde{r}} H(\tilde{r}) = e^{i\tilde{r}\sqrt{W_0^2 - 2m_0^2}} \sum_{n=0}^{\infty} \frac{g_n}{\tilde{r}^{n+1}}. \quad (2.3.20)$$

We have obtained the quasinormal frequencies using the numerical integration and by fixing different guess values of the frequency and found stable values corresponding to different overtones. These are tabulated in Tables 2.3.1 and 2.3.2. The nature of these frequencies thus obtained differs significantly from the nature of the pure Schwarzschild quasinormal frequencies. As the overtone number increases, the real oscillation frequency increases rapidly, which is the opposite behavior compared to the Schwarzschild black hole. On the other hand, it is known that the fundamental overtone will have the lowest damping and,



therefore, the longest life. This feature is present here. However, the rate of increase of the imaginary part of the frequency in our case is slow compared to the Schwarzschild black hole. The real vs. imaginary parts of the complex quasinormal frequencies for different  $m_0^2$ , overtones  $n$ , and multipole number  $l$  are plotted in Fig. 5.3.3.

### 2.3.3 Quasinormal frequencies for Schwarzschild de Sitter black holes

We come to the final example of the applicability of our theory and will numerically find out the quasinormal frequencies for Schwarzschild de Sitter black holes. Similar to the discussion stated in detail for the asymptotically flat black holes, the asymptotic master Eq.2.3.10 in  $r \rightarrow \infty$  for the present case takes the following form,

$$S''''(\tilde{r}) + \frac{12}{\tilde{r}} S'''(\tilde{r}) + \left(34 - \frac{2m_0^2 l^2}{\epsilon}\right) \frac{S''(\tilde{r})}{\tilde{r}^2} + \left(2 - \frac{m_0^2 l^2}{\epsilon}\right) \frac{8}{\tilde{r}^3} S'(\tilde{r}) = 0. \quad (2.3.21)$$

Taking the asymptotic solution to be of the form,  $S(\tilde{r}) = \tilde{r}^{-p}$ , the solution of the above equation for  $\epsilon = -1$  (dS black hole), one finds  $p = 0, 3$  and following conjugates

$$p_+ = \frac{1}{2} \left( 3 + \sqrt{9 - 8m_0^2 \tilde{l}^2} \right),$$

$$p_- = \frac{1}{2} \left( 3 - \sqrt{9 - 8m_0^2 \tilde{l}^2} \right).$$

The outgoing boundary condition sets an important constraint on our theoretical parameter, which is given by  $9 < 8m_0^2 \tilde{l}^2$ . Similar to the Schwarzschild case discussed before, we consider the following ansatz for the solution at the asymptotic infinity, taking into account outgoing mode ( $\tilde{r}^{-p_-} \equiv e^{-p_- \ln \tilde{r}}$ ), as

$$S_{dS}(\tilde{r}) = e^{-p_- \ln \tilde{r}} \sum_{n=0}^{\infty} \frac{g_n}{\tilde{r}^n} \equiv e^{-p_- \ln \tilde{r}} H_{dS}(r) \quad (2.3.22)$$

Applying the same numerical method, we again solve for the  $H_{dS}$  function. However, in order to solve numerically, we have taken into account the following constraints. The condition of outgoing mode at the horizon gives us a lower bound on  $m_0$  as

$$\frac{9}{8\tilde{l}^2} < m_0^2 = \frac{6\tilde{M}_3^6}{X_0^2 \tilde{l}^2} M_{Pl}^2 \quad (2.3.23)$$

The above equation exhibits the dependence of our model parameter  $m_0$  on the scalar hair parametrised by  $X_0$ . Now, since our present study considers the Schwarzschild de Sitter

	$l = 1$	$l = 2$	$l = 3$
$n$	$W_{0R} - iW_{0I}$	$W_{0R} - iW_{0I}$	$W_{0R} - iW_{0I}$
1	$0.743 - 0.261i$	$0.950 - 0.217i$	$1.151 - 0.203i$
2		$1.453 - 0.420i$	$1.653 - 0.334i$

**Table 2.3.3:** Quasinormal frequencies of Schwarzschild-dS black hole for  $m_0^2 = 10^{-6}$  and  $\tilde{l}^2 = 10^8$

black hole, assuming  $\mathcal{J} = 0$ , the value of the de Sitter cosmological constant can be set by the non-zero scalar hair  $X_0$ . Therefore, combining the above condition Eq. 2.3.23 with the value of the cosmological constant Eq. 2.3.8, we can find the following constraint on our model parameter space as,

$$\frac{3M_{Pl}^2 \tilde{M}_2^{12}}{32\tilde{M}_1^4} < \tilde{M}_3^6 \quad (2.3.24)$$

Our goal is to establish a possible connection with the observations and to extract the possible allowed range of values of the model parameters ( $\tilde{M}_1, \tilde{M}_2$  and  $\tilde{M}_3$ ). Therefore, we assume our present modified gravity model with the higher derivative scalar field Eq. 2.3.2 as a phenomenological model for our Milky way black hole with the present value of the cosmological constant of our universe. Therefore, we identify our theoretical value of the cosmological constant  $\Lambda_{th} = \tilde{M}_2^{12}/(4\tilde{M}_1^8 M_p^2)$  to that of the observed value  $\Lambda_{th} = \Lambda_{obs} \sim 10^{-47} GeV^2 \sim 10^{-123} M_{Pl}^2$ , and also take the size of the supermassive black hole at the center of the Milky Way galaxy to be  $r_0 \approx 1.17 \times 10^{10} m$ . With those values, one can arrive at the following constraint on our theory parameters,

$$1.6 \times 10^{-53} r_0^2 m^{-2} < m_0^2 \Rightarrow 9.45 \times 10^{-85} GeV^2 < \frac{\tilde{M}_3^6}{\tilde{M}_1^4} \quad (2.3.25)$$

$$\Rightarrow 0.1875 c^2 < \tilde{M}_3^6 M_{Pl}^2 \quad (2.3.26)$$

$$\Rightarrow 0.375 < \frac{\tilde{M}_3^6}{\tilde{M}_1^4 \Lambda}. \quad (2.3.27)$$

For the above constraint equation, we consider  $m_0 = 10^{-6}$ . As an example, choosing the following set of numerical values of the parameters  $\tilde{M}_1 \sim 10^{-7/4} GeV$  and  $\tilde{M}_2 \sim 10^{-5} GeV$  we get the condition

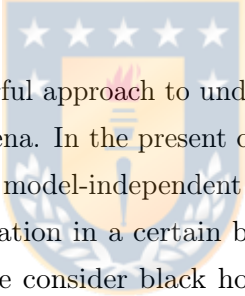
$$m_0^2 = 4 \frac{\tilde{M}_3^6 \tilde{M}_1^4 \Lambda}{\tilde{M}_2^{12}} M_{Pl}^2 r_0^2 \sim 4 \times 10^6 (M_{Pl}^2 \tilde{M}_3^6 GeV^{-6} r_0^2) \quad (2.3.28)$$

	$l = 1$	$l = 2$	$l = 3$
$n$	$W_{0R} - iW_{0I}$	$W_{0R} - iW_{0I}$	$W_{0R} - iW_{0I}$
1	$0.818 - 0.243i$	$1.014 - 0.204i$	$1.208 - 0.192i$
2		$1.495 - 0.417i$	$1.690 - 0.333i$

**Table 2.3.4:** Quasinormal frequencies of Schwarzschild-dS black hole for  $m_0^2 = 0.1$  and  $\tilde{l}^2 = 10^8$

which leads to  $m_0^2 \sim 10^{-6}$  in unit of  $r_0$  choosing  $\tilde{M}_3 = 10^{-2} GeV$ . Our numerical results for the quasinormal modes are given in the table 2.3.3, 2.3.4 for two sets of  $m_0^2$ . Our numerical analysis was unstable enough for this case to give the quasinormal modes for higher overtones. However, the qualitative behavior of the modes remains the same as that of the Schwarzschild black hole case discussed earlier.

## 2.4 Conclusion



Effective field theory is a powerful approach to understanding the low-energy behavior for a wide range of physical phenomena. In the present chapter, we applied this approach toward understanding black holes in a model-independent manner. In order to probe any physical system, the behavior of fluctuation in a certain background under consideration is most important. In this chapter, we consider black hole space-time with hair as a particular type of background whose properties can only be understood by looking at the nature of fluctuation around it. The conventional effective field theory approach deals with writing down the theory of background itself in terms of fundamental fields. In the present context, the approach was to consider the prior existence of a background of interest and then write down the most general theory for the fluctuations in the given background based on symmetry. This is the approach that has been successfully applied in inflationary cosmology, which is popularly known as an effective theory of inflation. In this chapter, we apply the same technique in the background of spherically symmetric black holes with hair which also enjoys the same symmetry. As mentioned earlier, our current investigation is motivated by the following question: *does the effective theory of black holes provide any information about the possible existence of hair?*

We have first written down the most general model-independent effective Lagrangian for the fluctuation in a given hairy black hole background. We have considered an asymptotically flat and de-Sitter black hole background for our detailed analysis. The background cosmological constant is assumed to be generated from the hair. Generally, the behavior of fluctuation

encodes essential information about background hair. Therefore, in order to understand the behavior of the fluctuation, we have chosen a particular set of effective theory parameters. By using the sixth-order WKB approximation associated with those fluctuations, we have computed the quasinormal modes, which appeared to carry different features when compared with that of usual black hole quasinormal modes. In general, for the four-dimensional Schwarzschild black hole in the asymptotically flat/dS background, the real oscillation frequency of the quasinormal modes decreases, and the imaginary part of the frequency increases with the increase of the overtone number ( $n$ ) while the multipole number ( $l$ ) is kept fixed. Interestingly what came out from our quasinormal mode analysis for the effective field theory fluctuation is that both the real and imaginary frequencies increase with increasing overtone number. Motivated by our effective field theory analysis, we also constructed a class of higher derivative scalar field theory. This theory also confirmed the aforementioned exciting behavior of the quasinormal modes.



## Chapter 3

# Gauged Q-Balls in the gauged Skyrme model



### Abstract

We analyze and discuss Q-balls and U(1) gauged Q-balls in the gauged Skyrme model. We find the constraints analytically on the frequency appearing in the Skyrme ansatz, which ensures the existence of such non-topological solitons. Asymptotically, this condensate of pions has an overall charge less than  $\pi/4$  in units of electronic charge,  $e$ . We also analyze how the minimal coupling with Maxwell changes constraints.

### 3.1 Introduction

There is no doubt that many of the most important problems in high energy physics and, especially, QCD are closely related to topologically non-trivial solutions (see (41; 42; 43; 45; 46; 57; 58)). Indeed, non-Abelian gauge theories are dominated by the non-perturbative effects as soon as the energy scale is not extremely large.

On the other hand, there is an essential class of classical solutions (which are denoted as “*non-topological solitons*”) which are extremely relevant both at the theoretical and phenomenological level (see (59; 60; 61; 62; 63; 64; 65; 66; 69) and references therein). The non-topological solitons analyzed in the present chapter are called (gauged) Q-balls. Such configurations are relevant both in astrophysics (due to the relations with bosons stars: see (70; 71)) and in particle physics (due to their tremendous cosmological implications (72; 73; 74; 75)). One of the leading open problems (which will be discussed in this chapter) is finding the necessary conditions for Q-balls and gauged Q-balls to exist in realistic situations. As the above references clearly show, unlike what happens with topological solitons, the existence of (gauged) Q-balls is closely related to the form of the effective interaction potential for the  $U(1)$  charge scalar field. Thus, one of the main goals of the present chapter is to derive an effective potential for the  $U(1)$  charged scalar field (which will be introduced in a moment) directly from the low energy limit of QCD, avoiding this way any arbitrariness in the choice of the potential.

At leading order in the large  $N_c$  't Hooft expansion, the Skyrme model is the low energy limit of QCD (77; 78; 79; 81; 82; 80). This model is a non-linear scalar field theory for an  $SU(N)$ -valued scalar field  $U$ ,  $N$  being the flavor number (we will consider the  $SU(2)$  case in the present chapter). The Skyrme model possesses a conserved topological charge interpreted as a Baryonic charge. Thus, configurations with vanishing Baryonic charges are interpreted as Pionic configurations, while configurations with non-vanishing topological charges contain Baryons. Hence, we will only consider configurations with vanishing topological charges in the present work. As we will see, one of the advantages of the Skyrme model is that the effective potential appearing in the “Q-ball equations” is uniquely determined by the geometry of the action (so that any arbitrariness in the choice of the potential disappears). On the other hand, the Skyrme model, until very recently, has always been considered a tough nut to crack from the analytic point of view (since, for instance, the BPS bound in terms of the Baryonic charge cannot be saturated; consequently, it is challenging to find analytic solutions with the usual methods adopted in the theory of BPS solitons). Even

more challenging is the gauged Skyrme model in which the minimal coupling with the Maxwell field is considered. In (68; 67), Q-balls were found in the baby Skyrme model with a V-shaped potential.

However, a systematic method to construct a generalized hedgehog ansatz which is neither static nor necessarily spherically symmetric but keeps all the other nice properties of the usual hedgehog ansatz alive have been developed in (83; 84; 85; 86; 87; 88; 90) for the Skyrme model, and such strategy has been proven useful also in the Einstein-Yang-Mills case in (106; 107; 108; 109; 110). Working in this ansatz, we can bring the Skyrme equation of motion in the form analogous to the equations in the complex scalar theories only after using a non-trivial change of variables applicable only for the non-gauged Skyrme model. Ansatz for the Maxwell field will consist of only electric potential. Under these ansatzes, the Skyrme and the gauge field variables depend only on the radial coordinate, simplifying the system enough to be analyzed while retaining many elegant features.

Our analysis highlights that ungauged Skyrme action and the equation of motion in the hedgehog ansatz have all the qualities supporting a Q-ball solution as specified by Coleman (66). Specifically, the qualities of the effective potential are qualified to host a Q-ball solution. Whenever a theory has an effective potential to host a Q-ball solution, it can be extended to a gauged Q-ball solution. Although, we were not yet able to find a numerical solution for a gauged Q-ball due to the sensitivity induced by the trigonometric functions in the equations. From our general understanding, we know they exist! We get the standard vital relation of energy per unit charge,  $\frac{E}{Q} = \omega$ , where  $\omega$  is the angular frequency of the Skyrme field in the internal space. Asymptotically, the overall physical charge  $Q_{gauged}^{phys}$  of the gauged Q-ball tends to be less than  $\pi/4$  in units of electronic charge,  $e$ . That is what we would expect for an astrophysical object.

The roadmap in this chapter is as follows; in section 2, we will introduce the gauged Skyrme model and its field equations. In section 3, we will review ungauged and gauged Q-balls of the complex scalar theories. In section 4, we will use the generalized hedgehog ansatz and analyze field equations. Sections 5 and 6 are dedicated to ungauged and gauged Q-balls, respectively. In section 7, we check the stability against small perturbations. In section 8, we discuss numerical analysis. In section 9, we look at the phenomenological implications for detecting gauged Q-balls and discuss why we have not yet detected any signatures. We end with a section about conclusions.

## 3.2 The gauged Skyrme model

The action of the  $U(1)$  gauged Skyrme model in four dimensions, which corresponds to the low energy limit of QCD at leading order in the 't Hooft expansion reads

$$I = \int \frac{d^4v}{4} \left[ K \text{Tr} \left( L^\mu L_\mu + \frac{\lambda}{8} G_{\mu\nu} G^{\mu\nu} \right) + 4K m^2 \text{Tr} (U + U^{-1} - 2\mathbb{1}) - F_{\mu\nu} F^{\mu\nu} \right], \quad (3.2.1)$$

$$L_\mu = U^{-1} D_\mu U, \quad G_{\mu\nu} = [L_\mu, L_\nu], \quad D_\mu = \nabla_\mu + A_\mu [t_3, \cdot], \quad d^4v = d^4x \sqrt{-g}, \quad (3.2.2)$$

$$U \in SU(2), \quad L_\mu = L_\mu^j t_j, \quad t_j = i\sigma_j, \quad F_{\mu\nu} = \partial_\mu A_\nu - \partial_\nu A_\mu, \quad (3.2.3)$$

where  $K$  and  $\lambda$  are the positive Skyrme couplings,  $d^4v$  is the four-dimensional volume element,  $g$  is the metric determinant,  $m$  is the Pions mass,  $A_\mu$  is the gauge potential,  $\nabla_\mu$  is the partial derivative, and  $\sigma_i$ 's are the Pauli matrices. The experimental values of the Skyrme couplings and Pion masses are

$$K \sim (93 \text{ MeV})^2 \quad \text{and} \quad \lambda \sim \frac{1}{29.7 K} \quad (3.2.4)$$

$$m_{\pi^\pm} \sim 140 \text{ MeV} \quad \text{and} \quad m_{\pi^0} \sim 135 \text{ MeV} \quad (3.2.5)$$

It is worth emphasizing that even when the field equations have to be solved numerically, a suitable ansatz can be extremely helpful, especially if one can reduce the three non-linear  $SU(2)$  coupled field equations for the gauged Skyrme model together with the four Maxwell equations (with the  $U(1)$  current arising from the Skyrme model) to just two coupled ODEs. In this way, the numerical task of analyzing the electromagnetic properties of the gauged Q-balls (to be discussed in the following sections) is vastly simplified.

### 3.2.1 Field equations

The field equations of the model are obtained by varying the action in Eq. (3.2.1) w.r.t. the  $U$  field and the Maxwell potential  $A_\mu$ . To perform this derivation it is useful to keep in mind the following relations

$$\begin{aligned} \delta_U L_\mu &= [L_\mu, U^{-1} \delta U] + D_\mu (U^{-1} \delta U), \\ \delta_U G_{\mu\nu} &= D_\nu [L_\mu, U^{-1} \delta U] - D_\mu [L_\nu, U^{-1} \delta U], \end{aligned}$$



where  $\delta_U$  denotes derivative w.r.t the  $U$  field, and

$$\begin{aligned}\frac{\delta}{\delta A^\mu} \left( \text{Tr}(L_\nu L^\nu) \right) &= 2\text{Tr}(\hat{O} L_\mu) , \\ \frac{\delta}{\delta A^\mu} \left( \text{Tr}(G_{\alpha\beta} G^{\alpha\beta}) \right) &= 4\text{Tr} \left( \hat{O} [L^\nu, G_{\mu\nu}] \right) .\end{aligned}$$

Here we have used

$$\frac{\delta G_{\beta}^{\alpha}}{\delta A^\mu} = \delta_{\mu\beta} [\hat{O}, L^\alpha] + \delta_\mu^\alpha [L_\beta, \hat{O}] ,$$

and we have defined

$$\frac{\delta L_\nu}{\delta A^\mu} = \delta_{\mu\nu} \hat{O} , \quad \hat{O} = U^{-1} [t_3, U] .$$

From the above, the field equations of the generalized gauged Skyrme model turns out to be

$$\begin{aligned}0 &= \frac{1}{\sqrt{-g}} \frac{K}{2} D^\mu \left[ \sqrt{-g} \left( L_\mu + \frac{\lambda}{4} D^\mu [L^\nu, G_{\mu\nu}] \right) \right] - 2Km^2 (U - U^{-1}) , \\ J^\nu &= \frac{1}{\sqrt{-g}} \nabla_\mu (\sqrt{-g} F^{\mu\nu}) ,\end{aligned}\tag{3.2.6}$$

where the current  $J_\mu$  is given by

$$J_\mu = \frac{K}{2} \text{Tr} \left[ \hat{O} \left( L_\mu + \frac{\lambda}{4} [L^\nu, G_{\mu\nu}] \right) \right] .\tag{3.2.7}$$

### 3.2.2 Energy-momentum tensor and topological charge

Using the standard definition

$$T_{\mu\nu} = -2 \frac{\partial \mathcal{L}}{\partial g^{\mu\nu}} + g_{\mu\nu} \mathcal{L} ,\tag{3.2.8}$$

we can compute the energy-momentum tensor of the theory under consideration

$$T_{\mu\nu} = T_{\mu\nu}^{\text{Sk}} + T_{\mu\nu}^{\text{mass}} + T_{\mu\nu}^{\text{U}(1)} ,\tag{3.2.9}$$

with  $T_{\mu\nu}^{\text{U}(1)}$  the energy-momentum tensor of the Maxwell field

$$T_{\mu\nu}^{\text{U}(1)} = F_{\mu\alpha} F_\nu^\alpha - \frac{1}{4} g_{\mu\nu} F_{\alpha\beta} F^{\alpha\beta} .$$

According to Eq. (3.2.8), a direct computation reveals that

$$\begin{aligned} T_{\mu\nu}^{\text{mass}} &= K m^2 g_{\mu\nu} \text{Tr}(U + U^{-1} - 2\mathbb{I}) , \\ T_{\mu\nu}^{\text{Sk}} &= -\frac{K}{2} \text{Tr} \left( L_\mu L_\nu - \frac{1}{2} g_{\mu\nu} L_\alpha L^\alpha + \frac{\lambda}{4} (g^{\alpha\beta} G_{\mu\alpha} G_{\nu\beta} - \frac{1}{4} g_{\mu\nu} G_{\alpha\beta} G^{\alpha\beta}) \right) , \end{aligned}$$

The topological charge of the gauged Skyrme model is given by:

$$B = \frac{1}{24\pi^2} \int_{\Sigma} \rho_B , \quad (3.2.10)$$

$$\rho_B = \epsilon^{ijk} \text{Tr} \left[ (U^{-1} \partial_i U) (U^{-1} \partial_j U) (U^{-1} \partial_k U) - \partial_i [3A_j t_3 (U^{-1} \partial_k U + (\partial_k U) U^{-1})] \right] . \quad (3.2.11)$$

Note that the second term in Eq. (3.2.10), the Callan-Witten term, guarantees both the conservation and the gauge invariance of the topological charge. When  $\Sigma$  is space-like,  $B$  is the Baryon charge of the configuration. However, in the following, we will consider configurations where the topological charge vanishes.

### 3.3 Review of Q-balls

This section will take a quick look at the fundamentals of Q-balls of complex scalar theories.

#### 3.3.1 Q-balls of complex scalar field

The simplest yet elegant version of Q-balls was given by Coleman (66). He demonstrated the existence of Q-ball configurations in the U(1) invariant theory of a single complex scalar field with non-derivative interactions.

$$L_{cs} = -\partial_\mu \phi \partial^\mu \phi^* - U(|\phi|^2) \quad (3.3.1)$$

with the U(1) invariant ansatz,  $\phi(t, r) = e^{i\omega t} f(r)$  and asymptotically  $f \rightarrow 0$ . The field equation and the mass of the free field are

$$\Delta f - \frac{dU(f)}{df} = 0 \quad (3.3.2)$$

$$m = \left. \frac{d^2 U}{df^2} \right|_{f=0} \quad (3.3.3)$$

where,  $\Delta$  is the Laplacian. The conserved charge is

$$Q = -i \int d^3x (\partial_0 \phi \phi^* - \phi \partial_0 \phi^*) \quad (3.3.4)$$

Q-ball is the absolute minima of energy for a fixed charge, and the charge is the number of particles. That is, this configuration of Q number of particles has lower energy than the energy of the Q free particles. The energy per unit charge is

$$\frac{E}{Q} = \omega < m \quad (3.3.5)$$

where  $m$  is the mass of the complex scalar field. Q-balls cease to exist for  $\omega > m$ .

### 3.3.2 Gagged Q-balls of complex scalar field

Gauged Q-balls are built upon the background theory of the complex scalar field. They exist in the same potential as that of the ungauged case. The single complex scalar field's gauged Q-balls were first studied in (121). The complex scalar field is coupled to the gauge field  $A_\mu$ . The fields are defined as

$$\phi(t, r) = f(r)e^{i\omega t} \quad \text{and} \quad g(r) = \omega - eA_0(r) \quad (3.3.6)$$

whose Lagrangian is

$$L_{gcs} = 4\pi \int dr r^2 \left[ \frac{1}{2}(f')^2 + \frac{1}{2e^2}(g')^2 + \frac{1}{2}f^2 g^2 - U(f) \right] \quad (3.3.7)$$

variation with  $f$  and  $g$  gives,

$$\Delta f + fg^2 - \frac{dU(f)}{df} = 0 \quad (3.3.8)$$

$$\Delta g - e^2 f^2 g = 0 \quad (3.3.9)$$

and the corresponding asymptotic ( $r \rightarrow \infty$ ) boundary conditions are

$$f \rightarrow 0 \quad \text{and} \quad g \rightarrow \omega \quad (A_0 \rightarrow 0) \quad (3.3.10)$$

with these conditions, numerical solutions for gauged Q-balls were found in (121). Asymptotically they also have  $U(f) \sim m^2 f^2/2$  and a linear eom

$$\Delta f + f(\omega^2 - m^2) = 0 \quad (3.3.11)$$

$$\implies f \sim \frac{1}{r} e^{-r\sqrt{m^2 - \omega^2}} \quad (3.3.12)$$

### 3.4 The ansatz and the corresponding field equations

Here we will generalize the ansatz introduced in (83) to the case of the ungauged Skyrme model. We will consider the flat metric in spherical coordinates:

$$ds^2 = -dt^2 + dr^2 + r^2 (d\theta^2 + \sin^2 \theta d\varphi^2)$$

As far as the  $SU(2)$ -valued configuration  $U$  is concerned we use the standard parameterization

$$U^{\pm 1}(x^\mu) = \cos(\alpha) \mathbf{1}_2 \pm \sin(\alpha) n^i t_i, \quad n^i n_i = 1, \quad (3.4.1)$$

$$n^1 = \sin \Theta \cos \Phi, \quad n^2 = \sin \Theta \sin \Phi, \quad n^3 = \cos \Theta. \quad (3.4.2)$$

The problem is finding a suitable ansatz that respects the above condition and simplifies the field equations as much as possible. A close look at Eq. (3.2.6) reveals that a good set of conditions is

$$\alpha = \alpha(r), \quad \Theta = \pi/2, \quad \Phi = \omega t. \quad (3.4.3)$$

As far as the  $U(1)$  gauge potential is concerned, the corresponding ansatz is

$$A_\mu dx^\mu = u(r) dt. \quad (3.4.4)$$

and let,

$$g(r) = \omega - 2u(r) \quad (3.4.5)$$

Plugging this ansatz in the eom 3.2.6 leads to

$$\begin{aligned} & (1 - \lambda g(r)^2 \sin^2 \alpha) \Delta \alpha(r) - 2\lambda g(r) g'(r) \alpha'(r) \sin^2 \alpha \\ & + \frac{1}{2} g(r)^2 \sin 2\alpha (1 - \lambda (\alpha'(r))^2) - 4m^2 \sin \alpha = 0, \end{aligned}$$

$$\Delta g(r) - 4Kg(r) \sin^2 \alpha (1 + \lambda(\alpha'(r))^2) = 0 \quad (3.4.6)$$

We will solve these equations to get Q-ball solutions, and we have checked that the following effective Lagrangian leads to 3.6.1!

$$L = 2\pi K \int dr r^2 \left[ g(r)^2 \sin^2 \alpha - (1 - \lambda g(r)^2 \sin^2 \alpha) (\alpha'(r))^2 + 8m^2 (\cos \alpha - 1) + \frac{1}{4K} (g'(r))^2 \right] \quad (3.4.7)$$

The total energy functionals in this ansatz are<sup>1</sup>

$$E_{gauged} = 4\pi K \int dr r^2 \left[ g^2 \sin^2 \alpha (1 + \lambda (\alpha')^2) + (\alpha')^2 - 8m^2 (\cos \alpha - 1) + \frac{1}{4K} (g')^2 \right] \quad (3.4.8)$$

and for the ungauged Skyrme model

$$E_{ungauged} = 4\pi K \int dr r^2 \left[ \omega^2 \sin^2 \alpha (1 + \lambda (\alpha')^2) + (\alpha')^2 - 8m^2 (\cos \alpha - 1) \right] \quad (3.4.9)$$

Now, we look at the charge in the gauged case,

$$\mathcal{Q}_{gauged} = 8\pi K \int dr r^2 g \sin^2 \alpha (1 + \lambda(\alpha')^2) \quad (3.4.10)$$

and for the non-gauged case,

$$\mathcal{Q}_{ungauged} = 8\pi K \omega \int dr r^2 \sin^2 \alpha (1 + \lambda(\alpha')^2) \quad (3.4.11)$$

These conserved charges  $\mathcal{Q}_{gauged}$  and  $\mathcal{Q}_{ungauged}$  are the number of pions, which is the difference between the number of positive and negative pions. From this, we get the physical charge, which is a multiple of electron charge  $e$ ,

$$\mathcal{Q}_{gauged}^{phys} = e \mathcal{Q}_{gauged} \quad (3.4.12)$$

$$\mathcal{Q}_{ungauged}^{phys} = e \mathcal{Q}_{ungauged} \quad (3.4.13)$$

In the case of ungauged Q-balls, the minimum energy solution is defined by

$$\delta (E - \omega \mathcal{Q}) = 0 \quad (3.4.14)$$

---

<sup>1</sup>Please check appendix A2.1 for calculational details

This variation leads to the equation of motion, and its solution will satisfy Eq. 3.4.14.

### 3.5 Q-Balls in Skyrme model

The first case is to analyze Q-balls in the ungauged Skyrme model with the hedgehog ansatz. That is, we switch off  $A_\mu = 0$  in the Eq. 3.4.7

$$L = 2\pi K \int dr r^2 [\omega^2 \sin^2 \alpha - (1 - \lambda \omega^2 \sin^2 \alpha) (\alpha'(r))^2 + 8m^2 (\cos \alpha - 1)] \quad (3.5.1)$$

and variation with respect to  $\alpha$  gives the equation of motion

$$[1 - \lambda \omega^2 \sin^2 \alpha] \Delta \alpha + \frac{1}{2} \omega^2 \sin 2\alpha (1 - \lambda (\alpha')^2) - 4m^2 \sin \alpha = 0 \quad (3.5.2)$$

The potential of the model is,

$$U(\alpha) = 8m^2 (1 - \cos \alpha) \quad (3.5.3)$$

and according to Coleman (66), new particles appear in the spectrum whenever the minima of  $U/\alpha^2$  is at some point  $\alpha_0 \neq 0$ . Although this condition was put forward for a theory with a linear kinetic term, we will show that the potential  $U(\alpha)$ , which is a part of Lagrangian with a non-linear kinetic term, also falls under the same umbrella. In figure 3.5.1, we see that the minima occur at every even multiple of  $\pi$  except at zero, that is,  $\alpha_0 = 2\pi$ , as all of them are the same point.

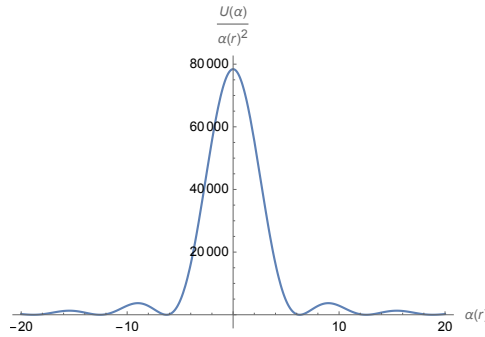


**Figure 3.5.1:** Minima of  $U(\alpha)$  at  $\alpha_0 \neq 0$ .

We will show its equivalence by linearizing the kinetic term with a change of variable that

lets us write the eom in a canonical form. A form familiar in the study of Q-balls,

$$H(\alpha) = \int^{\alpha} ds \sqrt{1 - \lambda\omega^2 \sin^2 s} \quad (3.5.4)$$

$$\Rightarrow \frac{\Delta H}{\sqrt{1 - \lambda\omega^2 \sin^2 \alpha}} = \Delta\alpha - \frac{\lambda\omega^2}{2} \frac{\sin 2\alpha (\nabla\alpha)^2}{1 - \lambda\omega^2 \sin^2 \alpha} \quad (3.5.5)$$

Using this, we can write the above equation in a form suitable for the Q-ball discussion

$$\begin{aligned} \Delta H + \frac{\omega^2 \sin 2\alpha - 2dU/d\alpha}{2\sqrt{1 - \lambda\omega^2 \sin^2 \alpha}} &= 0 \\ \frac{d^2 H(r)}{dr^2} + \frac{\omega^2 \sin 2\alpha}{2\sqrt{1 - \lambda\omega^2 \sin^2 \alpha}} - \frac{dU/d\alpha}{\sqrt{1 - \lambda\omega^2 \sin^2 \alpha}} &= -\frac{2}{r} \frac{dH(r)}{dr} \end{aligned} \quad (3.5.6)$$

where  $\alpha(r)$  is an inverse of the elliptic integral of the second kind, Eq. 3.5.4 and let  $\alpha(r) \equiv \mathcal{E}(H, \lambda\omega^2)$ . For the asymptotic case, that is, for  $r \rightarrow \infty$  the field  $H(r) \rightarrow 0$  giving  $\mathcal{E}(H, \lambda\omega^2) \sim H(r)$  and the EOM linearizes

$$\frac{d^2 H(r)}{dr^2} + (\omega^2 - 4m^2) H(r) = 0 \quad (3.5.7)$$

$$H(r) \rightarrow C \frac{e^{-r\sqrt{4m^2 - \omega^2}}}{r} \quad (3.5.8)$$

where C is a constant with a dimension of length. As already noted, the energetically favorable condition of  $\omega < m$  is also essential for the field's exponential decay. For a pionic Q-ball, we must have

$$0 < \omega \leq 2m = \omega_0 \quad (3.5.9)$$

When  $\omega > 2m$ , the asymptotic decay becomes oscillatory, resulting in a plane wave solution. In a way, the bounded configuration of the pions gets dispersed in the plane waves. We get the same exponential decay of the field from Eq. 3.5.2, which shows asymptotic behavior is independent of the change of variables. Please see the appendix A2.2 for the form of the asymptotic energy.

The EOM,

$$\frac{d^2 H(r)}{dr^2} + \frac{1}{2\sqrt{1 - \lambda\omega^2 \sin^2 \alpha}} \frac{d}{d\alpha} (\omega^2 \sin^2 \alpha - 2U) = -\frac{2}{r} \frac{dH(r)}{dr} \quad (3.5.10)$$

can be recast in a form resembling an energy conservation equation with

$$\frac{dH}{d\alpha} = \sqrt{1 - \lambda\omega^2 \sin^2 \alpha} \quad (3.5.11)$$

Plugging this identity in the EOM gives,

$$\frac{d^2 H}{dr^2} + \frac{1}{2} \frac{d}{dH} (\omega^2 \sin^2 \mathcal{E}(H, \lambda\omega^2) - 2U) = -\frac{2}{r} \frac{dH}{dr} \quad (3.5.12)$$

multiplying above equation by  $(dH/dr)$  and then integrating gives

$$\left(\frac{dH}{dr}\right)^2 + \omega^2 \sin^2 \mathcal{E}(H, \lambda\omega^2) - 2U = -\int \frac{4}{r} \left(\frac{dH}{dr}\right)^2 dr + \mathcal{C} \quad (3.5.13)$$

The effective potential is

$$V_{eff}(H) = -\omega^2 \sin^2 \mathcal{E}(H, \lambda\omega^2) + 2U \quad (3.5.14)$$

$$= -\omega^2 \sin^2 \mathcal{E}(H, \lambda\omega^2) + 8m^2 (1 - \cos \mathcal{E}(H, \lambda\omega^2)) \quad (3.5.15)$$

Now, we can check the Coleman criteria for a potential to host a Q-ball as in figure 3.5.1, and we can see that (figure 3.5.2) they come out to be the same.

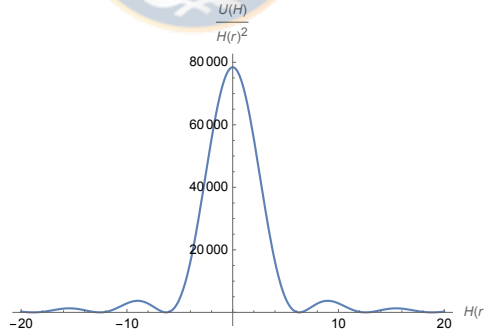


**Figure 3.5.2:** Minima of  $U(H)$  at  $H_0 \neq 0$ .

Hence, we have established that  $U(\alpha)$  has qualified to be a Q-ball potential. This is crucial because, with  $U(\alpha)$ , we have a foundation for the existence of gauged Q-balls. Whenever a potential supports an ungauged Q-ball solution, it also supports a gauged Q-ball. Change of variables is limited only to the case of ungauged Q-balls; therefore, we can't justify it for the gauged case. But with  $U(\alpha)$  qualified to be Q-ball potential, we are assured that gauged solutions exist!



Then we can write the energy conservation law with a dissipative term as

$$\left(\frac{dH}{dr}\right)^2 - V_{eff}(H) = - \int \frac{4}{r} \left(\frac{dH}{dr}\right)^2 dr + \mathcal{C} \tag{3.5.16}$$

We can paint an analogy of this equation of motion with the Newtonian equation of motion for a point particle subject to viscous damping if we think of  $r$  as a time coordinate and  $H(r)$  as the particle's position. Then the Q-ball solution is interpreted as the unit mass particle which moves in the effective potential  $(-V_{eff})$ , which is plotted in figure 3.5.3, along with the potential plot. In the plot 3.5.3d, we have  $\omega > 2m$ .

We can choose a starting position at time zero ( $r = 0$ ),  $H(0) \equiv H_0 \neq 0$ . So, we have  $dH/dr = 0$ , and this fixes the constant of integration to be  $\mathcal{C} = -V_{eff}(H_0)$ , which is like choosing the energy of the point particle system. From the effective potential plot 3.5.3b, we see that  $V_{eff}(H_0 \approx 6.27) = 0$ .

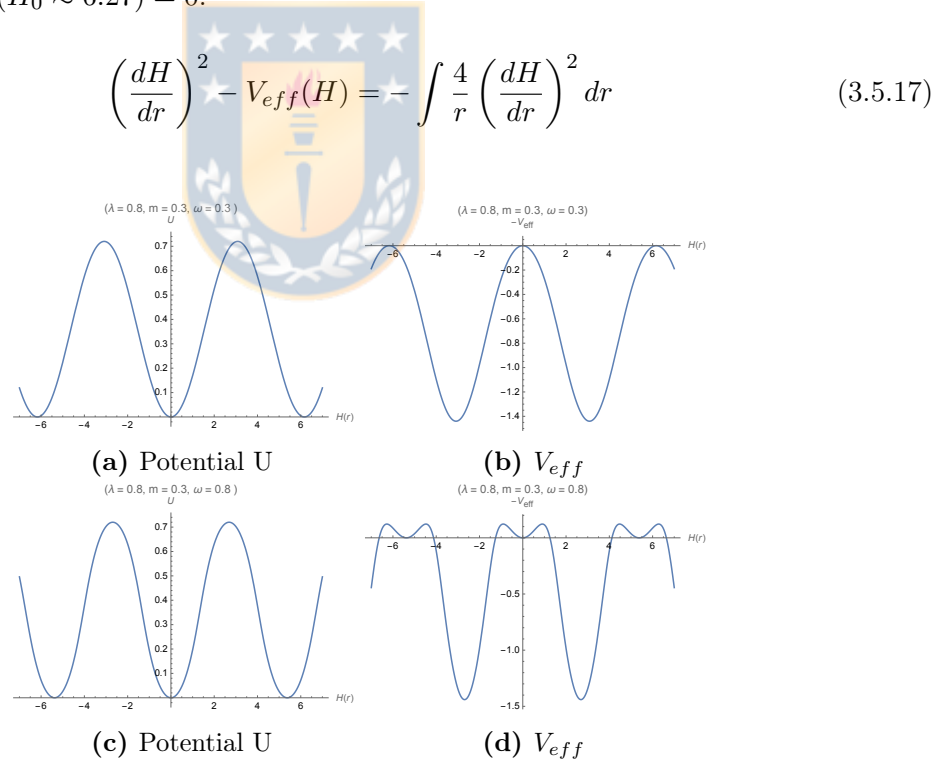


**Figure 3.5.3:**  $U(H)$  and  $V_{eff}$  plots

After choosing the starting point  $H_0$ . The particle will be stationary at  $H_0$  due to the frictional/viscous term, and once enough time passes (for large  $r = R \gg 1$ ), we can neglect the frictional term. After which, the particle will start sliding to the left and losing energy.

Eventually, it will reach its final destination. We can visualize this by looking at the  $-V_{eff}$  plot in figure 3.5.3b. For  $0 \leq r \leq R$ , the solution would be  $H \sim H_0$  which decreases to 0 as  $r \rightarrow \infty$ . The radius of the Q-ball will be given by  $R$ . So, at late times

$$\int_{H_0}^H \frac{dH}{\sqrt{V_{eff}(H)}} = r - R \quad (3.5.18)$$

The denominator should be real, which imposes

$$V_{eff}(H) \geq 0 \implies 8m^2 (1 - \cos \mathcal{E}(H, \lambda\omega^2)) \geq \omega^2 \sin^2 \mathcal{E}(H, \lambda\omega^2) \quad (3.5.19)$$

As we start going further out from the Q-ball, that is, from the radius  $R$ , the field  $H$  exponentially decreases. Due to which  $\mathcal{E}(H, \lambda\omega^2) \sim H(r) \ll 1$ , and the above bound manifests the Eq. 3.5.9.

$$\int_{H_0}^{H(r)} \frac{dH}{\sqrt{-\omega^2 \sin^2 \mathcal{E}(H, \lambda\omega^2) + 8m^2 (1 - \cos \mathcal{E}(H, \lambda\omega^2))}} = r - R \quad (3.5.20)$$

$$\implies \int_{\alpha_0}^{\alpha} d\alpha \sqrt{\frac{1 - \lambda\omega^2 \sin^2 \alpha}{-\omega^2 \sin^2 \alpha + 8m^2 (1 - \cos \alpha)}} = r - R \quad (3.5.21)$$

In theory, we have four parameters ( $\lambda, K, m$  and  $\omega$ ), out of which three are found experimentally except  $\omega$ . Hence, fixing three parameters, we have a restricted range for  $\omega$  to get a Q-ball. At a large distance, we can approximate the integral to be

$$\int_{H_0}^{H \ll 1} \frac{dH}{H} = \sqrt{-\omega^2 + 4m^2} (r - R) \quad (3.5.22)$$

$$\implies H_0 = H(r) e^{-\sqrt{4m^2 - \omega^2}(r-R)} \quad (3.5.23)$$

### 3.6 Gauged Q-balls in Skyrme model

To study the gauged case, we make a variation of the Lagrangian in Eq. 3.4.7 concerning  $\alpha(r)$  and  $g(r)$  at a fixed  $\omega$  to get the EOMs,

$$\begin{aligned} & (1 - \lambda g(r)^2 \sin^2 \alpha) \Delta \alpha(r) - 2\lambda g(r) g'(r) \alpha'(r) \sin^2 \alpha \\ & + \frac{1}{2} g(r)^2 \sin 2\alpha (1 - \lambda (\alpha'(r))^2) - 4m^2 \sin \alpha = 0 \end{aligned} \quad (3.6.1)$$

and,

$$\Delta g(r) - 4Kg(r) \sin^2 \alpha(1 + \lambda(\alpha'(r))^2) = 0 \quad (3.6.2)$$

Where  $\Delta = \nabla^2$  is the Laplacian. Eq. 3.6.2 is a constraint equation due to the absence of  $\dot{g}$  term in the Lagrangian.

Asymptotically at the leading order, the electric potential  $u(r) \rightarrow 0$ , yielding the boundary condition as  $g(r) \xrightarrow{r \rightarrow \infty} \omega$ . We can get crucial information from the charge using Eq. 3.6.2 for  $u(r)$  as,

$$\Delta u = -2Kg(r) \sin^2 \alpha(1 + \lambda(\alpha'(r))^2) \quad (3.6.3)$$

and plugging this in the Eq. 3.4.10 gives

$$\mathcal{Q}_{gauged} = -4\pi \int dr r^2 \Delta u \xrightarrow{r \rightarrow \infty} 2\pi r^2 g' = -\pi r^2 u' \quad (3.6.4)$$

$$\Rightarrow \lim_{r \rightarrow \infty} u(r) \sim \frac{\mathcal{Q}_{gauged}}{\pi r} + \mathcal{C} \quad (3.6.5)$$

Setting the integration constant  $\mathcal{C} = 0$  yields at the leading order  $g(r) \xrightarrow{r \rightarrow \infty} \omega$ . Now let us scrutinize the linearized asymptotic equations. Up to the subleading order in  $r$ , we have

$$g_\infty = \omega - \frac{2\mathcal{Q}_{gauged}}{\pi r} \quad (3.6.6)$$

Asymptotically,  $\sin \alpha \sim \alpha$  and with this, we get a linearized equation, and its solution has a similar form to that of the complex scalar field (123)

$$\alpha''(r) + \frac{2}{r}\alpha'(r) + \left( \omega^2 - \frac{4\omega\mathcal{Q}_{gauged}}{\pi r} - 4m^2 \right) \alpha(r) = 0 \quad (3.6.7)$$

$$\alpha(r)_\infty = c_1 \frac{e^{-r\sqrt{A^2}}}{\pi} {}_1F_1 \left( 1 + \frac{2\omega\mathcal{Q}_{gauged}}{\sqrt{A^2}\pi}; 2; 2r\sqrt{A^2} \right) + c_2 \frac{e^{-r\sqrt{A^2}}}{\pi} U \left( 1 + \frac{2\omega\mathcal{Q}_{gauged}}{\sqrt{A^2}\pi}, 2, 2r\sqrt{A^2} \right) \quad (3.6.8)$$

where  $A^2 = 4m^2 - \omega^2$  while  ${}_1F_1$  and  $U$  are the confluent hypergeometric functions of the first and second kind, respectively. The asymptotic fall-off can be deduced from them as

$$\alpha_\infty(r) \xrightarrow{r \rightarrow \infty} \frac{e^{-rA}}{r^{1 + \frac{2\omega\mathcal{Q}_{gauged}}{\pi A}}} \quad (3.6.9)$$

From this, we get the usual bound on the frequency,

$$\omega^2 \leq 4m^2 \quad (3.6.10)$$

### 3.6.1 Energy per unit charge

Energy and charge are parametrized by  $\omega$ , so we look at

$$\begin{aligned} \frac{dE_{gauged}}{d\omega} = 4\pi K \int dr r^2 \left\{ 2g \frac{dg}{d\omega} \sin^2 \alpha \left( 1 + \lambda (\alpha')^2 \right) + g^2 \frac{d}{d\omega} \left[ \sin^2 \alpha \left( 1 + \lambda (\alpha')^2 \right) \right] \right. \\ \left. + 2\alpha' \frac{d\alpha'}{d\omega} + 8m^2 \sin \alpha \frac{d\alpha}{d\omega} + \frac{1}{2K} g' \frac{dg'}{d\omega} \right\} \end{aligned} \quad (3.6.11)$$

Asymptotically both  $\alpha$  and  $g$  vanish so that we can drop the surface terms arising from integration by parts,

$$\begin{aligned} \frac{dE_{gauged}}{d\omega} = 4\pi K \int dr r^2 \left\{ 2g \frac{dg}{d\omega} \sin^2 \alpha \left( 1 + \lambda (\alpha')^2 \right) + g^2 \frac{d}{d\omega} \left[ \sin^2 \alpha \left( 1 + \lambda (\alpha')^2 \right) \right] \right. \\ \left. - 2 \left( \Delta \alpha - 4m^2 \sin \alpha \right) \frac{d\alpha}{d\omega} - \frac{2}{K} \Delta u \frac{du}{d\omega} \right\} \end{aligned} \quad (3.6.12)$$

Utilizing Eq. 3.6.1 we can write

$$\frac{dE_{gauged}}{d\omega} = 4\pi \int dr r^2 \left\{ g \frac{d}{d\omega} \left[ 2Kg \sin^2 \alpha \left( 1 + \lambda (\alpha')^2 \right) \right] - 2\Delta u \frac{du}{d\omega} \right\} \quad (3.6.13)$$

It further simplifies with the help of Eq. 3.6.3

$$\frac{dE_{gauged}}{d\omega} = 4\pi \int dr r^2 \left\{ (\omega - 2u) \frac{d}{d\omega} (-\Delta u) - 2\Delta u \frac{du}{d\omega} \right\} \quad (3.6.14)$$

$$= \omega \frac{dQ_{gauged}}{d\omega} + 8\pi \int dr r^2 \left( u \Delta \frac{du}{d\omega} - \Delta u \frac{du}{d\omega} \right) \quad (3.6.15)$$

Further, integrating by parts, we find that

$$\int dr r^2 u \Delta \frac{du}{d\omega} = \int dr r^2 \Delta u \frac{du}{d\omega} \quad (3.6.16)$$

This gives,

$$\frac{dE_{gauged}}{d\omega} = \omega \frac{dQ_{gauged}}{d\omega} \quad (3.6.17)$$

Therefore,

$$dE_{gauged} = \omega dQ_{gauged} \quad (3.6.18)$$

Following similar steps for ungauged case give us

$$dE_{ungauged} = \omega dQ_{ungauged} \quad (3.6.19)$$

### 3.7 Stability analysis

We check the classical stability of gauged Q-balls under small perturbations in  $\alpha(r)$  and  $g(r)$ . That is, we perturb around the background solutions  $\alpha_0(r)$  and  $g_0(r)$  and expand the EOMs up to the linear order in  $\epsilon$ . We will demonstrate the stability against small perturbations in the asymptotic region. It came to us as a surprise that there is no mention of a detailed analysis of asymptotic perturbations in the literature. Through this analysis, we were able to find a bound on the asymptotic physical charge  $Q_{gauged}^{phys}$ . Examining the classical stability of gauged Q-balls is highly non-trivial, and, in general, stability conditions are distinct from those of the ungauged Q-balls (126)

$$\alpha(r) = \alpha_0(r) + \epsilon a(r) \quad (3.7.1)$$

$$g(r) = g_0(r) + \epsilon b(r) \quad (3.7.2)$$

Expanding Eq. 3.6.1 and Eq. 3.6.2 till the first order in  $\epsilon$ , along with using the EOMs for the background fields, gives

$$\begin{aligned} & [-2\lambda b g_0 \sin^2 \alpha_0 + (1 - \lambda g_0^2 \sin 2\alpha_0) a] \Delta \alpha_0 + (1 - \lambda g_0^2 \sin^2 \alpha_0) \Delta a \\ & - \lambda \left[ 2 (g_0 b)' \alpha_0' \sin^2 \alpha_0 + (g_0^2)' a' \sin^2 \alpha_0 + (g_0^2)' a \alpha_0' \sin 2\alpha_0 \right] \\ & + (g_0^2 a \cos 2\alpha_0 + 2g_0 b \sin 2\alpha) (1 - \lambda (\alpha_0')^2) - \lambda g_0^2 a' \alpha_0' \sin 2\alpha_0 - 4m^2 a \cos \alpha_0 = 0 \end{aligned} \quad (3.7.3)$$

and

$$\Delta b - 4K \left[ 2\lambda g_0 a' \alpha_0' \sin^2 \alpha_0 + (g_0 a \sin 2\alpha_0 + b \sin^2 \alpha_0) (1 + \lambda (\alpha_0')^2) \right] = 0 \quad (3.7.4)$$

In the asymptotic limit  $\alpha_0 \sim \alpha_\infty$  and  $g_0 \sim g_\infty$ , and we will analyze them up to the order of  $\mathcal{O}(r^{-2})$ .

The perturbation equation boils down to an ODE resembling the Hydrogen atom ODE

$$\Delta a + \left( \frac{4Q_{gauged}^2}{\pi^2 r^2} - 4\omega \frac{Q_{gauged}}{\pi r} - A^2 \right) a = 0 \quad (3.7.5)$$

$$\Delta b = 0 \quad (3.7.6)$$

We can get rid of the first derivatives  $a'$  and  $b'$  by a change of variable; that is, we define

$$a = \frac{\Psi_1}{r} \quad \text{and} \quad b = \frac{\Psi_2}{r} \quad (3.7.7)$$

with this, we get

$$\Psi_1'' + \left( \frac{4Q_{gauged}^2}{\pi^2 r^2} - 4\omega \frac{Q_{gauged}}{\pi r} - A^2 \right) \Psi_1 = 0 \quad (3.7.8)$$

$$\Psi_2'' = 0 \quad (3.7.9)$$

To check for stability, we write these equations analogously to the Schrodinger equation with an eigenvalue of  $F^2$ . This is because if the perturbation is stable, it will have the same sign as the potential.

$$-\Psi_1'' + \left( A^2 + 4\omega \frac{Q_{gauged}}{\pi r} - \frac{4Q_{gauged}^2}{\pi^2 r^2} \right) \Psi_1 = F^2 \Psi_1 \quad (3.7.10)$$

$$-\Psi_2'' = F^2 \Psi_2 \quad (3.7.11)$$

The solutions are Whittaker functions,

$$\Psi_1 = c_1 M_{p,q} \left( 2ir \sqrt{F^2 - A^2} \right) + c_2 W_{p,q} \left( 2ir \sqrt{F^2 - A^2} \right) \quad (3.7.12)$$

where,  $p = \frac{2iQ_{gauged}\omega}{\pi\sqrt{F^2-A^2}}$  and  $q = \frac{\sqrt{\pi^2-16Q_{gauged}^2}}{2\pi}$

$$\Psi_2 = c_3 e^{-r\sqrt{-F^2}} + c_4 e^{r\sqrt{-F^2}} \quad (3.7.13)$$

We can expand Whittaker functions in terms of confluent hypergeometric functions,

$$M_{p,q}\left(2ir\sqrt{F^2 - A^2}\right) = e^{-ir\sqrt{F^2 - A^2}} \left(2ir\sqrt{F^2 - A^2}\right)^{\frac{1}{2}+q} {}_1F_1\left[\frac{1}{2} + q - p; 1 + 2q, 2ir\sqrt{F^2 - A^2}\right] \quad (3.7.14)$$

The confluent hypergeometric function is defined only for  $1 + 2q > 0$  (124), due to which we get a bound on the charge as

$$-\frac{\pi}{4}e \leq Q_{gauged}^{phys}(\infty) \leq \frac{\pi}{4}e \quad (3.7.15)$$

### 3.8 Phenomenological implications

Phenomenological signatures of gauged Q-balls could exist in the stream of particles evaporating off the surface of the Q-balls. Evaporation of global U(1) Q-balls was first studied in (127), at the leading semiclassical order where the Q-ball was considered a classical background. With the Yukawa interaction, they calculated the neutrino pair production rate. This analysis was extended to the case of gauged Q-balls in (128), with the coupling of the scalar field with fermions by Yukawa interaction.

Gauged Q-balls could arise as the Bose-Einstein condensed phase of pions in the early Universe, along with possible implications on cosmic evolution. Their formation in the early Universe during the QCD epoch could have left some scars on the primordial gravitational waves (PGW) and primordial black holes (PBH). In (129), authors discussed the possible gravitational wave signatures arising from the pion condensation in the early Universe. They demonstrated that with the increased sensitivity of future detectors like LISA and SKA, we should be able to detect signatures of pion condensates, primarily due to the enhancement of the PGW spectra and change in the fraction of PBHs with a mass more significant than one solar mass.

### 3.9 Conclusion

Skyrme model fixes the potential form, leaving no room for arbitrariness in the potential. The hedgehog ansatz allows us to analyze the Skyrme equations of motion, which has a fertile ground for hosting ungauged and gauged Q-balls. We saw in figure 3.5.1 the potential satisfies Coleman's condition for the existence of Q-balls. The ungauged Q-ball is the

solution seen in the plot of the effective potential 3.5.3b. It could be visualized as a point particle that sits at the peak of the  $V_{eff}$  for a very long analog time (which is  $r$ ) until the frictional term is negligible, which then rolls down to zero asymptotically.

Whenever a potential supports an ungauged Q-ball solution, it usually also supports a gauged Q-ball, which can be found numerically. We are still in the process of numerical evaluation of the solution. The reason for not yet accomplishing it is the intricacies and sensitivities involved with the Skyrme eom, specifically the trigonometric functions.





## Chapter 4

# But, what about Quantum Gravity?

Quantum gravity is a theoretical framework that attempts to merge quantum mechanics and general relativity to explain the behavior of gravity at the quantum level. This is a highly active area of research, and there are currently several different approaches to developing a consistent theory of quantum gravity. Some primary methods include string theory, loop quantum gravity, and causal dynamical triangulation. Despite significant progress, a complete and consistent theory of quantum gravity remains an open problem in physics.

### 4.1 Roadblocks in quantizing gravity

1. *The principles of quantum mechanics and general relativity are challenging to reconcile:* Quantum mechanics and general relativity is two of the most successful theories in physics, but they are based on fundamentally different principles. Quantum mechanics describes the behavior of matter and energy at the microscopic level, while general relativity describes the behavior of space-time and gravity at the macroscopic level. However, these two theories are incompatible, and it is not clear how to combine them into a single consistent framework.
2. *Quantum gravity is a highly non-linear theory:* The gravitational field is a non-linear field, which means that it exhibits a complex and highly non-linear behavior. This makes it challenging to study using the methods of quantum mechanics, which are based on the assumption of linearity. As a result, developing a consistent theory of quantum gravity is a complex and challenging problem.
3. *Quantum gravity is plagued by infinities and other singularities:* Many of the attempts to

quantize the gravitational field have been beset by infinities and other singularities, which arise due to the non-linear nature of gravity. These infinities and singularities make it challenging to define a consistent and well-behaved theory of quantum gravity. They are one of the main obstacles to progress in this field.

4. *There is a lack of experimental data and observations to guide the development of quantum gravity:* Unlike other areas of physics, there is a lack of empirical data and observations that can be used to guide the development of quantum gravity. This makes it difficult to test the theoretical predictions of quantum gravity and to determine whether they are consistent with the observed behavior of the universe.

## 4.2 Wait, but why should we quantize gravity?

The idea of quantizing gravity, or describing the gravitational force as a quantum mechanical phenomenon, arises from the fact that the other fundamental forces in nature, such as electromagnetism and the strong and weak nuclear forces, are described by quantum field theories. These theories successfully explain a wide range of phenomena, from the behavior of atoms and molecules to the interactions of elementary particles. Therefore, it is natural to ask whether gravity can also be described by a quantum field theory, in which the gravitational force would be mediated by quantum mechanical particles known as gravitons.

It is exciting and essential to try to quantize gravity for several reasons. First, a consistent theory of quantum gravity would provide a more fundamental description of the gravitational force. It could potentially explain phenomena currently not well understood, such as the nature of dark matter and the Universe's origin. Second, a quantum theory of gravity would be required to understand the behavior of gravitational systems in regimes where quantum effects are essential, such as in the early Universe or near black holes. Finally, a quantum theory of gravity would provide a framework for reconciling general relativity, which describes gravity on large scales, with quantum mechanics, which represents the behavior of microscopic systems. Overall, quantizing gravity is a challenging but fascinating problem in theoretical physics that could have important implications for our understanding of the Universe.

### 4.3 But, what about the path integral of gravity?

The gravitational path integral is a mathematical technique used in quantum gravity to calculate the amplitude for a gravitational field to evolve from one configuration to another. It is the sum of all possible classical gravitational field configurations between the initial and final states, weighted by each configuration's exponent of the classical gravitational action. The gravitational path integral is a way to extend the concept of the path integral, which is typically used in quantum mechanics and quantum field theory, to the case of gravity.

That sounds promising, but one of the biggest challenges is to define the measure. In path integral formalism, the measure is a mathematical concept that describes the weight or probability of a particular path or trajectory of a particle or system. The measure is a crucial part of the path integral formalism, as it determines the probability of a particle or system is in a particular state and can help to predict its behavior in different situations. The measure is typically determined by quantum mechanics principles and depends on the specific system being studied.

We tried to define a path integral measure in the case of 2+1 AdS pure gravity, but more on that in chapters 6 and 7. So, now let's get back to the background discussion of path integral by discussing scenarios where it has led to intriguing results and insights!

#### 4.3.1 Euclidean quantum gravity

We are far from having a theory of QG. Perhaps the gravitational field is not quantized in nature, and something more fundamental lurks behind the four-dimensional Universe's curtains. In any case, we can relish the semi-classical effects of quantum fields and classical backgrounds. To name a few significant advancements, the black hole entropy (130; 131) (a.k.a. Bekenstein–Hawking entropy), the Hawking radiation (131). More recently, the quantum corrected background metric forms horizons around naked singularities in 2+1 AdS gravity (132; 133; 134; 135).

The framework of Euclidean QG captures some of the essences of the black hole thermodynamics as the wick-rotated gravitational action is a free energy of the gravitational system (136). With the wick rotation, we can define the partition function for gravity.

The partition function is a mathematical function used to calculate a physical system's thermodynamic properties in statistical mechanics. It is typically denoted by the letter "Z". It is defined as the sum of the Boltzmann factors for each possible state of the system,

weighted by the degeneracy (number of ways in which a given state can be achieved) of that state. The partition function is a critical quantity in statistical mechanics because it encodes all of the information about the statistical properties of the system, such as its internal energy, entropy, and heat capacity. We can derive Hawking radiation (137), black hole entropy (136), and log-corrections to the black hole entropy with the partition function.

#### 4.3.1.1 Wait, but how is it related to a path integral?

The partition function and the path integral are two closely related concepts in statistical mechanics and quantum field theory. Their relation comes from the fact that they are expressions of the same underlying principle: the sum of all possible configurations or paths. In the case of the partition function, the configurations are the possible states of the system, and the sum is over the Boltzmann factors for each state. In the case of the path integral, the configurations are the possible paths a particle can take, and the sum is over the exponents of the classical action for each path. Thus, both the partition function and the path integral are expressions of the idea that the behavior of a physical system can be understood by summing over all possible configurations or paths.

Both of them can supply different aspects of the theory. Namely, statistical information like microstates of the black hole could be explained through partition function. While something like a transition amplitude or the probability of a black hole metric completely evaporating away in radiation could be studied through a path integral. In this case, the transition will be between a black hole metric and a flat metric.

## 4.4 But, what would it imply if nature doesn't follow QG?

If it turns out that gravity cannot be quantized, or described as a quantum mechanical phenomenon, then it would have significant implications for our understanding of the fundamental nature of the Universe. It would mean that gravity is fundamentally different from the other fundamental forces in nature, such as electromagnetism and the strong and weak nuclear forces described by quantum field theories. This would imply that there is no quantum version of the gravitational force and that gravity cannot be explained in terms of the exchange of gravitons or other quantum mechanical particles.

If gravity is not quantizable, then it would also have implications for our understanding of the behavior of gravitational systems in regimes where quantum effects are essential. For example, it would mean that we cannot use quantum mechanics to explain the behavior of

the early Universe or the behavior of objects near black holes. This would be a significant limitation on our ability to understand and predict the behavior of these systems.

Overall, the question of whether gravity can be quantized is a fundamental one that is still the subject of much debate and research in theoretical physics. If it turns out that gravity cannot be quantized, then it would have far-reaching implications for our understanding of the Universe and the fundamental forces that govern it.



## Chapter 5

# Quantum Corrections to a Finite Temperature BIon



### Abstract

In this chapter, we will analyze a finite temperature BIon, which is a finite temperature brane-anti-brane wormhole configuration. We will analyze the quantum fluctuations to this BIon solution using Euclidean quantum gravity. It will be observed that these quantum fluctuations produce logarithmic corrections to the entropy of this finite temperature BIon solution. These corrections to the entropy also correct the internal energy and the specific heat for this finite temperature BIon. We will also analyze the critical points for this finite temperature Bionic system, and analyze the effects of quantum corrections on the stability of this system.

## 5.1 Introduction

In string theory, it is possible to analyze certain physical objects in a region of spacetime in terms of very different objects. Thus, it is possible to analyze a system of many coincident strings in terms of D-brane geometry, and this is done in the BIon solution (138; 139). So, this BIon solution can describe an F-string coming out of the D3-brane or a D3-brane parallel to an anti-D3-brane, such that a wormhole connects them with an F-string charge. This configuration is called as the brane-antibrane-wormhole configuration. It is also possible

to use such a solution to analyze D-branes probing a thermal background (140; 141). This can be done using the blackfold approach (142; 143; 144; 145). In this method, a large number of coincident D-branes form a brane probe. Furthermore, as this probe is in thermal equilibrium with the background, this method has been used to heat up a BIon. This was done by putting it in a hot background. It is also possible to analyze the thermodynamics of this finite temperature BIon solution (140; 141). In this chapter, we will analyze the effects of thermal fluctuations on the thermodynamics of this system.

The entropy-area law of black holes thermodynamics (146; 147), is expected to get modified near the Planck scale due to quantum fluctuations (148). These quantum fluctuations in the geometry of any black holes are expected to produce thermal fluctuations in their associated thermodynamics. It is interesting to note that the thermal fluctuations produce a logarithmic correction term to the thermodynamics of black holes (149; 150; 151; 152). The consequences of such logarithmic correction have been studied for a charged AdS black hole (155), charged hairy black hole (156), a black saturn (157), a Hayward black hole (158) a small singly spinning Kerr-AdS black hole (159), and a dyonic charged AdS black hole (160). In non-perturbative quantum general relativity, the density of microstates were associated with the conformal blocks has been used to obtain logarithmic corrections to the entropy (161). It has also been demonstrated that the Cardy formula can produce logarithmic correction terms for all black holes whose microscopic degrees of freedom are characterized by a conformal field theory (162). The logarithmic correction has also been studied from the black hole in the presence of matter fields (163) and dilatonic black holes (164). Leading order quantum corrections to the semi-classical black hole entropy have been obtained (165), and applied to Gödel black hole (166; 167). The logarithmic corrections were also used to study different aspects of regular black holes satisfying the weak energy condition (168), three-dimensional black holes with soft hairy boundary conditions (169), and certain aspects of Kerr/CFT correspondence (170). The logarithmic corrected entropy also corrects some hydrodynamical quantities, and so the the field theory dual to such corrected solutions has also been studied (175; 171; 172; 174; 173).

The logarithmic corrections to the entropy of various black holes have also been obtained using the Euclidean Quantum Gravity (176; 177; 178). In this approach, Euclidean Quantum Gravity (179) is used to obtain the partition function for the black hole, which is then used to obtain the logarithmic corrections to the thermodynamics of that black hole. As the logarithmic corrections occur almost universally in the thermodynamics of black holes, in this chapter, we will analyze the consequences of such corrections for a thermal BIon. We

compute the quantum correction to the black hole entropy, internal energy, specific heat using the Euclidean Quantum Gravity (179). We find that the logarithmic correction affects the critical points, and the corrections significantly change the stability of this system.

## 5.2 Gravitational Partition Function

Now, we start with the Euclidean Quantum Gravity that is obtained by performing a Wick rotation on the temporal coordinates in the path integral. Thus, we obtain the gravitational partition function in Euclidean Quantum Gravity (179),

$$Z = \int [\mathcal{D}] e^{-\mathcal{I}_E} = \int_0^\infty \rho(E) e^{-\beta E} dE, \quad (5.2.1)$$

where  $\mathcal{I}_E$  is the Euclidean action for the BIon solution (140; 141), and  $\beta \propto 1/T$ . The density of states  $\rho(E)$  is easily obtained from (5.2.1) by performing an inverse Laplace transform, so that one obtains

$$\rho(E) = \frac{1}{2\pi i} \int_{a-i\infty}^{a+i\infty} e^{S(\beta)} d\beta. \quad (5.2.2)$$

Here,  $S(\beta)$  is the entropy, and its exact form is given in terms of the partition function and the total energy as  $S(\beta) = \beta E + \ln Z$ , where  $S_0 = S(\beta_0)$ . The integral (5.2.2) can be evaluated using the method of steepest decent, around the saddle point  $\beta_0$ , so that  $[\partial S(\beta)/\partial \beta]_{\beta=\beta_0}$  vanishes, and the equilibrium relation  $E = -[\partial \ln Z(\beta)/\partial \beta]_{\beta=\beta_0}$  is satisfied. Therefore, the equilibrium temperature is given by  $T_0 = 1/\beta_0$ , and we can expand the entropy  $S(\beta)$  around the equilibrium point  $\beta_0$  as follows

$$S(\beta) = S_0 + \frac{1}{2}(\beta - \beta_0)^2 \left[ \frac{\partial^2 S(\beta)}{\partial \beta^2} \right]_{\beta=\beta_0} + \dots \quad (5.2.3)$$

Here, the first term  $S_0 = S(\beta_0)$  denotes the entropy at the equilibrium, the second term represents the first-order correction over it. If we restrict ourselves to this first order and replace (5.2.3) with (5.2.2), we obtain

$$\rho(E) = \frac{e^{S_0}}{\sqrt{2\pi}} \left\{ \left[ \frac{\partial^2 S(\beta)}{\partial \beta^2} \right]_{\beta=\beta_0} \right\}^{-\frac{1}{2}}, \quad (5.2.4)$$



for  $[\partial^2 S(\beta)/\partial\beta^2]_{\beta=\beta_0} > 0$ , where we choose  $a = \beta_0$  and  $\beta - \beta_0 = ix$  with  $x$  being a real variable. Thus, the expression of the microcanonical entropy  $\mathcal{S}$  turns out to be (149; 150)

$$\mathcal{S} = \ln \rho(E) = S_0 - \frac{1}{2} \ln \left\{ \left[ \frac{\partial^2 S(\beta)}{\partial\beta^2} \right]_{\beta=\beta_0} \right\}. \quad (5.2.5)$$

Note that the entropy  $S(\beta)$  given in (5.2.3) is different from  $\mathcal{S}$  as given by (5.2.5), the former  $S(\beta)$  being the entropy at any temperature, whereas the latter one,  $\mathcal{S}$  is the corrected microcanonical entropy at equilibrium, which is computed by incorporating small fluctuations around the thermal equilibrium. However, the result obtained in (5.2.5) is completely model-independent and, it can be applied to any canonical thermodynamical system including a BIon solution. Thus, the first-order correction is solely governed by the term  $\ln[\partial^2 S(\beta)/\partial\beta^2]_{\beta=\beta_0}$ . This can be simplified to a generic form of the entropy correction given by  $\ln(CT^2)$  (149; 150).

Now for a system with equilibrium temperature  $\beta_0$ , and the equilibrium entropy  $S_0$ , the fluctuation around this equilibrium entropy,  $\ln[\partial^2 S(\beta)/\partial\beta^2]_{\beta=\beta_0}$  do not depend on  $\beta_0$  or  $S_0$ . However, the exact form of these fluctuations can be obtained by assuming that this system is dual to a conformal field theory, and using the modular invariance of the conformal field theory (150; 151). This is done by assuming that  $S(\beta) = a\beta^m + b\beta^{-n}$ , with  $m, n, a/b > 0$ , and observing that at equilibrium this function has an extremum, with  $\beta_0 = (nb/am)^{1/m+n}$ . Using this observation, it can be demonstrated that this term  $[\partial^2 S(\beta)/\partial\beta^2]_{\beta=\beta_0}$  (which represents first-order correction around the equilibrium) has to be proportional to  $\ln[S_0\beta_0^2]$  (149; 150; 151; 152). As the Hawking temperature,  $T$  for the black hole is obtained at the equilibrium, so we identified the equilibrium temperature  $\beta_0$  with  $T$ . Thus, the thermal fluctuations around the equilibrium entropy can be expressed in terms of the equilibrium entropy  $S_0$  and equilibrium temperature  $T$ . It may be noted that such corrections to the entropy of AdS black holes have been obtained from the entropy of the boundary theory using AdS/CFT correspondence (180; 181; 182; 183), and it has been observed that the corrections to entropy can be expressed as a logarithmic function of the original equilibrium temperature  $T$ .

As this correction term is proportional to the logarithmic function of the area, it is of the universal form of the leading order corrections to the entropy of the black hole (189; 190; 191; 192; 193; 194). It may be noted that even though the form of these corrections is universal, the exact value of the constant of proportionality to these corrections is model

dependent (189; 190; 191; 192; 193; 194). Hence, as the constant of proportionality is model dependent, we will use a free parameter  $\gamma = [0, 1]$  (184; 185; 186; 187; 188). Now it is obvious that when we neglect these thermal fluctuations  $\gamma \rightarrow 0$ , we obtain the original equilibrium results. Furthermore, for  $\gamma \neq 0$ , these corrections are proportional to the logarithmic function of the area, and hence are the leading order corrections to the entropy (189; 190; 191; 192; 193; 194). Furthermore, as these are the leading order corrections to the equilibrium entropy, so they are expected to be less than the original equilibrium entropy of the black hole (for the perturbative expansion to be valid) (184; 185; 186; 187; 188). It may be noted that when the black hole is large, we can neglect thermal fluctuations, and at that stage, the original equilibrium entropy can describe the system. Thus,  $S_0$  is a good approximation to entropy when  $S_0 \gg \ln(S_0 T^2)$ . However, as the black hole reduces in size due to Hawking radiation, we need to consider the corrections to entropy due to thermal fluctuations. Thus, we need to consider  $\gamma \ln(S_0 T^2)$ , when  $S_0 > \ln(S_0 T^2)$ . These corrections are still smaller than the original equilibrium entropy, but they are large enough to change the behavior of the system, so they cannot be neglected. At first, we can use the leading order corrections, and then we have to use higher order corrections. These corrections can be obtained by considering higher-order perturbative corrections around the equilibrium (195; 196). However, as the black hole approaches the Planck scale and  $S_0 \sim \ln(S_0 T^2)$ , the perturbative expansion around equilibrium breakdown and this expansion cannot be used to obtain the corrections to the entropy. This corresponds to the breaking of spacetime manifold by quantum fluctuations, which occur near Planck scale (197; 198). So, this perturbative approximation cannot be used for analyzing Planck-scale black holes.

Now, as this expansion for leading order corrections, holds for any black hole whose degrees of freedom can be analyzed using a CFT (150; 151; 152), and it has been argued that degrees of freedom of a BIon can also be analyzed using a CFT (153; 154), we can use these corrections for analyzing a BIon. So, we propose that the quantum correction to the entropy of a BIon can be expressed as

$$\mathcal{S} = S_0 - \frac{\gamma}{2} \ln(S_0 T^2) \mathcal{Y} \sim S_0 - \frac{\gamma}{2} \ln(S_0 T^2) - \frac{\gamma}{2} \mathcal{Y}, \quad (5.2.6)$$

where  $S_0$  is the original entropy of the BIon solution (140; 141), and  $\mathcal{Y}$  in general, is a function of other quantities (such as the properties of branes and string charges). Thus, a full analysis of this system should incorporate such quantities, but as a toy model, we will only analyze the corrections produced by  $\gamma \ln(S_0 T^2)/2$  on the thermodynamics of such a

system and neglect the effect of  $\mathcal{Y}$ . This can possibly be justified by fixing certain quantities in the system and analyzing it as a toy model. So, here the last term of (5.2.6), along with the higher order corrections to entropy (199) are neglected, and the leading order corrections to the entropy from thermal fluctuations are considered.

It may be noted that such logarithmic corrections terms are universal, and occur in almost all approaches to quantum gravity. However, the coefficient of such logarithmic correction term is model dependent (189; 190; 191; 192; 193; 194). As the corrected expression used in this chapter involves a free parameter  $\gamma = [0, 1]$  (184; 185; 186; 187; 188), it will hold even using different approaches. Any other approach to this problem can only change the value of this coefficient  $\gamma$ , which is not fixed in this chapter. Thus, the validity of the (5.2.6) can be argued on general grounds, and the main aim of the chapter is to analyze the effects of such logarithmic corrections on the thermodynamics of a BIon solution.

So, to obtain quantum corrections to the entropy of a BIon solution, we need to use the original entropy  $S_0$  and original equilibrium temperature  $T$  of the BIon solution (140; 141). Now a Bionic system is a flat spacetime configuration of a D-brane parallel to an anti-D-brane, connected by a wormhole, which has an F-string charge. Geometrically, it is composed of  $\mathcal{N}$  coincident D-branes which are infinitely extended, and has  $\mathcal{K}$  units of F-string charge, ending in a throat, with minimal radius  $\sigma_0$  (at temperature  $T$ ). To construct a wormhole solution from this, all we have to do is to attach a mirror solution at the end of the throat.

It is well known that the blackfold action can be used to describe the D-brane for probing the zero-temperature background. However, it was shown that one can also use DBI action for probing the thermal backgrounds (141), where it is ensured that the brane is not affected by the thermal background, but the degrees of freedom living on the brane are 'warmed up' due to the temperature of thermal background. Thus, the thermal background acts as a heat bath to the D-brane probe, and due to this, the probe stays in thermal equilibrium with the thermal background, which is a ten-dimensional hot flat space. This is constructed in the blackfold approach. Thus the thermal generalization of the BIon solution has been carried out, and the thermodynamic quantities for this configuration are given by (140; 141)

$$M = \frac{4T_{D3}^2}{\pi T^4} \int_{\sigma_0}^{\infty} d\sigma \frac{\sigma^2 (4 \cosh^2 \alpha + 1) F(\sigma)}{\sqrt{F^2(\sigma) - F^2(\sigma_0)} \cosh^4 \alpha}, \quad (5.2.7)$$

$$S_0 = \frac{4T_{D3}^2}{\pi T^5} \int_{\sigma_0}^{\infty} d\sigma \frac{4\sigma^2 F(\sigma)}{\sqrt{F^2(\sigma) - F^2(\sigma_0)} \cosh^4 \alpha}, \quad (5.2.8)$$

$$\mathcal{F} = \frac{4T_{D3}^2}{\pi T^4} \int_{\sigma_0}^{\infty} d\sigma \sqrt{1+z'^2(\sigma)} F(\sigma), \quad (5.2.9)$$

where  $M$  is the total mass,  $S_0$  is the entropy and  $\mathcal{F}$  is free energy of the BIon. Here,  $T_{D3}$  is the D3-brane tension,  $z$  is a transverse coordinate to the branes and  $F(\sigma) = \sigma^2(4 \cosh^2 \alpha - 3)/\cosh^4 \alpha$ , with  $\sigma$  being the world volume coordinate and  $\sigma_0$  being the minimal (sphere) radius of the throat or wormhole. Here  $\alpha$  is a function of the temperature. The chemical potentials for the D3-brane and F-string are as follows

$$\mu_{D3} = 8\pi T_{D3} \int_{\sigma_0}^{\infty} d\sigma \frac{\sigma^2 \tanh \alpha \cos \zeta F(\sigma)}{\sqrt{F^2(\sigma) - F^2(\sigma_0)}} \quad (5.2.10)$$

$$\mu_{F1} = 2T_{F1} \int_{\sigma_0}^{\infty} d\sigma \frac{\tanh \alpha \cos \zeta F(\sigma)}{\sqrt{F^2(\sigma) - F^2(\sigma_0)}} \quad (5.2.11)$$

It should be noted that these relations satisfy the first law of thermodynamics  $dM = TdS_0 + \mu_{D3}d\mathcal{N} + \mu_{F1}d\mathcal{K}$  as well as the Smarr relation,  $4(M - \mu_{D3}\mathcal{N} - \mu_{F1}\mathcal{K}) - 5TS_0 = 0$ . One can also calculate internal energy and the specific heat of the BIon solution as

$$U_0 = \frac{4T_{D3}^2}{\pi T^4} \int_{\sigma_0}^{\infty} d\sigma F(\sigma) \left[ \sqrt{1+z'^2(\sigma)} + \frac{4\sigma^2}{\sqrt{F^2(\sigma) - F^2(\sigma_0)} \cosh^4 \alpha} \right], \quad (5.2.12)$$

$$C_0 = T \left( \frac{dS_0}{dT} \right) = -\frac{20T_{D3}^2}{\pi T^5} \int_{\sigma_0}^{\infty} d\sigma \frac{4\sigma^2 F(\sigma)}{\sqrt{F^2(\sigma) - F^2(\sigma_0)} \cosh^4 \alpha}, \quad (5.2.13)$$

which indicates that the system has a negative specific heat.

### 5.3 Corrected Thermodynamics for the BIon

Let us now look for the thermal corrections to the above equations by considering logarithmic correction to the entropy  $S$  given by the equation (5.2.6). The entropy (5.2.8) of  $\mathcal{N}$  coincident D-branes, with a throat solution gets corrected as

$$S = \frac{4T_{D3}^2}{\pi T^5} \int_{\sigma_0}^{\infty} d\sigma \frac{4\sigma^2 F(\sigma)}{\cosh^4 \alpha \sqrt{F^2(\sigma) - F^2(\sigma_0)}} - \frac{\gamma}{2} \ln \left[ \frac{4T_{D3}^2}{\pi T^3} \int_{\sigma_0}^{\infty} d\sigma \frac{4\sigma^2 F(\sigma)}{\cosh^4 \alpha \sqrt{F^2(\sigma) - F^2(\sigma_0)}} \right]. \quad (5.3.1)$$

In order to analyze the expression for the corrected entropy, we can assume  $\cosh^2 \alpha(\sigma_0) = \frac{3}{4}$ , which means that  $F(\sigma_0) = 0$  produces a relatively easy solution. It is indeed a possible

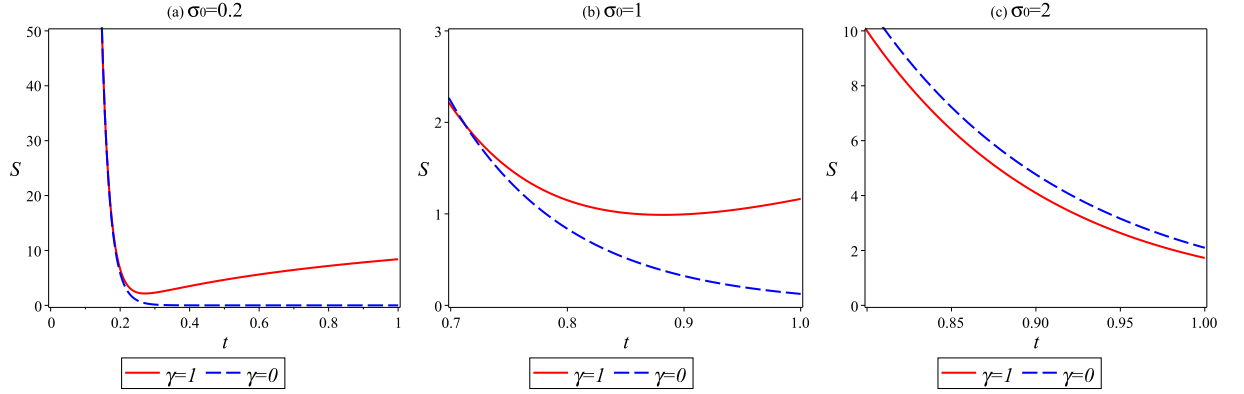


**Figure 5.3.1:** Behavior of the corrected entropy as a function of  $t \equiv \bar{T}$  for  $\mathcal{K} = 1$  and  $T_{D3} = 1$ .

solution of the equation of motion at  $\sigma_0$  (140). However, we would like to work on a regime where the branch is connected to the extremal Blon (140). In this formulation one obtains

$$\cosh^2 \alpha = \frac{3 \cos \frac{\delta}{3} + \sqrt{3} \cos \frac{\delta}{3}}{\cos \delta}, \quad (5.3.2)$$

where  $\cos \delta = \bar{T}^4 \sqrt{1 + \mathcal{K}^2/\sigma^4}$ , with  $\bar{T}^4 = 9\pi^2 T^4 \mathcal{N}/(4\sqrt{3}T_{D3})$ . We further assume an infinitesimal  $\delta$  (corresponding to  $\sigma^2 > \mathcal{K}$  at low temperature  $\bar{T} \approx 1$ ), so that  $\cos \delta \approx 1$  and  $\sin \delta \approx \delta \approx \bar{T}^4 [1 + 1/(2\sigma^4)]$ . Here we have considered  $\mathcal{K} = 1$ , as it can always be absorbed

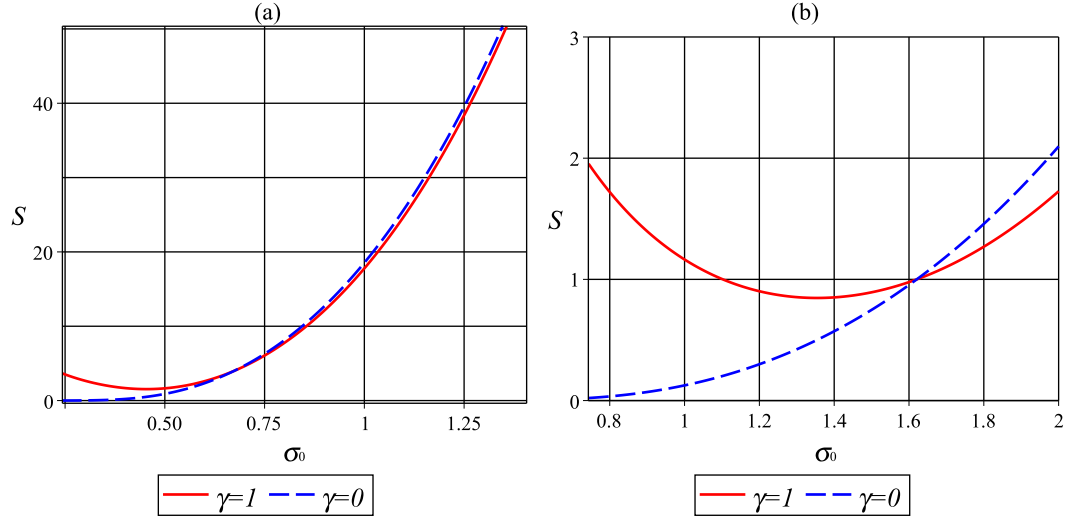


**Figure 5.3.2:** Behavior of the corrected entropy as a function of  $\sigma_0$  for  $\mathcal{K} = 1$ ,  $T_{D3} = 1$  (a)  $\bar{T} = 0.5$  (b)  $\bar{T} = 1$ .

in  $\sigma$  by means of a re-scaling. Now the remaining parameter is  $T_{D3}$ , which we can set to one,  $T_{D3} = 1$ . So, we can plot the corrected entropy (5.3.1) by varying the  $\bar{T}$ ,  $\sigma_0$  and  $\gamma$  as depicted in Figs. 5.3.1, 5.3.2 and 5.3.3. In Fig. 5.3.1, we draw the corrected entropy in terms of  $\bar{T}$  for different values of  $\sigma_0$ . We should note that there is a minimal radius  $\sigma_{min} = \bar{T}^2(1 - \bar{T}^8)^{-\frac{1}{4}}$  corresponding to each plots, with  $\sigma_0 \geq \sigma_{min}$ . In panel (a) of Fig. 5.3.1, we have considered  $\sigma_0 = 0.2$ , such that  $\bar{T} \geq 0.45$  and, in such a situation, we can see that the corrected entropy is larger than the uncorrected one. This means that the logarithmic corrections have increased the value of the entropy. A similar thing happens in panel (b), where  $\sigma_0 = 1$ , thus,  $\bar{T} \geq 0.9$ . However, the system behaves differently, when we consider  $\sigma_0 = 2$  and  $\bar{T} \geq 0.99$ , as shown in Fig. 5.3.1(c). Here we see that the corrected entropy is smaller than the uncorrected entropy. Therefore, the behavior of the entropy with the logarithmic correction depends on both the parameters, namely, the temperature and  $\sigma_0$ .

In Fig. 5.3.2, we plot the corrected entropy as a function of  $\sigma_0$  for  $\bar{T} \geq 0.5$ , i.e.  $\sigma_{min} = 0.25$ . In this case, we see that there exists a critical  $\sigma_c$  for each of the plots, and when the value of  $\sigma_0$  is less than the value of  $\sigma_c$ , the corrected entropy is larger than the uncorrected one. Whereas, when  $\sigma_0 > \sigma_c$ , the corrected entropy is less. However, the critical points depend on the temperature, for instance, in the case when  $\bar{T} = 0.5$ , i.e. in Fig. 5.3.2(a), we notice that  $\sigma_c \approx 0.7$ , while in Fig. 5.3.2(b), i.e. for  $\bar{T} \approx 1$ ,  $\sigma_c \approx 1.6$ . We should note that the region compatible with our assumption is  $\sigma_0 > 1$ . Fig. 5.3.3 demonstrates the behavior of the entropy with respect to  $\gamma$ , which is the coefficient that determines the amount of corrections on the system. By choosing  $\bar{T} \geq 1$ , we can see that the entropy is a decreasing function of  $\gamma$  for  $\sigma_0 = 2$ , while it is an increasing function of  $\gamma$  for  $\sigma_0 = 1$ . It means that for the small throat (smaller than  $\sigma_c$ ), the thermal fluctuation increases the entropy, which may yield more stability to the system, with a maximum value of the entropy. On the other hand, a bigger throat may make the system unstable.

The logarithmic correction also modifies the internal energy and the specific heat. Let us analyze the effects of the modification of the internal energy first, which we compute as follows

$$U = \frac{4T_{D3}^2}{\pi T^4} \int_{\sigma_0}^{\infty} d\sigma F(\sigma) \left[ \sqrt{1 + z'^2(\sigma)} + \frac{4\sigma^2}{\sqrt{F^2(\sigma) - F^2(\sigma_0)} \cosh^4 \alpha} \right]$$

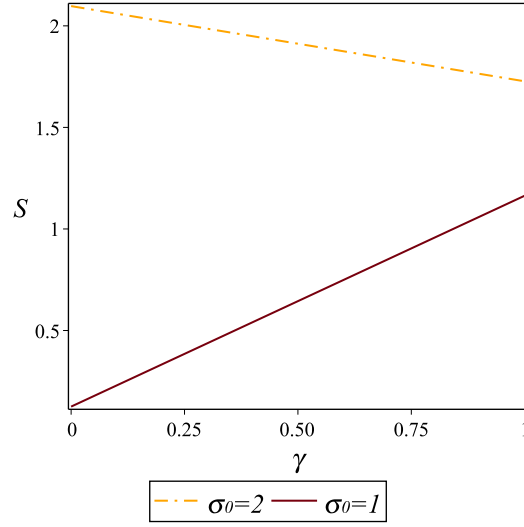


**Figure 5.3.3:** Behavior of the corrected entropy in terms of  $\gamma$  to see cases of  $\gamma = 0$  and  $\gamma = 1$ . We set  $\mathcal{K} = 1$ ,  $\bar{T} = 1$  and  $T_{D3} = 1$ .

$$-\frac{\gamma T}{2} \ln \left[ \frac{4T_{D3}^2}{\pi T^3} \int_{\sigma_0}^{\infty} d\sigma \frac{4\sigma^2 F(\sigma)}{\sqrt{F^2(\sigma) - F^2(\sigma_0)} \cosh^4 \alpha} \right]. \quad (5.3.3)$$

We can perform a graphical analysis similar to the entropy to give similar results. However, we focus only on the internal energy behavior with the parameter  $\gamma$  variation. Fig. 5.3.4

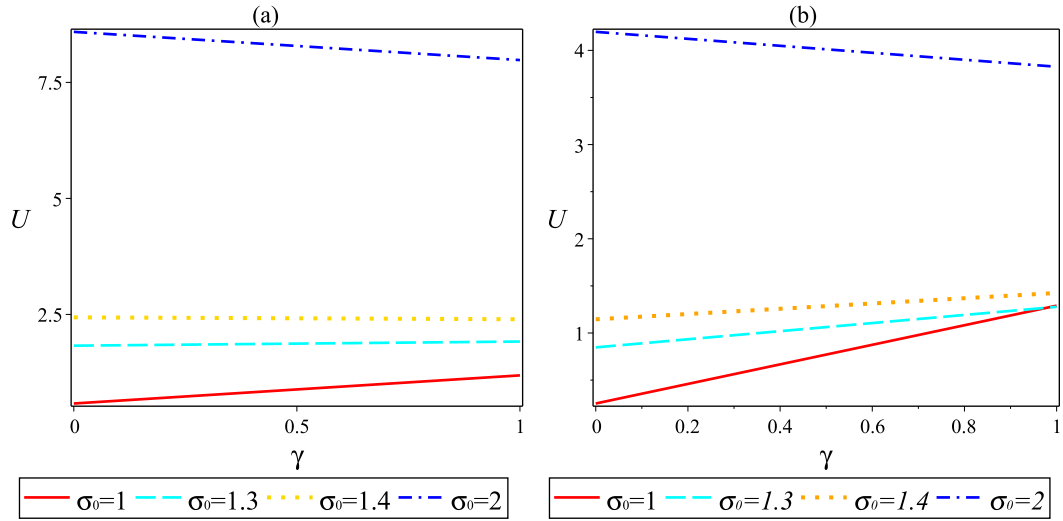


**Figure 5.3.4:** Behavior of internal energy in terms of  $\gamma$ , with  $\mathcal{K} = 1$  and  $T_{D3} = 1$  (a)  $\bar{T} = 0.9$  (b)  $\bar{T} = 1$ .

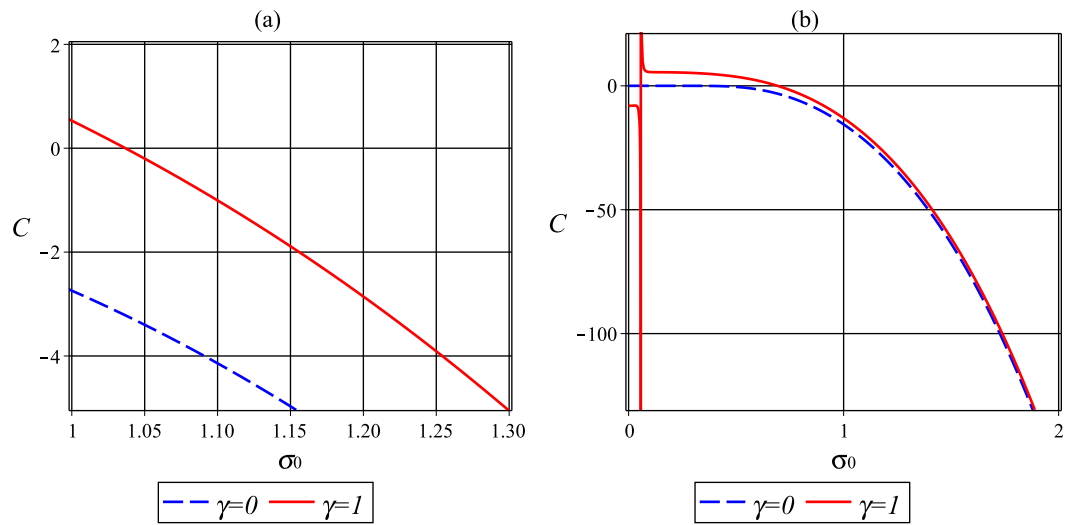


**Figure 5.3.5:** Behavior of the specific heat with respect  $\sigma_0$  for  $\mathcal{K} = 1$  and  $T_{D3} = 1$  (a)  $\bar{T} = 0.9$  (b)  $\bar{T} = 0.7$ .

shows that, although the variation of the internal energy is smaller with the logarithmic corrections, however, the slope of the increasing or decreasing functions depends on the value of the temperature and the radius of the throat, as expected. For a larger radius, the entropy is decreased due to thermal fluctuations, while for a smaller radius, the entropy is increased. Let us now see the effects of the specific heat. The exact expression of the

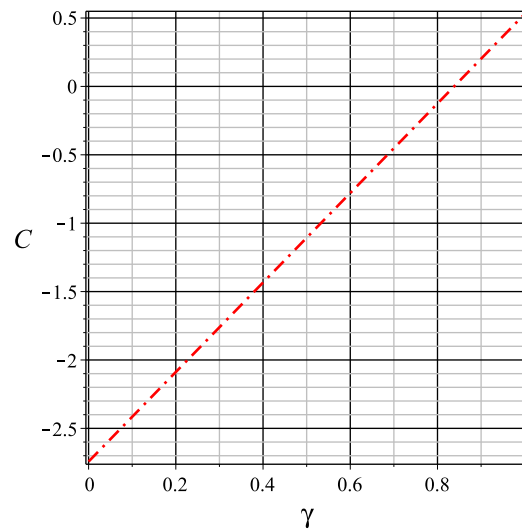


**Figure 5.3.6:** Behavior of the specific heat with respect to  $\gamma$  for  $\mathcal{K} = 1$ ,  $\bar{T} = 0.9$  and  $T_{D3} = 1$ .



corrected specific heat is given by

$$C = T \frac{d}{dT} \left( S - \frac{\gamma}{2} \ln[ST^2] \right), \quad (5.3.4)$$

which has been analyzed in Fig. 5.3.5. Here, we show the effect of the logarithmic correction on the specific heat inside the allowed region  $1 \leq \sigma_0$  for Fig. 5.3.5(a), and for the whole range in Fig. 5.3.5(b) in order to explore the general approximate behavior. In the case of  $\gamma = 0$ , we find that the specific heat is entirely negative; however, in the presence of thermal fluctuations, there are some regions where it is positive. This means that in the presence of the logarithmic correction, there is a special radius  $\sigma_s$  for which the specific heat is negative,  $\sigma_0 > \sigma_s$ , while it is positive for  $\sigma_0 < \sigma_s$ . Here again the value of the  $\sigma_s$  depends on the temperature, for instance, in Fig. 5.3.5(a) it is obvious that when we choose  $\bar{T} = 0.9$ , we obtain  $\sigma_s \approx 1.03$ . On the other hand, in Fig. 5.3.5(b), when we increase  $\sigma_0$ , the difference between the corrected and uncorrected case slowly vanishes. It indicates that the thermal fluctuation becomes relevant for the smaller radius. Also, we can see from Fig. 5.3.5(b) an asymptotic behavior which may be interpreted as a first-order phase transition as found in (140). Here we show that it occurs due to thermal fluctuations. We can confirm this by analyzing the free energy ( $\mathcal{F}$ ) and find that  $\frac{\partial \mathcal{F}}{\partial T} = 0$  at the phase transition point. It is indicated that we have a first-order phase transition in this system.

Also, we demonstrate the variation of the specific heat with the parameter  $\gamma$  in Fig. 5.3.6.

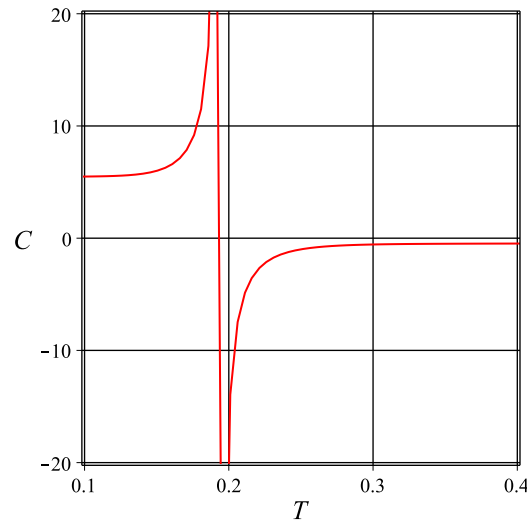


**Figure 5.3.7:** Behavior of the specific heat with respect to  $\bar{T}$  for  $\mathcal{K} = 1$ ,  $\sigma_0 = 0.02$  and  $T_{D3} = 1$ .

It is evident that the effect of the logarithmic correction is to increase the specific heat and, for  $\gamma > 0.65$  (approximately) the specific heat is entirely positive, while for  $\gamma = 0$ , it is completely negative. Finally in the Fig. 5.3.7, we can analyze the variation of the specific heat with  $\bar{T}$  to plot its asymptotic behavior. At this asymptotic point, the first derivative of the free energy with respect to the temperature is zero, so it is a first-order phase transition.

## 5.4 Conclusion

Quantum fluctuations are essential when dealing with objects of very small length scales. They can be neglected when the object is large compared to the Planck scale, but quantum fluctuation becomes vital for small objects. Now at the Planck scale, the background spacetime breaks down, and it isn't easy to analyze this system. However, there is a stage before such a total breakdown when the quantum fluctuations can not be neglected but can be analyzed as perturbations around a fixed spacetime. This corresponds to analyzing thermal fluctuations around equilibrium for a black hole. We analyze the quantum corrections for the Bionic systems using such fluctuations around the equilibrium. We explicitly include the correction terms produced by such thermal fluctuations. After including these correction terms, we also analyze the system's behavior at the critical points. Moreover, we demonstrate that these correction terms are essential by analyzing the stability conditions for this system. In fact, we can show numerically that these quantum fluctuation affects the critical points, thus affecting the stability of the system. The stability increases under certain conditions. For instance, when the throat is more minor, the inclusion of fluctuations increases the stability. Our analysis explicitly shows how the quantum fluctuation terms become essential with the decrease of the radius. In Fig. 5.3.5(b), we observe that by increasing the radius  $\sigma_0$ , the correction term slowly vanishes, and the corrected result becomes identical to the uncorrected one. Apart from the stability analysis, we have computed the corrections to the internal energy and specific heat due to the quantum fluctuation. We confirmed that the first-order phase transition occurs in this system by analyzing the free energy. We have also analyzed the change in the behavior of the corrected system with the temperature.

It may be noted that here we have only analyzed the system numerically. However, to demonstrate that the system actually has phase transition, it is essential to analyze it analytically. It would thus be necessary to examine this system analytically. However, as this system is very complicated, it might be interesting to study a simpler model of black branes analytically. Such an analysis can give a better under fluctuations that affect the

system. It is possible to construct a BIon system's stabilizing system of M2-branes, and M5-branes (200). It would be interesting to analyze the system at a finite temperature. Then the thermodynamics of this system can be studied. It would be possible to study the quantum fluctuations to the geometry of a BIon in M-theory, which could produce thermal fluctuations in the thermodynamics of this system. It would be interesting to analyze the critical points for such a system and study the effects of these fluctuations on the stability of this system. It may also be noted that the thermodynamics of the AdS black hole has been studied in M-theory (201; 202). It is possible to analyze the quantum corrections to these black holes, which can also be done in Euclidean Quantum Gravity. It would also be interesting to generalize the work of this chapter to such AdS black holes in M-theory.



## Chapter 6

# Lorentzian path integral of 3D pure gravity

### 6.1 Introduction

In this chapter, we try to analyze the path integral for pure 3D gravity by using Hamiltonian formalism, which will assist in defining the path integral measure and the boundary term of the action. For a non-relativistic point particle, the path integral can be viewed as a lattice regularization in analogy with Riemann integral. We divide the time interval into small units of  $\epsilon$  and sum over all paths in each interval of measure  $\epsilon$ .

$$K \sim \int \prod_{i=1}^{N-1} dx_i e^{-iS(x)/\hbar} \quad (6.1.1)$$

The Hamiltonian formalism allows us to paint a picture analogous to a point particle. ADM decomposition lets us foliate the 2+1 D spacetime into constant time hypersurface. Now we can see where it is going; it is analogous to dividing the time interval into  $\epsilon$ 's for the point particle. So, we must have fixed initial and final surfaces and sum over all the geometries to get the gravitational path integral. For example, consider the initial and final surfaces to be of the naked singularity and BTZ black hole, respectively. This builds a platform for calculating transition amplitudes/probabilities between these geometries. That sounds ambitious and promising, but unfortunately, we can't go very far with it!

The set of all surfaces is called super-space, and the metric defined in this space is the

Wheeler-DeWitt metric ( $G_{ijkl}$ ). We define the gravitational measure by again drawing inspiration from the point particle. The point particle Lagrangian is

$$L_{pp} = g_{\mu\nu} \dot{x}^\mu \dot{x}^\nu - V \quad (6.1.2)$$

and the determinant of the coefficient of the kinetic term, that is,  $|g_{\mu\nu}|$  goes into defining the probability amplitude or the transition amplitude between any two quantum wave functions

$$Z_{pp} = \langle \psi | \phi \rangle = \int dx \sqrt{-g} \psi^* \phi \quad (6.1.3)$$

In the next section, we will see how we can write the gravitational Lagrangian in a form analogous to  $L_{pp}$ ,

$$L = \int d^2x \left[ \frac{\sqrt{g}}{4N} G^{ijkl} \dot{g}_{ij} \dot{g}_{kl} - \frac{\sqrt{g}}{N} G^{ijkl} (\dot{g}_{ij} N_{l|k} + N_{i|j} N_{l|k}) + N \sqrt{g} (R - 2\Lambda) \right] \quad (6.1.4)$$

## 6.2 Proposal for the gravitational path integral measure

We have a spacetime manifold with topology  $\mathbb{R} \times \Sigma$ , where  $\Sigma$  is a time constant spacelike hypersurface which in the case of 2+1 gravity is just a two-geometry or a two-dimensional surface. That is, we slice the bulk manifold for constant times  $t$ .  $\Sigma$  will have coordinates  $x^i$ , where ( $i = 1, 2$ ) along with an induced metric  $g_{ij}(t, x)$ . Normal deformation or displacement of  $\Sigma$  is given in terms of a lapse function  $N = (-g^{00})^{-1/2}$  while the shift function gives the deformations along the hypersurface  $N^i = g^{ij} g_{oj}$ .

Induced metric on  $\Sigma$  is given using the metric on the full spacetime  $g_{\mu\nu}$  as

$$g_{ij} = e^\mu{}_i e^\nu{}_j g_{\mu\nu} \quad (6.2.1)$$

Extrinsic curvature contains the velocity term

$$K_{ij} = \frac{1}{2N} (-\dot{g}_{ij} + N_{i|j} + N_{j|i}) \quad (6.2.2)$$

here the vertical bars in  $N_{i|j}$  represent covariant derivative with respect to the induced metric  $g_{ij}$  in  $\Sigma$ . The next step is to separate second-time derivatives from the gravitational

Lagrangian by adding a divergence term

$$L = \int d^2x \mathcal{L} = \int d^2x N \sqrt{{}^{(2)}g} \left( K^{ij} K_{ij} - K^2 + {}^{(2)}R - 2\Lambda \right) - \int d^2x \left[ 2\partial_t(\sqrt{{}^{(2)}g}K) - \partial_i \left( \sqrt{{}^{(2)}g}K N^i - \sqrt{{}^{(2)}g}g^{ij}\partial_j N \right) \right] \quad (6.2.3)$$

We can write this Lagrangian in the form of kinetic and potential term

$$L = \int d^2x \left[ \frac{\sqrt{{}^{(2)}g}}{4N} G^{ijkl} \dot{g}_{ij} \dot{g}_{kl} - \frac{\sqrt{{}^{(2)}g}}{N} G^{ijkl} (\dot{g}_{ij} N_{l|k} + N_{i|j} N_{l|k}) + N \sqrt{{}^{(2)}g} ({}^{(2)}R - 2\Lambda) \right] - \int d^2x \left[ 2\partial_t(\sqrt{{}^{(2)}g}K) - \partial_i \left( \sqrt{{}^{(2)}g}K N^i - \sqrt{{}^{(2)}g}g^{ij}\partial_j N \right) \right] \quad (6.2.4)$$

where,

$$G_{ijkl} = \frac{1}{2} (g_{ik}g_{jl} + g_{il}g_{jk} - 2g_{ij}g_{kl}) \quad (6.2.5)$$

$$G^{ijkl} = \frac{1}{2} (g^{ik}g^{jl} + g^{il}g^{jk} - 2g^{ij}g^{kl}) \quad (6.2.6)$$

is known as the Wheeler-DeWitt metric. This is a metric on the superspace, which is a space of all  $g_{ij}$  associated with a surface  $\Sigma$ . From now on exclusively in this chapter we will write  $N^\perp \equiv N$ ,  $\sqrt{{}^{(2)}g} \equiv \sqrt{g}$  and  ${}^{(2)}R$  is the intrinsic curvature associated with  $\Sigma$  which depends on  $g_{ij}$ . So, we have

$$L = \int d^2x \left[ \frac{\sqrt{g}}{4N} G^{ijkl} \dot{g}_{ij} \dot{g}_{kl} - \frac{\sqrt{g}}{N} G^{ijkl} (\dot{g}_{ij} N_{l|k} + N_{i|j} N_{l|k}) + N \sqrt{g} (R - 2\Lambda) \right] \quad (6.2.7)$$

The coefficient of the kinetic term is taken to be the weight functional for the measure

$$w[g] = \sqrt{-\left(\frac{\sqrt{g}}{4N}\right)^3 |G|} = \frac{1}{8N^{3/2}g^{3/4}} \quad (6.2.8)$$

Details of the calculation of  $|G|$  are given in the appendix A3. Here the dynamics are over the space of metrics, which is the superspace, with the metric on the superspace being  $G_{ijkl}$ . So the path integral will sum over all the three-geometries.

$$Z = \int \frac{\mathcal{D}g_{ij} \mathcal{D}\dot{g}_{ij}}{8N^{3/2}g^{3/4}} e^{-\frac{i}{\hbar} (\int dt L[g_{ij}, \dot{g}_{ij}] + \mathcal{B}[g_{ij}, \dot{g}_{ij}])} \quad (6.2.9)$$

### 6.3 Gravitational Hamiltonian and the Boundary term

We now make a transition from the configuration space  $(g_{ij}, \dot{g}_{ij})$  to the phase space  $(g_{ij}, \pi^{ij})$  by defining the conjugate momenta of  $g_{ij}$

$$\pi^{ij} = \frac{\partial \mathcal{L}}{\partial \dot{g}_{ij}} = -\sqrt{g} (K^{ij} - K g^{ij}) \quad (6.3.1)$$

$$\begin{aligned} \pi^i_j &= -\sqrt{g} (K^i_j - K \delta^i_j) \\ &= -\frac{\sqrt{g}}{N} \left[ \frac{1}{2} (N^i_{|j} + g_{jl} g^{ik} N^l_{|k}) - N^k_{|k} \delta^i_j \right] \end{aligned} \quad (6.3.2)$$

We can now express the velocities in terms of conjugate momenta  $\pi^{ij}$

$$\dot{g}_{ij} = \frac{2N}{\sqrt{g}} (\pi_{ij} - \pi g_{ij}) + N_{i|j} + N_{j|i} \quad (6.3.3)$$

With that, we can write down the canonical Hamiltonian for gravity

$$\begin{aligned} \mathcal{H}_c &= \pi^{ij} \dot{g}_{ij} - \mathcal{L} \\ H &= \int d^2x \mathcal{H}_c = \int d^2x [N\mathcal{H} + N^i \mathcal{H}_i] \\ &= \int d^2x \left[ \frac{N}{\sqrt{g}} G_{ijkl} \pi^{ij} \pi^{kl} - N\sqrt{g} (R - 2\Lambda) - 2N_i \pi^{ij}_{|j} \right] \end{aligned} \quad (6.3.4)$$

The constraints are

$$\mathcal{H} = \frac{1}{\sqrt{g}} G_{ijkl} \pi^{ij} \pi^{kl} - \sqrt{g} (R - 2\Lambda) \quad (6.3.5)$$

$$\mathcal{H}_i = -2\pi^{ij}_{|j} \quad (6.3.6)$$

The action in phase space variables is

$$I[g_{ij}, \pi^{ij}] = \frac{1}{16\pi G_3} \int dt L + \mathcal{B} = \frac{1}{16\pi G_3} \int dt d^2x [\pi^{ij} \dot{g}_{ij} - \mathcal{H}_c] + \mathcal{B} \quad (6.3.7)$$

We will set  $G_3 = \frac{1}{8}$  only in this chapter. Einstein's equation can be reproduced as Hamilton's equation of motion ( $\dot{g}_{ij} = \delta H_c / \delta \pi^{ij}$ ;  $\dot{\pi}^{ij} = -\delta H_c / \delta g_{ij}$ ) by demanding the surface terms to vanish which is done by taking the variation of the boundary term to be negative of the surface terms (203), to within a constant. The geometries we are interested in are time-independent  $\dot{g}_{ij} = 0$ , so the action after taking into account constraints  $\mathcal{H} = 0$  and

$\mathcal{H}_i = 0$  consists of the surface terms. The action, in terms of the constraints, is

$$I = -\frac{1}{2\pi} \int dt d^2x [N\mathcal{H}_\perp + N^i\mathcal{H}_i] + \mathcal{B}[g_{ij}, \pi^{ij}] \quad (6.3.8)$$

whose variation produces surface terms to be canceled by the boundary term.

$$\begin{aligned} \delta I = & -\frac{1}{2\pi} \int dt d^2x [A^{ij}\delta g_{ij} + B_{ij}\delta\pi^{ij}] \\ & + \frac{1}{2\pi} \int dt ds_l \left[ g^{1/2} G^{ijkl} (\hat{\xi}^\perp \delta g_{ij;k} - \hat{\xi}_{,k}^\perp \delta g_{ij}) + 2\hat{\xi}^i \delta\pi^l{}_i + (2\hat{\xi}^i \pi^k{}_m g^{lm} - \hat{\xi}^l \pi^i{}_m g^{km}) \delta g_{ik} \right] \\ & + \delta \mathcal{B} = 0 \end{aligned} \quad (6.3.9)$$

The boundary term is

$$\delta \mathcal{B} = -\frac{1}{2\pi} \int dt ds_l \left[ g^{1/2} G^{ijkl} (\hat{\xi}^\perp \delta g_{ij;k} - \hat{\xi}_{,k}^\perp \delta g_{ij}) + 2\hat{\xi}^i \delta\pi^l{}_i + (2\hat{\xi}^i \pi^k{}_m g^{lm} - \hat{\xi}^l \pi^i{}_m g^{km}) \delta g_{ik} \right] \quad (6.3.10)$$

where, the surface integral contains a normal vector  $n_l = \delta_l^r \sqrt{g_{rr}}$  pointing in the radial direction

$$ds_l = n_l d\phi \sqrt{g_{\phi\phi}} = d\phi \sqrt{g_{rr} g_{\phi\phi}} \delta_l^r \quad (6.3.11)$$

$\hat{\xi}^\mu$  are the deformation vectors related to the  $N^\mu$  and killing vectors as

$$\hat{\xi}^\perp = N \xi^t \quad (6.3.12)$$

$$\hat{\xi}^r = \xi^r + N^r \xi^t \quad (6.3.13)$$

$$\hat{\xi}^\phi = \xi^\phi + N^\phi \xi^t \quad (6.3.14)$$

The conformal killing vectors are (204)

$$\xi^t = lT(t, \phi) + \frac{l^3}{r^2} \bar{T}(t, \phi) + O(r^{-4}) \quad (6.3.15)$$

$$\xi^r = rR(t, \phi) + O(r^{-1}) \quad (6.3.16)$$

$$\xi^\phi = \Phi(t, \phi) + \frac{l^2}{r^2} \bar{\Phi}(t, \phi) + O(r^{-4}) \quad (6.3.17)$$



and relations among them are

$$l\partial_t T(t, \phi) = \partial_\phi \Phi(t, \phi) = -R(t, \phi) \quad (6.3.18)$$

$$l\partial_t \Phi(t, \phi) = \partial_\phi T(t, \phi) \quad (6.3.19)$$

$$\bar{T}(t, \phi) = -\frac{l}{2} \partial_t R(t, \phi) \quad (6.3.20)$$

$$\bar{\Phi}(t, \phi) = \frac{1}{2} \partial_\phi R(t, \phi) \quad (6.3.21)$$

We can break down all these expressions into left movers and right movers by looking at

$$\begin{aligned} l\partial_t^2 T(t, \phi) &= \partial_\phi \partial_t \Phi(t, \phi) \quad \text{and} \quad l\partial_\phi \partial_t \Phi(t, \phi) = \partial_\phi^2 T(t, \phi) \\ l\partial_\phi \partial_t T(t, \phi) &= \partial_\phi^2 \Phi(t, \phi) \quad \text{and} \quad l\partial_t^2 \Phi(t, \phi) = \partial_\phi \partial_t T(t, \phi) \\ \implies \square T &= 0 \quad \text{and} \quad \square \Phi = 0 \end{aligned} \quad (6.3.22)$$

Before looking at the solutions of these wave equations, let's make a coordinate transformation to  $x^\pm$

$$t = \frac{l}{2}(x^+ + x^-) \quad \text{and} \quad \phi = \frac{1}{2}(x^+ - x^-) \quad (6.3.23)$$

$$l\partial_t = \partial_+ + \partial_- \quad \text{and} \quad \partial_\phi = \partial_+ - \partial_- \quad (6.3.24)$$

In these coordinates, solutions to the wave equations are

$$T(t, \phi) = T^+(x^+) + T^-(x^-) \quad (6.3.25)$$

$$\Phi(t, \phi) = T^+(x^+) - T^-(x^-) \quad (6.3.26)$$

using which we get

$$R = -(\partial_+ T^+ + \partial_- T^-) \quad (6.3.27)$$

$$\bar{T} = \frac{1}{2}(\partial_+^2 T^+ + \partial_-^2 T^-) \quad (6.3.28)$$

$$\bar{\Phi} = -\frac{1}{2}(\partial_+^2 T^+ - \partial_-^2 T^-) \quad (6.3.29)$$

Now the asymptotic Killing vectors can be decomposed into left and right coordinates

$$\xi^t = l(T^+ + T^-) + \frac{l^3}{2r^2}(\partial_+^2 T^+ + \partial_-^2 T^-) + O(r^{-4}) \quad (6.3.30)$$

$$\xi^r = -r (\partial_+ T^+ + \partial_- T^-) + O(r^{-1}) \quad (6.3.31)$$

$$\xi^\phi = T^+ - T^- - \frac{l^2}{2r^2} (\partial_+^2 T^+ - \partial_-^2 T^-) + O(r^{-4}) \quad (6.3.32)$$

Let

$$\xi^+ = T^+ + \frac{l^2}{2r^2} \partial_-^2 T^- \quad \text{and} \quad \xi^- = T^- + \frac{l^2}{2r^2} \partial_+^2 T^+ \quad (6.3.33)$$

$$\implies \xi^t = l(\xi^+ + \xi^-) \quad \text{and} \quad \xi^\phi = \xi^+ - \xi^- \quad (6.3.34)$$

The boundary conditions specify the behavior of the canonical coordinates  $(g_{ij}, \pi^{ij})$  and of  $N^\mu$  at the spatial infinity, which at the classical level should have the form of

$$ds^2 \rightarrow -r^2 dt^2 + \frac{dr^2}{r^2} + r^2 d\phi^2$$

Boundary conditions follow from (204), and the sub-leading terms might hold the information on the quantum structure of the geometry

$$g_{rr} = \frac{l^2}{r^2}, \quad g_{r\phi} = \frac{f_{r\phi}}{r^3}, \quad g_{\phi\phi} = r^2 + Ml^2 \quad (6.3.35)$$

$$N = r + \frac{f^\perp}{r}, \quad N^r = \frac{f^r}{r}, \quad N^\phi = \frac{f^\phi}{r^2} \quad (6.3.36)$$

$$\pi^r_r \sim O(r^{-3}), \quad \pi^r_\phi \sim J/l + O(r^{-2}), \quad \pi^\phi_r \sim O(r^{-4}), \quad \pi^\phi_\phi \sim O(r^{-3}) \quad (6.3.37)$$

and for the inverse

$$g^{rr} \sim g_{\phi\phi} = r^2 + Ml^2, \quad g^{r\phi} \sim -g_{r\phi} = -\frac{f_{r\phi}}{r^3}, \quad g^{\phi\phi} \sim g_{rr} = \frac{1}{r^2} \quad (6.3.38)$$

variations -

$$\delta g_{rr} = 0, \quad \delta g_{r\phi} = \frac{\delta f_{r\phi}}{r^3}, \quad \delta g_{\phi\phi} = \delta M \quad (6.3.39)$$

Under these boundary conditions, the leading contributions to the boundary term are

$$\begin{aligned} \delta \mathcal{B} &= - \lim_{r \rightarrow \infty} \frac{1}{2\pi} \int dt d\phi \left\{ \xi^t \delta M + \xi^\phi \delta J \right\} \\ &= - \lim_{r \rightarrow \infty} \frac{1}{2\pi} \int dt d\phi \delta \left\{ \xi^t M + \xi^\phi J \right\} \end{aligned} \quad (6.3.40)$$

This can be integrated to give the boundary term along with a constant of integration

$$\mathcal{B} = -(t_2 - t_1) \left( \xi^t M + \xi^\phi J \right) \quad (6.3.41)$$

The path integral over the phase space variables is

$$Z = \int \mathcal{D}g_{ij} \mathcal{D}\pi^{ij} \sqrt{-\left(\frac{\sqrt{g}}{4N}\right)^3 |G|} e^{-\frac{i}{2\pi\hbar} \left( \int dt d^2x [\pi^{ij} \dot{g}_{ij} - \mathcal{H}_c] + 2\pi\mathcal{B} \right)} \quad (6.3.42)$$

We calculated the boundary term for the mini-superspace and not the full superspace, so the partition function for the mini-superspace is

$$Z = \int \frac{dM dJ}{8N^{3/2}g^{3/4}} e^{\frac{i(t_2-t_1)}{\hbar} (\xi^t M + \xi^\phi J)} \quad (6.3.43)$$

For the mini-superspace geometries, we have

$$N^{3/2}g^{3/4} = r^{3/2} \quad (6.3.44)$$

and the r here is like trace index, which we must integrate out! After that

$$Z = \frac{1}{8} \int_{-\infty}^{\infty} dM \int_{-M}^M dJ e^{\frac{i(t_2-t_1)}{\hbar} (\xi^t M + \xi^\phi J)} \quad (6.3.45)$$

$$= \frac{\hbar}{4(t_2-t_1)\xi^\phi} \int_{-\infty}^{\infty} dM \sin\left(\frac{(t_2-t_1)\xi^\phi}{\hbar} M\right) e^{-i\frac{(t_2-t_1)}{\hbar} \xi^t M} \quad (6.3.46)$$

This is an oscillatory integral, and we don't know how to handle it! Picard-Lefschetz's theory has recently been applied to oscillatory integrals (205) to make the Lorentzian path integral more robust! The crux of the approach implements the steepest descent over complex contours to make the integral absolutely convergent. The problem we ran into applying these techniques in 2+1 gravity is that the saddle points of the action are not well-defined as it is linear in M and J, not quadratic.

## Chapter 7

# Partition function of 3D pure gravity

### 7.1 Introduction

The path toward understanding the quantum mechanics of the gravitational field is arduous. The natural setting of the universe is in terms of the Lorentzian signature for the metric. Lorentzian signature geometries are harder to tame, and so far, there have not been significant advancements in our understanding of quantum gravity (QG). Experiments were the key to initial successes and further developments of the quantum mechanics and quantum field theories of electrodynamics, strong and weak interactions in the 20th century. Of course, the other side of this success story is theory and mathematics. Developing theories and experiments are essential for advancing our fundamental understanding of nature. That being said, we are still struggling to shed some light on the QG because of the lack of experiments and observations. Unfortunately, this chapter will discuss theoretical results toward our understanding of the QG. Hopefully, we will have more to say on the experimental side in the future!

We will focus on the  $2 + 1$  AdS pure gravity as this theory is rich in various features shared by  $3 + 1$  gravity. There are numerous reasons to study  $2 + 1$  AdS gravity; one of them is they have zero degrees of freedom (DoF). Even with the simplicity of the zero DoF, we are faced with the challenges of handling a Lorentzian metric and an oscillatory integral, as we saw in the previous chapter. We want to simplify the model by tweaking a few game rules. Doing so puts us in a different physical scenario, the Euclidean world, in contrast with the Lorentzian world. These two worlds are not equivalent, as a coordinate transformation does not relate to them. We can still learn some exciting features from the Euclidean sector,

which could improve our insights into the Lorentzian sector.

Euclidean sector allows us to define a canonical ensemble of inverse temperature  $\beta$ . We can construct a canonical partition function for this ensemble and derive various thermodynamical quantities, like the internal energy and entropy. We can think of this canonical ensemble as one of an ideal gas as the individual geometries don't interact with each other.

## 7.2 BTZ mini-superspace of 2+1 AdS gravity

The BTZ mini-superspace contains all the 2 + 1 AdS stationary geometries. They consist of BTZ black holes, conical defects and excesses (CD/CE), and over-spinning (OS) singularities, (4; 5). The Euclidean mini-superspace consists of the metric with imaginary Lorentzian time ( $t = -i\tau$ ),

$$ds^2 = N^2(r)d\tau^2 + \frac{dr^2}{N^2(r)} + r^2 \left( d\phi + N^\phi(r)d\tau \right)^2 \quad (7.2.1)$$

$$N^2(r) = \left( \frac{r^2}{l^2} - 8GM + \frac{16G^2J^2}{r^2} \right), \quad N^\phi(r) = -\frac{4GJ}{r^2} \quad (7.2.2)$$

where,  $M, J \in \mathcal{R}$ . Geometries are classified based on the values of  $M$  and  $J$ . BTZ black hole have  $M \geq J/l \geq 0$ , CD/CE have  $M < -|J|/l$  and OS have  $|M| \leq |J|/l$ . We will discard OS geometries in this discussion and focus exclusively on the BTZ black hole and CD/CE.

Roots of  $N^2(r) = 0$  correspond to the horizons ( $r_\pm$ ) of the black hole,

$$r_\pm = \pm l\sqrt{2G} \left[ \sqrt{M + iJ/l} \pm \sqrt{M - iJ/l} \right] \quad (7.2.3)$$

$$M = \frac{r_+^2 + r_-^2}{8Gl^2} \quad \text{and} \quad J = \frac{ir_+r_-}{4Gl} \quad (7.2.4)$$

For NS we have,  $M < 0$  and  $J \leq |M|$  with  $M = -|M|$ . The roots of  $N^2(r) = 0$  for NS are given by  $\lambda_\pm$

$$\lambda_\pm = \mp il\sqrt{2G} \left[ \sqrt{|M| + iJ/l} \pm \sqrt{|M| - iJ/l} \right] \quad (7.2.5)$$

$$|M| = -\frac{\lambda_+^2 + \lambda_-^2}{8Gl^2} \quad \text{and} \quad J = \frac{i\lambda_+\lambda_-}{4Gl} \quad (7.2.6)$$

### 7.3 Temperature of Naked Singularities (NS)

In the Euclidean version of geometries, the period in time and angular coordinate correspond to the  $\beta$  and  $\Phi$ . The periods of the Euclidean BTZ were found in (206) by making identifications in hyperbolic three-space  $\mathbb{H}^3$ . The boundary topology of the Lorentzian solution is cylindrical, which turns into a two-torus with a Dehn twist after identifying in  $\tau$  and  $\phi$ . Here, we extend this analysis to the Euclidean version of the BTZ mini-superspace naked singularities (CD/CE).

We proceed by changing the coordinates to the cartesian coordinates for the upper half-plane.

$$x = \left( \frac{r^2 - \lambda_-^2}{r^2 - \lambda_+^2} \right)^{1/2} \cos \left( \frac{|\lambda_+|}{l} \phi + \frac{\lambda_-}{l^2} \tau \right) e^{\frac{|\lambda_+|}{i^2} \tau - \frac{\lambda_-}{l} \phi} \quad (7.3.1)$$

$$y = \left( \frac{r^2 - \lambda_-^2}{r^2 - \lambda_+^2} \right)^{1/2} \sin \left( \frac{|\lambda_+|}{l} \phi + \frac{\lambda_-}{l^2} \tau \right) e^{\frac{|\lambda_+|}{i^2} \tau - \frac{\lambda_-}{l} \phi} \quad (7.3.2)$$

$$z = \left( \frac{\lambda_-^2 - \lambda_+^2}{r^2 - \lambda_+^2} \right)^{1/2} e^{\frac{|\lambda_+|}{i^2} \tau - \frac{\lambda_-}{l} \phi} \quad (7.3.3)$$

where,  $|\lambda_+| = i\lambda_+$  and  $r \geq \lambda_-$ . This is startling as the Euclidean NS acquires a horizon in the form of  $\lambda_-$ . The singularity is only exposed for the geometries with  $J = 0$ . The metric in these coordinates is

$$ds^2 = \frac{l^2}{z^2} (dx^2 + dy^2 + dz^2) \quad (7.3.4)$$

These coordinates are invariant under the identifications ( $\tau \sim \tau + \beta$ ,  $\phi \sim \phi + \Phi$ ), where the periods are

$$\beta^{NS} = \frac{2\pi l^2 |\lambda_+|}{\lambda_-^2 - \lambda_+^2} \quad \text{and} \quad \Phi^{NS} = \frac{2\pi l \lambda_-}{\lambda_-^2 - \lambda_+^2} \quad (7.3.5)$$

If we wake up in the Euclidean world, we won't be able to differentiate between the time and angular directions as both are circular. The temperature has to be well-defined, so the inverse temperature  $\beta$  has to be associated with the periodicity in the time direction. This discloses to us which is the actual temporal direction. The temperature of  $AdS_3$  vacuum with  $|M| = 1$  and  $J = 0$  is

$$\beta^{AdS_3} = \frac{2\pi l}{\sqrt{8G}} \quad (7.3.6)$$

For the BTZ black hole, the periods are,

$$\beta^{BTZ} = \frac{2\pi l^2 r_+}{r_+^2 - r_-^2} \quad \text{and} \quad \Phi^{BTZ} = \frac{2\pi l |r_-|}{r_+^2 - r_-^2} \quad (7.3.7)$$

## 7.4 Partition function

The well-known Euclidean action for the BTZ black is (4; 206)

$$I_{BTZ} = -\beta^{BTZ} (M - \Omega^{BTZ} J) + \frac{\pi l}{\sqrt{2G}} \left[ \sqrt{M + iJ/l} + \sqrt{M - iJ/l} \right] \quad (7.4.1)$$

The first two terms come from the asymptotic boundary, while the last term is from the interior boundary at the outer horizon. In the same spirit, we have the Euclidean action for a Euclidean naked singularity is

$$I_{NS} = \beta^{NS} (|M| + \Omega^{NS} J) + \frac{i\pi l}{\sqrt{2G}} \left[ \sqrt{|M| + iJ/l} - \sqrt{|M| - iJ/l} \right] \quad (7.4.2)$$

In the saddle point approximation, we can recover the Bekenstein-Hawking entropy for the BTZ black hole along with the log correction, which arises from the Jacobian of the partition function. The partition function has the form,

$$\mathcal{Z}[\beta, \Phi] = \frac{G}{\hbar} \int dM dJ \rho(M, J) e^{I[\beta, \Phi; M, J]/\hbar} \quad (7.4.3)$$

The Jacobian of the transformation of  $(M, J)$  to  $(r_+, r_-)$

$$|\mathcal{J}| = -\frac{i(r_+^2 - r_-^2)}{16G^2} \quad (7.4.4)$$

The partition function measure holds the information coming from the quantum regime and makes itself explicit as a logarithmic correction

$$dM dJ = |\mathcal{J}| dr_+ dr_- \quad (7.4.5)$$

The partition function in 7.4.3 becomes,

$$\mathcal{Z}_{BTZ}[\beta, \Phi] = -\frac{i}{16} \int dr_+ dr_- \frac{(r_+^2 - r_-^2)}{G^2 \hbar^2} e^{-\beta \left( \frac{r_+^2 + r_-^2}{8Gl^2 \hbar} - \Omega \frac{ir_+ r_-}{4Gl \hbar} \right) + \frac{2\pi r_+}{4G \hbar}}$$

$$\approx e^{-\beta\left(\frac{r_+^2+r_-^2}{8Gl^2\hbar}-\Omega\frac{ir_+r_-}{4Gl\hbar}\right)+\frac{2\pi r_+}{4G\hbar}+\ln\left(\frac{r_+^2-r_-^2}{G^2\hbar^2}\right)} \quad (7.4.6)$$

Therefore, we have

$$\ln \mathcal{Z}_{BTZ}[\beta, \Phi] \approx -\beta\left(\frac{r_+^2+r_-^2}{8Gl^2\hbar}-\Omega\frac{ir_+r_-}{4Gl\hbar}\right)+\frac{2\pi r_+}{4G\hbar}+\ln\left(\frac{r_+^2-r_-^2}{G^2\hbar^2}\right) \quad (7.4.7)$$

The canonical ensemble entropy is

$$\begin{aligned} S_{BH} &= (1 - \beta\partial_\beta) \ln \mathcal{Z}_{BTZ}[\beta, \Phi] \\ &= \frac{2\pi r_+}{4G\hbar} + \ln\left(\frac{r_+^2-r_-^2}{G^2\hbar^2}\right) \end{aligned} \quad (7.4.8)$$

The log correction matches the log correction found by doing CFT calculations in the microcanonical ensemble but with a different numerical coefficient (3/2 for the CFT calculations). Logarithmic correction to the BTZ black hole entropy was first found by Carlip (207), and he speculated that the numerical factor of 3/2 would be universal if the entropy is calculated from a single CFT. This numerical factor is nothing more than an artifact of the CFT calculation. Although, this numerical factor and the form of the log correction match its 3 + 1 counterpart (208). Here, we got the quantum correction to the black hole entropy without implementing any techniques from CFT.

Using similar tools for the Euclidean naked singularity, which has forged an outer horizon-like artifact ( $\lambda_-$ ), we get

$$\ln \mathcal{Z}_{NS}[\beta, \Phi] \approx \beta\left(-\frac{\lambda_+^2+\lambda_-^2}{8Gl^2\hbar}+\Omega\frac{i\lambda_+\lambda_-}{4Gl\hbar}\right)+\frac{2\pi\lambda_-}{4G\hbar}+\ln\left(\frac{\lambda_-^2-\lambda_+^2}{G^2\hbar^2}\right) \quad (7.4.9)$$

The canonical ensemble entropy is

$$\begin{aligned} S_{NS} &= (1 - \beta\partial_\beta) \ln \mathcal{Z}_{NS}[\beta, \Phi] \\ &= \frac{2\pi\lambda_-}{4G\hbar} + \ln\left(\frac{\lambda_-^2-\lambda_+^2}{G^2\hbar^2}\right) \end{aligned} \quad (7.4.10)$$

For non-spinning NS, entropy consists only of the log term,

$$S_{NS} = \ln\left(\frac{8|M|l^2}{G\hbar^2}\right) \quad (7.4.11)$$



## Chapter 8

# Conclusion

Overall, we have shown how fruitful it is to use EFTs as it is a powerful approach to understanding the vast spectrum of low-energy physics. Here, we applied this approach in four dimensions for analyzing hairy black holes and Q-balls in the Skyrme model. Both of these solutions come from theories that have a spontaneously broken symmetry,  $r$ -diffeomorphism for the hairy black hole, and approximated chiral symmetry for Q-balls. EFTs, let us isolate these relevant degrees of freedom that reveals interesting physics!

In the 2nd chapter, we addressed the question: *does the effective theory of black holes provide any information about the possible existence of hair?*, and the answer is yes, it indeed does! Asymptotically flat/dS hairy Schwarzschild black holes have features in quasinormal modes, which are in contrast with the non-hairy black holes. Specifically, with an increase in the overtone number, the hairy black holes exhibit an increase in the real and imaginary frequency parts of the quasinormal oscillations. For non-hairy black holes, only the imaginary part of the frequency increases while the real part decreases. In this way, we have a proposal for the possible detection signature of the hairy black hole in the gravitational wave data. One more exciting thing to note is that the scalar hair gave rise to the cosmological constant in the case of the dS black hole.

In the 3rd chapter, we addressed the question: *Can Q-balls, ungauged and gauged, exist in the Skyrme model?*, and the answer is yes! The existence of ungauged Q-balls can be easily seen through the lens of a point particle living in the  $V_{eff}$ , figure 3.5.3b. While we have still not found a numerical solution for a gauged Q-ball, we are confident that they exist based on the form of the potential. We demonstrated this following the hedgehog ansatz, under

which the potential and effective potential satisfy all the conditions put forth by Coleman (66).

Q-balls provide a foundation to study pion stars, making studying Q-balls in the Skyrme model a perfect and realistic candidate! So far, we have not detected a pion star. Still, it is reasonable to consider their existence, given that neutron stars exist. Besides black holes, neutron stars are the densest known object in the Universe. In a way, they represent a penultimate state for the densest object, which helps gain insights into black hole physics. But nature could host another intermediate state between a neutron star and a black hole, a pion star as a combination of two and three quarks is abundant in the Universe. Studying pion stars will give us unprecedented insights into compact objects and black holes.

In the 5th chapter, we explored quantum fluctuations around the equilibrium of a BIon configuration. The analysis was carried out solely numerically. Through this, we found that the fluctuations give rise to corrections in the thermodynamic properties of the configurations; specifically, the entropy receives log corrections. This analysis parallels that of a black hole. We also demonstrated numerically that these quantum fluctuations affect the critical points, thus affecting the system's stability. The stability increases under certain conditions. For instance, when the throat is smaller, the inclusion of fluctuations increases the stability. This numerical analysis can be used to study black holes.

Chapters 6 and 7 highlight the hardships involved in path integral quantization of gravity. We put forward a proposal for the path integral measure, but the equations are still intractable. The proposed measure comes with the determinant of the Wheeler-DeWitt metric

$$w[g] = \sqrt{-\left(\frac{\sqrt{(2)g}}{4N}\right)^3 |G|} \quad (8.0.1)$$

Finding a well-defined measure could allow us to study exciting properties of the 2 + 1 D pure gravity, like the transition amplitude/probability for the evaporation of the BTZ black hole. Without matter fields, this probability should be zero; a well-defined measure will allow us to calculate it.

Using Euclidean techniques, we analyzed the thermal properties of the BTZ mini-superspace. Specifically, we considered Euclidean BTZ black holes and naked singularities (conical defects and excesses). The Euclidean version of 2+1 D NS was not studied before, so we carefully analyzed it in the cartesian coordinates and found periodicities in time and

angular direction. Surprisingly, Euclidean NS gets a horizon-like artifact given by  $\lambda_-$ . The temperature and angular potential are

$$\beta^{NS} = \frac{2\pi l^2 |\lambda_+|}{\lambda_-^2 - \lambda_+^2} \quad \text{and} \quad \Phi^{NS} = \frac{2\pi l \lambda_-}{\lambda_-^2 - \lambda_+^2} \quad (8.0.2)$$

In the saddle point approximation for the geometries in the BTZ mini-superspace, we got the logarithmic correction to the black hole entropy coming from the Jacobian of the transformation of  $(M, J)$  to  $(r_+, r_-)$ ,

$$S_{BH} = \frac{2\pi r_+}{4G\hbar} + \ln \left( \frac{r_+^2 - r_-^2}{G^2 \hbar^2} \right) \quad (8.0.3)$$

Previously, the logarithmic corrections were calculated using CFT techniques, but here we showed the corrections without employing CFT. We also calculated the entropy of NS with logarithmic correction.

$$S_{NS} = \frac{2\pi \lambda_-}{4G\hbar} + \ln \left( \frac{\lambda_-^2 - \lambda_+^2}{G^2 \hbar^2} \right) \quad (8.0.4)$$

That is the story so far! It is exceptionally challenging to probe gravity at quantum scales. With the path integral approach, we run into two significant issues measure and oscillatory integral. However, new ways of handling Lorentzian path integrals, Picard-Lefschetz theory, have come into the light, like in the simple toy model of the FRW cosmology (205). We tried that approach for the BTZ mini-superspace, but it is not applicable as this technique requires an action quadratic in  $M$  and  $J$ .

# Appendix A

## A1 Supplements for the EFT of Black holes

Solving Einstein's equation, we get

$$\begin{aligned} \Lambda(r) = & \frac{M_{Pl}^2}{g(r)} \left( -\frac{f'(r)R'(r)}{4f(r)R(r)} + \frac{g'(r)R'(r)}{4g(r)R(r)} + \frac{g(r)}{R(r)} - \frac{R''(r)}{2R(r)} \right) \\ & - \left( \frac{f'^2(r)}{2f^2(r)} + \frac{f'(r)g'(r)}{4g^{3/2}(r)\sqrt{f(r)}} - \frac{f'(r)R'(r)}{4f(r)R(r)} + \frac{R'^2(r)}{4R^2(r)} - \frac{f''(r)}{4f(r)} \right) \frac{\alpha(r)}{g(r)} + \frac{f'(r)}{2f(r)g(r)} \alpha'(r), \end{aligned} \quad (\text{A1.1})$$

$$\begin{aligned} c(r) = & \frac{M_{Pl}^2 R'(r)}{4R(r)} \left( \frac{f'(r)}{f(r)} + \frac{g'(r)}{g(r)} - \frac{R''(r)}{2R(r)} + \frac{R'^2(r)}{R^2(r)} \right) \\ & - \left( \frac{f'^2(r)}{2f^2(r)} + \frac{f'(r)g'(r)}{4g^{3/2}(r)\sqrt{f(r)}} - \frac{f'(r)R'(r)}{4f(r)R(r)} + \frac{R'^2(r)}{4R^2(r)} - \frac{f''(r)}{4f(r)} \right) \alpha(r) + \frac{f'(r)}{4f(r)} \alpha'(r). \end{aligned} \quad (\text{A1.2})$$

## A2 Q-balls

### A2.1 Energy of Q-balls

The total energy functional in this ansatz can be calculated using the above effective Lagrangian is,

$$E = \int d^3x \sqrt{-g} T_{00} = \int d^3x \sqrt{-g} \left[ T_{00}^{\text{Sk}} + T_{00}^{\text{mass}} + T_{00}^{\text{U}(1)} \right] \quad (\text{A2.1})$$

$$\begin{aligned} = & -4\pi K \int dr r^2 \text{Tr} \left[ \frac{1}{2} L_0^2 + \frac{1}{2} L_r^2 + \frac{\lambda}{8} G_{0r}^2 + 2m^2 (U + U^{-1} - 2\mathbb{I}) \right. \\ & \left. - \frac{2}{K} \left( g^{\alpha\beta} F_{0\alpha} F_{0\beta} + \frac{1}{4} g^{\alpha\rho} g^{\sigma\beta} F_{\alpha\beta} F_{\rho\sigma} \right) \right] \end{aligned} \quad (\text{A2.2})$$

where,

$$\begin{aligned}\frac{1}{2}\text{Tr} L_0^2 &= -g^2 \sin^2 \alpha \\ \frac{1}{2}\text{Tr} L_r^2 &= -(\alpha')^2 \\ \frac{1}{8}\text{Tr} G_{0r}^2 &= -g^2 (\alpha')^2 \sin^2 \alpha \\ \text{Tr}(U + U^{-1} - 2\mathbb{I}) &= 4(\cos \alpha - 1) \\ T_{00}^{\text{U}(1)} &= \frac{1}{8}(g')^2\end{aligned}$$

Putting it all together

$$E_{\text{gauged}} = 4\pi K \int dr r^2 \left[ g^2 \sin^2 \alpha \left( 1 + \lambda (\alpha')^2 \right) + (\alpha')^2 - 8m^2 (\cos \alpha - 1) + \frac{1}{4K} (g')^2 \right] \quad (\text{A2.3})$$

and for the ungauged Skyrme model

$$\begin{aligned}E_{\text{ungauged}} &= \int d^3x \sqrt{-g} (T_{00}^{\text{Sk}} + T_{00}^{\text{mass}}) \\ &= 4\pi K \int dr r^2 \left[ \omega^2 \sin^2 \alpha \left( 1 + \lambda (\alpha')^2 \right) + (\alpha')^2 - 8m^2 (\cos \alpha - 1) \right] \quad (\text{A2.4})\end{aligned}$$

## A2.2 Asymptotic energy of ungauged Q-balls

The energy of this system from A2.4 as  $r \rightarrow \infty$  goes to zero exponentially fast.

$$\begin{aligned}E_{\text{ungauged}} &= 4\pi K \int dr r^2 \left[ \omega^2 \sin^2 H + (H')^2 (1 + \lambda \omega^2 \sin^2 H) - \frac{8m^2}{K} (\cos H - 1) \right] \\ \implies E_{\text{ungauged}} &\xrightarrow{R \rightarrow \infty} 4\pi K \int^R dr r^2 [(H')^2 + (\omega^2 + \omega_0^2) H^2] \quad (\text{A2.5}) \\ \implies E_{\text{ungauged}} &= 32\pi K C^2 m^2 \int^R dr e^{-r\sqrt{\omega_0^2 - \omega^2}} \rightarrow 0\end{aligned}$$

## A3 Determinant of the Wheeler-DeWitt metric

Wheeler-DeWitt metric is a metric on the superspace that depends on three functions  $g_{ij}$ . Let us denote the set of indices as  $A = \{11, 12, 22\}$  so that we have the components of  $g_{ij}$  as  $g_A$ . Using this notation, we can see that the metric  $G_{ijkl} = G_{AB}$  is three-dimensional.

Its form in 3 dimensions is different from the one in 4 dimensions.

$$G_{ijkl} = \frac{1}{2} (g_{ik}g_{jl} + g_{il}g_{jk} - 2g_{ij}g_{kl}) \quad (\text{A3.1})$$

$$G^{ijkl} = \frac{1}{2} (g^{ik}g^{jl} + g^{il}g^{jk} - 2g^{ij}g^{kl}) \quad (\text{A3.2})$$

One should require that  $G_{ijkl}G^{klmn} = 1/2 [\delta_i^m \delta_j^n + \delta_j^m \delta_i^n]$ , which is the identity in the space of symmetric tensors:  $1/2 [\delta_i^m \delta_j^n + \delta_j^m \delta_i^n] A_{mn} = A_{ij}$ . Then,

$$G_{ijkl} = \frac{1}{2} (g_{ik}g_{jl} + g_{il}g_{jk} - 2/(D-1)g_{ij}g_{kl}) \quad (\text{A3.3})$$

where  $D =$  (number of spatial dimensions), so  $2/(D-1) = 2$  in our case. Then  $G_{ijkl}G^{ijkl} = D(D+1)/2 =$  (number of independent components of a symmetric tensor), which in our case is 3.

If we take their product, we can realize that they are indeed inverse of each other.

$$G_{ijkl}G^{ijkl} = 3 \quad (\text{A3.4})$$

In the matrix form for  $g_{12} = 0$

$$\begin{pmatrix} 0 & 0 & -g_{11}g_{22} \\ 0 & g_{11}g_{22} & 0 \\ -g_{11}g_{22} & 0 & 0 \end{pmatrix} \begin{pmatrix} 0 & 0 & -g^{11}g^{22} \\ 0 & g^{11}g^{22} & 0 \\ -g^{11}g^{22} & 0 & 0 \end{pmatrix} = \begin{pmatrix} 1 & 0 & 0 \\ 0 & 1 & 0 \\ 0 & 0 & 1 \end{pmatrix} \quad (\text{A3.5})$$

$$G_{ijkl} = G_{AB} = \begin{pmatrix} G_{1111} & G_{1112} & G_{1122} \\ G_{1112} & 2G_{1212} & G_{1222} \\ G_{1122} & G_{1222} & G_{2222} \end{pmatrix} \quad (\text{A3.6})$$

$$= \begin{pmatrix} 0 & 0 & (g_{12})^2 - g_{11}g_{22} \\ 0 & -[(g_{12})^2 - g_{11}g_{22}] & 0 \\ (g_{12})^2 - g_{11}g_{22} & 0 & 0 \end{pmatrix} \quad (\text{A3.7})$$

The determinant of the W-DW metric is

$$\text{Det } G_{ijkl} = [(g_{12})^2 - g_{11}g_{22}]^3 \quad (\text{A3.8})$$

$$G^{AB} = G^{ijkl} = \frac{1}{2} (g^{ik} g^{jl} + g^{il} g^{jk} - 2g^{ij} g^{kl}) \quad (\text{A3.9})$$

$$\Rightarrow G^{AB} = \begin{pmatrix} 0 & 0 & (g^{12})^2 - g^{11}g^{22} \\ 0 & -[(g^{12})^2 - g^{11}g^{22}] & 0 \\ (g^{12})^2 - g^{11}g^{22} & 0 & 0 \end{pmatrix} \quad (\text{A3.10})$$

The determinant of the inverse W-DW metric  $G^{AB}$  is

$$\text{Det } G^{AB} = [(g^{12})^2 - g^{11}g^{22}]^3 = -|g^{ij}|^3 = -|g_{ij}|^{-3}. \quad (\text{A3.11})$$

For  $g_{12} = 0$ ,

$$G^{AB} = \begin{pmatrix} 0 & 0 & -g^{11}g^{22} \\ 0 & g^{11}g^{22} & 0 \\ -g^{11}g^{22} & 0 & 0 \end{pmatrix} \quad (\text{A3.12})$$

The determinant of the inverse W-DW metric  $G^{AB}$  is

$$\text{Det } G^{AB} = -[g^{11}g^{22}]^3 \quad (\text{A3.13})$$

# Bibliography

- [1] Chakrabarti, Sayan, Chougule, Sumeet, and Debaprasad Maity. "Effective Field Theory of Hairy Black Holes and Their flat/dS limit." arXiv, (2018). <https://doi.org/10.1103/PhysRevD.100.064015>.
- [2] B. Pourhassan, S. Dey, S. Chougule and M. Faizal, "Quantum corrections to a finite temperature BIon," *Class. Quant. Grav.* **37**, no.13, 135004 (2020) doi:10.1088/1361-6382/ab90a3 [arXiv:1905.03624 [hep-th]].
- [3] B. P. Abbott *et al.* [LIGO Scientific and Virgo], "Observation of Gravitational Waves from a Binary Black Hole Merger," *Phys. Rev. Lett.* **116**, no.6, 061102 (2016) doi:10.1103/PhysRevLett.116.061102 [arXiv:1602.03837 [gr-qc]].
- [4] M. Banados, C. Teitelboim and J. Zanelli, "The Black hole in three-dimensional space-time," *Phys. Rev. Lett.* **69**, 1849-1851 (1992) doi:10.1103/PhysRevLett.69.1849 [arXiv:hep-th/9204099 [hep-th]].
- [5] M. Banados, M. Henneaux, C. Teitelboim and J. Zanelli, "Geometry of the (2+1) black hole," *Phys. Rev. D* **48**, 1506-1525 (1993) [erratum: *Phys. Rev. D* **88**, 069902 (2013)] doi:10.1103/PhysRevD.48.1506 [arXiv:gr-qc/9302012 [gr-qc]].
- [6] J. F. Donoghue, "Introduction to the effective field theory description of gravity," [arXiv:gr-qc/9512024 [gr-qc]].
- [7] J. F. Donoghue, "Quantum General Relativity and Effective Field Theory," [arXiv:2211.09902 [hep-th]].
- [8] G. 't Hooft and M. J. G. Veltman, "One loop divergencies in the theory of gravitation," *Ann. Inst. H. Poincare Phys. Theor. A* **20**, 69-94 (1974)
- [9] P. Kraus and E. T. Tomboulis, "Photons and gravitons as Goldstone



- bosons, and the cosmological constant,” *Phys. Rev. D* **66**, 045015 (2002) doi:10.1103/PhysRevD.66.045015 [arXiv:hep-th/0203221 [hep-th]].
- [10] D. Robinson, Four decades of black holes uniqueness theorems, in *The Kerr Spacetime: Rotating Black Holes in General Relativity*, eds. D.L. Wiltshire and M. Visser and S. M. Scott (Cambridge University Press, 2009); P. T. Chrusciel, J. L. Costa and M. Heusler, *Living Rev. Rel.* **15**, 7 (2012) [arXiv:1205.6112]; R. Ruffini and J. A. Wheeler, *Phys. Today* **24**, 1 (1971).
- [11] J. D. Bekenstein, *Phys. Rev. Lett.* **28**, 452 (1972); J. D. Bekenstein, *Phys. Rev.* **D5**, 1239 (1972); J. D. Bekenstein, *Phys. Rev.* **D5**, 2403 (1972); J. D. Bekenstein, *Phys. Rev.* **D51**, 6608 (1995).
- [12] A. Nicolis, R. Rattazzi and E. Trincherini, *Phys. Rev.* **D79**, 064036 (2009) [arXiv:0811.2197] ; C. Deffayet, S. Deser and G. Esposito-Farese, *Phys. Rev.* **D80**, 064015 (2009) [arXiv:0906.1967]; C. Deffayet, X. Gao, D. A. Steer and G. Zahariade, *Phys. Rev.* **D84**, 064039 (2011) [arXiv:1103.3260]. T. Kobayashi, M. Yamaguchi and J. Yokoyama, *Prog. Theor. Phys.* **126**, 511 (2011) [arXiv:1105.5723].
- [13] L. Hui and A. Nicolis, *Phys. Rev. Lett.* **110**, 241104 (2013) [arXiv:1202.1296].
- [14] Thomas P. Sotiriou and Shuang-Yong Zhou, *Phys. Rev. Lett.*, **112**, 251102 (2014).
- [15] E. Babichev and C. Charmousis, *JHEP* **1408**, 106 (2014) [arXiv:1312.3204]; C. Charmousis, T. Kolyvaris, E. Papantonopoulos and M. Tsoukalas, *JHEP* **1407**, 085 (2014) [arXiv:1404.1024]; Y. Zhong, B. M. Gu, S. W. Wei and Y. X. Liu, *Eur.Phys.J.* **C76**, 377 (2016) [arXiv:1503.00126]; C. Charmousis and D. Iosifidis, arXiv:1501.05167; E. Babichev, C. Charmousis and M. Hassaine, *JCAP* **1505**, 031 (2015) [arXiv:1503.02545].
- [16] B. P. Abbott *et al.* [LIGO Scientific and Virgo Collaborations], *Phys. Rev. Lett.* **119** (2017) no.16, 161101.
- [17] B. P. Abbott *et al.* [LIGO Scientific and Virgo Collaborations], *Astrophys. J.* **851** (2017) no.2, L35
- [18] C. A. R. Herdeiro, Eugen Radu, *Int.J.Mod.Phys.* **D24**, 1542014 (2015) [arXiv:1504.08209].
- [19] C. Cheung, A. L. Fitzpatrick, J. Kaplan, L. Senatore, and P. Creminelli, *Journal of High Energy Physics*, 2008(03), 014 (2008).

- [20] R. Kase, L. A. Gergely, and S. Tsujikawa, *Phys. Rev.* **D90**, 124019 (2014) [arXiv:1406.2402]
- [21] O. J. Tattersall, P. G. Ferreira, and M. Lagos, *Phys. Rev.* **D97**, 044021 (2018); [arXiv:1711.01992].
- [22] G. Franciolini, L. Hui, R. Penco, L. Santoni and E. Trincherini, *JHEP* 1902, 127 (2019); [arXiv:1810.07706].
- [23] Marc Henneaux, Cristián Martínez, Ricardo Troncoso, and Jorge Zanelli, *Phys. Rev. D* 65, 104007 (2002)
- [24] Cristián Martínez, Ricardo Troncoso, and Jorge Zanelli, *Phys. Rev. D* 70, 084035 (2004)
- [25] Steven S. Gubser, *Phys.Rev.* **D78**, 065034 (2008).
- [26] P. Breitenlohner, D. Z. Freedman, *Annals Phys.* **144**, 249 (1982).
- [27] S. Iyer and C. M. Will, *Phys. Rev* **D35**, 3621 (1987)
- [28] R. A. Konoplya, A. Zhidenko and A. F. Zinhailo, arXiv: 1904.10333
- [29] R. A. Konoplya, *Phys. Rev.* **D68**, 024018 (2003)
- [30] N. Arkani-Hamed, H. -C. Cheng, M. A. Luty, and S. Mukohyama. *Journal of High Energy Physics*, 2004(05):074, 2004.
- [31] N. Arkani-Hamed, P. Creminelli, S. Mukohyama, and M. Zaldarriaga. *Journal of Cosmology and Astroparticle Physics*, 2004(04):001, 2004.
- [32] S. Chandrasekhar and S. L. Detweiler, *Proceedings of the Royal Society of London A*, 344(1639), 441–452 (1975).
- [33] H. -P. Nollert, *Class. Quant. Grav.* **16**, R159 (1999).
- [34] K. D. Kokkotas and B. G. Schmidt, *Living Rev. Rel.* **2**, 2 (1999)
- [35] E. Berti, V. Cardoso and A. O. Starinets, *Class. Quant. Grav.* **26** (2009) 163001
- [36] R. A. Konoplya and A. Zhidenko, *Rev. Mod. Phys.* **83** (2011) 793
- [37] H. -P. Nollert, *Class. Quant. Grav.* **16**, R159 (1999).
- [38] K. D. Kokkotas and B. G. Schmidt, *Living Rev. Rel.* **2**, 2 (1999)
- [39] E. Berti, V. Cardoso and A. O. Starinets, *Class. Quant. Grav.* **26** (2009) 163001

- [40] R. A. Konoplya and A. Zhidenko, *Rev. Mod. Phys.* **83** (2011) 793
- [41] J. Greensite, *An Introduction to the Confinement Problem* (Lecture Notes in Physics, Vol. 821), Springer, 2011.
- [42] G. Ripka, *Dual Superconductor Models of Color Confinement* (Lecture Notes in Physics, 639, 2004).
- [43] N. Manton and P. Sutcliffe, *Topological Solitons*, (Cambridge University Press, Cambridge, 2007).
- [44] J. A. Frieman, G. B. Gelmini, M. Gleiser and E. W. Kolb, “Solitogenesis: Primordial Origin of Nontopological Solitons,” *Phys. Rev. Lett.* **60**, 2101 (1988) doi:10.1103/PhysRevLett.60.2101
- [45] A. Balachandran, G. Marmo, B. Skagerstam, A. Stern, *Classical Topology and Quantum States*, World Scientific (1991).
- [46] M. Shifman, “*Advanced Topics in Quantum Field Theory: A Lecture Course*” Cambridge University Press, (2012).
- [47] A. Kusenko and M. E. Shaposhnikov, “*Supersymmetric Q balls as dark matter*,” *Phys. Lett.* **B418** (1998) 46–54, [[hep-ph/9709492](#)].
- [48] A. Kusenko, V. Kuzmin, M. E. Shaposhnikov, and P. G. Tinyakov, “*Experimental signatures of supersymmetric dark matter Q balls*,” *Phys. Rev. Lett.* **80** (1998) 3185–3188, [[hep-ph/9712212](#)].
- [49] A. Kusenko and P. J. Steinhardt, “*Q ball candidates for selfinteracting dark matter*,” *Phys. Rev. Lett.* **87** (2001) 141301, [[astro-ph/0106008](#)].
- [50] E. Pontón, Y. Bai, and B. Jain, “*Electroweak Symmetric Dark Matter Balls*,” *JHEP* **09** (2019) 011, [[1906.10739](#)].
- [51] Y. Bai and J. Berger, “*Nucleus Capture by Macroscopic Dark Matter*,” *JHEP* **05** (2020) 160, [[1912.02813](#)].
- [52] Y. Bai, S. Lu, and N. Orlofsky, “*Q-monopole-ball: a topological and nontopological soliton*,” *JHEP* **01** (2022) 109, [[2111.10360](#)].
- [53] K. Enqvist and J. McDonald, “*Q balls and baryogenesis in the MSSM*,” *Phys. Lett. B* **425** (1998) 309–321, [[hep-ph/9711514](#)].

- [54] E. Krylov, A. Levin, and V. Rubakov, “*Cosmological phase transition, baryon asymmetry and dark matter Q-balls,*” *Phys. Rev.* **D87** (2013) 083528, [[1301.0354](#)].
- [55] A. Kusenko and A. Mazumdar, “*Gravitational waves from fragmentation of a primordial scalar condensate into Q-balls,*” *Phys. Rev. Lett.* **101** (2008) 211301, [[0807.4554](#)].
- [56] D. Croon, A. Kusenko, A. Mazumdar, and G. White, “*Solitogenesis and Gravitational Waves,*” *Phys. Rev. D* **101** (2020) 085010, [[1910.09562](#)].
- [57] M. Shifman, A. Yung, “*Supersymmetric Solitons*” Cambridge University Press, (2009).
- [58] E. J. Weinberg, *Classical Solutions in Quantum Field Theory*, Cambridge, 2012.
- [59] G. Rosen. *Journ. Math. Phys.* 9 (1968) 996, 999.
- [60] D. Kaup, *Phys. Rev.* 172 (1968) 1331.
- [61] R. Ruffini and S. Bonazzola, *Phys. Rev.* 187 (1969) 1767.
- [62] P. Vinciarelli, *Nuovo Cimento Lett.* 4 (1972) 905.
- [63] T.D. Lee, G.C. Wick. *Phys. Rev. D* 9 (1974) 229.
- [64] A. Chodos. R.J. Jaffe. K. Johnson. C.B. Thorn, V.F. Weisskopf, *Phys. Rev. D* 9 (1974) 3471.
- [65] R. Friedberg. T.D. Lee, A. Sirlin. *Phys. Rev. D* 13 (1976) 2739; *Nucl. Phys. B* 115(1976) 1; *Nucl. Phys. B* 115(1976)32.
- [66] S. Coleman, *Nucl. Phys.* **B 262** (1985) 263-283.
- [67] C. Adam, P. Klimas, J. Sánchez-Guillén, and A. Wereszczyński *Phys. Rev. D* 80, (2009) 105013
- [68] Jakub Lis, *Phys. Rev. D* 84, (2011) 085030.
- [69] A. M. Safian, S. Coleman, M. Axenides, *Nucl. Phys.* **B 297** (1988) 498-514.
- [70] T. D. Lee, Y. Pang, *Physics Reports* **221** (1992), 251-350.
- [71] S. Liebling, C. Palenzuela, *Dynamical boson stars*, *Living Rev Relativ* (2017) 20: 5.
- [72] E. Ya. Nugaev, A. V. Shkerin, *Journal of Experimental and Theoretical Physics* **130**, 301–320 (2020).
- [73] I. Affleck and M. Dine, *Nucl. Phys. B* 249, 361 (1985).

- [74] J. A. Frieman, G. B. Gelmini, M. Gleiser, E. W. Kolb, *Phys. Rev. Lett.* **60**, 2101 (1988).
- [75] A. Kusenko and M. E. Shaposhnikov, *Phys. Lett. B* **418**, 46 (1998); arXiv: hep-ph/9709492.
- [76] K. Takayama and M. Oka, *Nucl. Phys.* A551, 637 (1993).
- [77] T. Skyrme, *Proc. R. Soc. London A* **260**, 127 (1961); *Proc. R. Soc. London A* **262**, 237 (1961); *Nucl. Phys.* **31**, 556 (1962).
- [78] C. G. Callan Jr. and E. Witten, *Nucl. Phys. B* **239** (1984) 161-176.
- [79] E. Witten, *Nucl. Phys.* **B 223** (1983), 422; *Nucl. Phys.* **B 223**, 433 (1983).
- [80] G. S. Adkins, C. R. Nappi, E. Witten, *Nucl. Phys.* **B 228** (1983), 552-566.
- [81] A. P. Balachandran, V. P. Nair, N. Panchapakesan, S. G. Rajeev, *Phys. Rev.* **D 28** (1983), 2830.
- [82] A. P. Balachandran, A. Barducci, F. Lizzi, V.G.J. Rodgers, A. Stern, *Phys. Rev. Lett.* **52** (1984), 887; A.P. Balachandran, F. Lizzi, V.G.J. Rodgers, A. Stern, *Nucl. Phys.* **B 256**, 525-556 (1985).
- [83] F. Canfora, *Phys. Rev.* **D 88**, (2013), 065028
- [84] F. Canfora, *Eur. Phys. J.* **C78**, no. 11, 929 (2018); F. Canfora, S.-H. Oh, A. Vera, *Eur. Phys. J.* **C79** (2019) no.6, 485; F. Canfora, S. Carignano, M. Lagos, M. Mannarelli and A. Vera, *Phys. Rev. D* **103**, no. 7, 076003 (2021); G. Barriga, F. Canfora, M. Torres and A. Vera, *Phys. Rev. D* **103**, no.9, 096023 (2021).
- [85] F. Canfora, M. Lagos, A. Vera, *Eur. Phys. J. C* **80** (2020) 8, 697.
- [86] S. Chen, Y. Li, Y. Yang, *Phys. Rev.* **D 89** (2014), 025007.
- [87] E. Ayon-Beato, F. Canfora, J. Zanelli, *Phys. Lett.* **B 752**, (2016) 201-205; P. D. Alvarez, F. Canfora, N. Dimakis and A. Paliathanasis, *Phys. Lett.* **B 773**, (2017) 401-407; L. Aviles, F. Canfora, N. Dimakis, D. Hidalgo, *Phys. Rev.* **D 96** (2017), 125005; F. Canfora, M. Lagos, S. H. Oh, J. Oliva and A. Vera, *Phys. Rev. D* **98**, no. 8, 085003 (2018); F. Canfora, N. Dimakis, A. Paliathanasis, *Eur.Phys.J.* **C79** (2019) no.2, 139.
- [88] P. D. Alvarez, S. L. Cacciatori, F. Canfora, B. L. Cerchiai, *Phys. Rev. D* **101** (2020) 12, 125011.

- [89] S. L. Cacciatori, F. Canfora, M. Lagos, F. Muscolino and A. Vera, [arXiv:2105.10789 [hep-th]].
- [90] E. Ayon-Beato, F. Canfora, M. Lagos, J. Oliva and A. Vera, Eur. Phys. J. C **80**, no. 5, 384 (2020).
- [91] A. I. Larkin, Yu. N. Ovchinnikov, Zh. Eksp. Teor. Fiz. 47: 1136 (1964); Sov. Phys. JETP. 20: 762; P. Fulde, R. A. Ferrell, Phys. Rev. 135: A550 (1964).
- [92] L. Marleau, Phys. Lett. B **235**, 141 (1990) Erratum: [Phys. Lett. B **244**, 580 (1990)]; L. Marleau, Phys. Rev. D **43**, 885 (1991); Phys. Rev. D **45**, 1776 (1992).
- [93] S. B. Gudnason and M. Nitta, JHEP **1709**, 028 (2017).
- [94] R. P. Feynman, Nucl. Phys. B188 (1981) 479-512.
- [95] R. P. Feynman, Phys. Rev. 91 (1953) 30; Phys. Rev. 94 (1954) 262.
- [96] A. M. Polyakov, Phys. Lett. B 59, 82 (1975); Nucl. Phys. B 120, 429 (1977).
- [97] A. Kovner, B. Rosenstein, Mod.Phys.Lett.A 7 (1992) 2287-2298; Phys. Rev. Lett. 67, 1490 (1991).
- [98] Ian I. Kogan, Alex Kovner, Published in: "At the frontier of particle physics" Vol. 4 2335-2407, e-Print: hep-th/0205026 [hep-th]; A. Kovner, Int.J.Mod.Phys.A 17 (2002) 2113-2164.
- [99] D. Karabali, C.-j. Kim, V.P. Nair, Phys.Lett.B 434 (1998) 103-109; Nucl.Phys.B 524 (1998) 661-694; Phys.Rev.D 64 (2001) 025011.
- [100] A. Agarwal, D. Karabali, V.P. Nair, Nucl.Phys.B 790 (2008) 216-239; A. Agarwal, V.P. Nair, Nucl.Phys.B 816 (2009) 117-138.
- [101] V.P. Nair, Phys.Rev.D 85 (2012) 105019; D. Karabali, V.P. Nair, Phys.Rev.D 98 (2018) 10, 105009.
- [102] R. G. Leigh, D. Minic, and A. Yelnikov, Phys. Rev. Lett. 96, 222001 (2006); Phys. Rev. D 76, 065018 (2007).
- [103] M.J. Teper, Phys. Rev. D 59 (1999) 014512, hep-lat/9804008.
- [104] B. Lucini, M. Teper, Phys. Rev. D 66 (2002) 097502, hep-lat/0206027.
- [105] B. Bringoltz, M. Teper, Phys. Lett. B 645 (2007) 383, hep-th/0611286.

- [106] F. Canfora, S.-H. Oh, P. Salgado-Rebolledo, *Phys.Rev.D* 96 (2017) 8, 084038.
- [107] F. Canfora, A. Gomberoff, S.-H. Oh, F. Rojas, P. Salgado-Rebolledo, *JHEP* 06 (2019) 081.
- [108] F. Canfora, S.-H. Oh, *Eur.Phys.J.C* 81 (2021) 5, 432.
- [109] F. Canfora, *Eur.Phys.J.C* 81 (2021) 11, 1032.
- [110] F. Canfora, D. Flores-Alfonso, M. Lagos and A. Vera, *Phys. Rev. D* **104**, no.12, 125002 (2021).
- [111] B. A. Bernevig, T. L. Hughes, *Topological Insulators and Topological Superconductors*, Princeton University Press (2013).
- [112] K. Fukushima, V. Skokov, *Polyakov loop modeling for hot QCD*, *Prog. Part. Nucl. Phys.* 96 (2017) 154-199.
- [113] M. Hanada, H. Shimada, N. Wintergerst, *JHEP* 08 (2021) 039.
- [114] R.P. Treat, *Nuovo Cim.A* 6 (1971) 121-128.
- [115] Sidney R. Coleman, *Phys.Lett.B* 70 (1977) 59-60.
- [116] Y Nutku, *J. Phys. A: Math. Gen.* 16 (1983) L583-L586.
- [117] K. Rajagopal, N. Turok, *Nucl. Phys. B*375, 299 (1992).
- [118] H. Goldberg, D. Nash, M. T. Vaughn, *Phys. Rev. D* 46, 2585 (1992).
- [119] C. R. Hu, S. G. Matinyan, B. Muller, A. Trayanov, T. M. Gould, S. D. H. Hsu, E. R. Poppitz, *Phys. Rev. D* 52, 2402 (1995).
- [120] C. R. Hu, S. G. Matinyan, B. Muller, D. Sweet, *Phys. Rev. D* 53, 3823, 1996.
- [121] K. Lee, J. Stein-Schabes, R. Watkins, and L. Widrow *Phys. Rev. D* 39, 1665, (1989).
- [122] I. Gulamov, E. Nugaev, and M. Smolyakov *Phys. Rev. D* 89, 085006
- [123] I. Gulamov, E. Nugaev, A. Panin and M. Smolyakov *Phys. Rev. D* 92, 045011
- [124] [DLMF] NIST Digital Library of Mathematical Functions. <http://dlmf.nist.gov/>, Release 1.1.5 of 2022-03-15. F. W. J. Olver, A. B. Olde Daalhuis, D. W. Lozier, B. I. Schneider, R. F. Boisvert, C. W. Clark, B. R. Miller, B. V. Saunders, H. S. Cohl, and M. A. McClain, eds. See, Eq. 13.2.2

- [125] Detection of the Characteristic Pion-Decay Signature in Supernova Remnants. Fermi-LAT Collaboration, M. Ackermann (DESY) et al. *Science* 339 (2013) 807
- [126] A. Panin and M. Smolyakov, *Phys. Rev. D* 95, 065006
- [127] A. COHEN, S. COLEMAN, H. GEORGI and A. MANOHAR, *Nuclear Physics B* 272 (1986) 301-321
- [128] Jeong-Pyong Hong, Masahiro Kawasaki, *Phys. Rev. D* 96, 103526 (2017)
- [129] V. Vovchenko, B. Brandt, F. Cuteri, G. Endrődi, F. Hajkarim, and J. Schaffner-Bielich *Phys. Rev. Lett.* 126, 012701 (2021)
- [130] Bekenstein, J.D. Black holes and the second law. *Lett. Nuovo Cimento* 4, 737–740 (1972). <https://doi.org/10.1007/BF02757029>
- [131] Hawking, S.W. Particle creation by black holes. *Commun.Math. Phys.* 43, 199–220 (1975). <https://doi.org/10.1007/BF02345020>
- [132] M. Casals, A. Fabbri, C. Martínez and J. Zanelli, “Quantum-corrected rotating black holes and naked singularities in  $(2+1)$  dimensions,” *Phys. Rev. D* **99**, no.10, 104023 (2019) doi:10.1103/PhysRevD.99.104023 [arXiv:1902.01583 [hep-th]]
- [133] M. Casals, A. Fabbri, C. Martínez and J. Zanelli, “Quantum fields as Cosmic Censors in  $(2 + 1)$ -dimensions,” *Int. J. Mod. Phys. D* **27**, no.11, 1843011 (2018) doi:10.1142/S0218271818430113
- [134] M. Casals, A. Fabbri, C. Martínez and J. Zanelli, “Quantum Backreaction on Three-Dimensional Black Holes and Naked Singularities,” *Phys. Rev. Lett.* **118**, no.13, 131102 (2017) doi:10.1103/PhysRevLett.118.131102 [arXiv:1608.05366 [gr-qc]]
- [135] M. Casals, A. Fabbri, C. Martínez and J. Zanelli, “Quantum dress for a naked singularity,” *Phys. Lett. B* **760**, 244-248 (2016) doi:10.1016/j.physletb.2016.06.044 [arXiv:1605.06078 [hep-th]]
- [136] G. W. Gibbons and S. W. Hawking, “Action Integrals and Partition Functions in Quantum Gravity,” *Phys. Rev. D* **15**, 2752-2756 (1977) doi:10.1103/PhysRevD.15.2752
- [137] J. B. Hartle and S. W. Hawking, *Phys. Rev. D* **13**, 2188-2203 (1976) doi:10.1103/PhysRevD.13.2188
- [138] J. Callan, G. Curtis and J. M. Maldacena, *Nucl. Phys. B* 513, 198 (1998)



- [139] G. W. Gibbons, Nucl. Phys. B 514, 603 (1998)
- [140] G. Grignani, T. Harmark, A. Marini, N. A. Obers and M. Orselli, Nucl. Phys. B 851, 462 (2011)
- [141] G. Grignani, T. Harmark, A. Marini, N. A. Obers, and M. Orselli, JHEP 1106, 058 (2011)
- [142] R. Emparan, T. Harmark, V. Niarchos, N. A. Obers and M. J. Rodriguez, JHEP 10, 110 (2007)
- [143] R. Emparan, T. Harmark, V. Niarchos and N. A. Obers, Phys. Rev. Lett. 102, 191301 (2009)
- [144] R. Emparan, T. Harmark, V. Niarchos and N. A. Obers, JHEP 03, 063 (2010)
- [145] R. Emparan, T. Harmark, V. Niarchos and N. A. Obers, JHEP 04, 046 (2010)
- [146] S. W. Hawking, Nature 248, 30 (1974)
- [147] J. D. Bekenstein, Phys. Rev. D 23, 287 (1981)
- [148] S. K. Rama, Phys. Lett. B 457, 268 (1999)
- [149] S. S. More, Class. Quantum Grav. 22, 4129 (2005)
- [150] S. Das, P. Majumdar and R. K. Bhaduri, Class. Quantum Grav. 19, 2355 (2002)
- [151] S. Carlip, Class. Quantum Grav. 17, 4175 (2000)
- [152] B. Pourhassan, M. Faizal, Z. Zaz and A. Bhat, Phys. Lett. B 773, 325 (2017)
- [153] E. Poppitz and M. Unsal, JHEP 0907, 060 (2009)
- [154] M. M. Anber and E. Poppitz, JHEP 1106, 136 (2011)
- [155] B. Pourhassan and M. Faizal, Europhys. Lett. 111, 40006 (2015)
- [156] J. Sadeghi, B. Pourhassan and F. Rahimi, Can. J. Phys. 92, 1638 (2014)
- [157] M. Faizal and B. Pourhassan, Phys. Lett. B 751, 487 (2015)
- [158] B. Pourhassan, M. Faizal and U. Debnath, Eur. Phys. J. C 76, 145 (2016)
- [159] B. Pourhassan and M. Faizal, Nucl. Phys. B 913, 834 (2016)
- [160] J. Sadeghi, B. Pourhassan and M. Rostami, Phys. Rev. D 94, 064006 (2016)

- [161] A. Ashtekar, *Lectures on non-perturbative canonical gravity*, World Scientific: Singapore (1991)
- [162] T. R. Govindarajan, R. K. Kaul and V. Suneeta, *Class. Quantum Gravity* 18, 2877 (2001)
- [163] R. B. Mann and S. N. Solodukhin, *Nucl. Phys. B* 523, 293 (1998)
- [164] J. Jing and M. L. Yan, *Phys. Rev. D* 63, 24003 (2001)
- [165] R. K. Kaul and P. Majumdar, *Phys. Rev. Lett.* 84, 5255 (2000)
- [166] A. Pourdarvish, J. Sadeghi, H. Farahani and B. Pourhassan, *Int. J. Theor. Phys.* 52, 3560 (2013)
- [167] B. Pourhassan, K. Kokabi and Z. Sabery, *Ann. Phys.* 399, 181 (2018).
- [168] N. Morales-Durán, A. F. Vargas, P. Hoyos-Restrepo and P. Bargueno, *Eur. Phys. J. C* 76, 559 (2016)
- [169] D. Grumiller, A. Perez, D. Tempo and R. Troncoso, *JHEP* 08, 107 (2017)
- [170] A. Pathak, A. P. Porfyriadis, A. Strominger and O. Varela, *JHEP* 04, 090 (2017)
- [171] G. Policastro, D. T. Son and A. O. Starinets, *JHEP* 09, 043 (2002)
- [172] P. Kovtun, D. T. Son and A. O. Starinets, *JHEP* 10, 064 (2003)
- [173] A. Buchel and J. T. Liu, *Phys. Rev. Lett.* 93, 090602 (2004)
- [174] J. Sadeghi, B. Pourhassan and S. Heshmatian, *Adv. High Energy Phys.* 2013, 759804 (2013)
- [175] B. Pourhassan and M. Faizal, *Eur. Phys. J. C* 77, 96 (2017)
- [176] J. R. Mureika, J. W. Moffat and M. Faizal, *Phys. Lett. B* 757, 528 (2016)
- [177] A. Sen, *Gen. Rel. Grav.* 44, 1947 (2012)
- [178] A. Sen, *JHEP* 04, 156 (2013)
- [179] G. W. Gibbons and S. W. Hawking, *Phys. Rev. D* 15, 2752 (1977)
- [180] S. Mukherji and S. S. Pal, *JHEP* 0205, 026 (2002)
- [181] J. E. Lidsey, S. Nojiri, S. D. Odintsov and S. Ogushi, *Phys. Lett. B* 544, 337 (2002)

- [182] M. H. Dehghani and A. Khoddam-Mohammadi, *Phys. Rev. D* 67, 084006 (2003)
- [183] S. Das and V. Husain, *Class. Quantum Grav.* 20, 4387 (2003)
- [184] B. Pourhassan and M. Faizal, *Eur. Phys. J. C* 77, 2, 96 (2017)
- [185] S. Upadhyay, *Phys. Lett. B* 775, 130 (2017)
- [186] A. Haldar and R. Biswas, *Gen. Rel. Grav.* 50, no. 6, 69 (2018)
- [187] S. Upadhyay, *Gen. Rel. Grav.* 50, no. 10, 128 (2018)
- [188] B. Pourhassan, M. Faizal and S. Capozziello, *Annals Phys.* 377, 108 (2017)
- [189] S. N. Solodukhin, *Phys. Lett. B* 802, 135235 (2020)
- [190] S. Karan, G. Banerjee and B. Panda, *JHEP* 1908, 056 (2019)
- [191] O. Asin, J. Ben Achour, M. Geiller, K. Noui and A. Perez, *Phys. Rev. D* 91, 084005 (2015)
- [192] C. Keeler, F. Larsen and P. Lisboa, *Phys. Rev. D* 90, 4, 043011 (2014)
- [193] R. Aros, D. E. Diaz and A. Montecinos, *Phys. Rev. D* 88, 10, 104024 (2013)
- [194] A. Castro, V. Godet, F. Larsen and Y. Zeng, *JHEP* 1805, 079 (2018)
- [195] S. S. More, *Class. Quantum Grav.* 22, 4129 (2005)
- [196] B. Pourhassan, K. Kokabi and S. Rangyan, *Gen. Rel. Grav.* 49, 144 (2017)
- [197] T. Padmanabhan, S. Chakraborty and D. Kothawala, *Gen. Rel. Grav.* 48, 55 (2016)
- [198] S. Chakraborty, D. Kothawala and A. Pesci, *Phys. Lett. B* 797, 134877 (2019)
- [199] B. Pourhassan, S. Upadhyay and H. Farahani, *Int. J. Mod. Phys. A* 34, 1950158 (2019)
- [200] C. Krishnan, *Nucl. Phys. Proc. Suppl.* 192, 132 (2009)
- [201] S. Katmadas and A. Tomasiello, *JHEP* 1512, 111 (2015)
- [202] A. Belhaj, M. Chabab, H. El Moumni, K. Masmar and M. B. Sedra, *Eur. Phys. J. C* 76, 73 (2016)
- [203] T. Regge and C. Teitelboim, "Role of Surface Integrals in the Hamiltonian Formulation of General Relativity," *Annals Phys.* 88, 286 (1974) doi:10.1016/0003-4916(74)90404-7

- [204] J. D. Brown and M. Henneaux, “Central Charges in the Canonical Realization of Asymptotic Symmetries: An Example from Three-Dimensional Gravity,” *Commun. Math. Phys.* **104**, 207-226 (1986) doi:10.1007/BF01211590
- [205] J. Feldbrugge, J. L. Lehners and N. Turok, “Lorentzian Quantum Cosmology,” *Phys. Rev. D* **95**, no.10, 103508 (2017) doi:10.1103/PhysRevD.95.103508 [arXiv:1703.02076 [hep-th]].
- [206] S. Carlip and C. Teitelboim, “Aspects of black hole quantum mechanics and thermodynamics in (2+1)-dimensions,” *Phys. Rev. D* **51**, 622-631 (1995) doi:10.1103/PhysRevD.51.622 [arXiv:gr-qc/9405070 [gr-qc]].
- [207] S. Carlip, “Logarithmic corrections to black hole entropy from the Cardy formula,” *Class. Quant. Grav.* **17**, 4175-4186 (2000) doi:10.1088/0264-9381/17/20/302 [arXiv:gr-qc/0005017 [gr-qc]].
- [208] R. K. Kaul and P. Majumdar, “Logarithmic correction to the Bekenstein-Hawking entropy,” *Phys. Rev. Lett.* **84**, 5255-5257 (2000) doi:10.1103/PhysRevLett.84.5255 [arXiv:gr-qc/0002040 [gr-qc]].

